ISSN 2079-1372 ***DOI: 10.31891/2079-1372***

THE INTERNATIONAL SCIENTIFIC JOURNAL

PROBLEMS OF TRIBOLOGY

Volume 30 ***No 3/117-2025***

МІЖНАРОДНИЙ НАУКОВИЙ ЖУРНАЛ

ПРОБЛЕМИ ТРИБОЛОГІЇ

PROBLEMS OF TRIBOLOGY

INTERNATIONAL SCIENTIFIC JOURNAL

Published since 1996, four time a year

Volume 30 No 3/117-2025

Establishers:
Khmelnytskyi National University (Ukraine)
Lublin University of Technology (Poland)

Associated establisher:
Vytautas Magnus University (Lithuania)

Editorial board address:
International scientific journal "Problems of Tribology",
Khmelnytskyi National University,
Instytutska str. 11, Khmelnytskyi, 29016, Ukraine
phone +380975546925

Indexed: CrossRef, DOAJ, Ulrichsweb, ASCI, Google Scholar, Index Copernicus

E-mail: tribology@khmnu.edu.ua

Internet: http://tribology.khnu.km.ua

ПРОБЛЕМИ ТРИБОЛОГІЇ

МІЖНАРОДНИЙ НАУКОВИЙ ЖУРНАЛ

Видається з 1996 р. ***Виходить 4 рази на рік***

Том 30 **№ 3/117-2025**

Співзасновники:
Хмельницький національний університет (Україна)
Університет Люблінська Політехніка (Польща)

Асоційований співзасновник:

Університет Вітовта Великого (Литва)

Адреса редакції:
Україна, 29016, м. Хмельницький, вул. Інститутська 11, к. 4-401
Хмельницький національний університет, редакція журналу "Проблеми трибології"
тел. +380975546925, **E-mail**: tribology@khmnu.edu.ua

Internet: http://tribology.khnu.km.ua

Зареєстровано Міністерством юстиції України
Свідоцтво про держреєстрацію друкованого ЗМІ: Серія КВ № 1917 від 14.03. 1996 р.
(перереєстрація № 24271-14111ПР від 22.10.2019 року)

Входить до переліку наукових фахових видань України
(Наказ Міністерства освіти і науки України № 612/07.05.19. Категорія Б.)

Індексується в МНБ: CrossRef, DOAJ, Ulrichsweb, ASCI, Google Scholar, Index Copernicus

Рекомендовано до друку рішенням вченої ради ХНУ, протокол № 2 від 11.09.2025 р.

ISSN 2079-1372 Problems of Tribology, V. 30, No 3/117-2025

Problems of Tribology
Website: http://tribology.khnu.km.ua/index.php/ProbTrib
E-mail: tribosenator@gmail.com

CONTENTS

***ISSN 2079-1372 Problems of Tribology**, V. 30, No 3/117-2025*

Problems of Tribology
Website: http://tribology.khnu.km.ua/index.php/ProbTrib
E-mail: tribosenator@gmail.com

ЗМІСТ

ISSN 2079-1372 Problems of Tribology, V. 30, No 3/117-2025, 6-12

Problems of Tribology
Website: http://tribology.khnu.km.ua/index.php/ProbTrib
E-mail: tribosenator@gmail.com

DOI: https://doi.org/10.31891/2079-1372-2025-117-3-6-12

Theoretical foundations of glow discharge nitriding of internal local recesses on metallic surfaces

M.S. Stechyshyn[000-0001-5780-2790], **O.V. Dykha***[0000-0003-3020-9625], **M.Ye. Skyba**[0009-0006-1451-4186] ,
D.V. Zdorenko[0009-0004-3872-3797], **V.V. Liukhovets**[0000-0002-6978-7820]

Khmelnytskyi national University, Ukraine
**E-mail: tribosenator@gmail.com*

Received: 02 June 2025: Revised 20 June 2025: Accept: 10 July 2025

Abstract

This paper presents a comprehensive analysis of internal local recesses on metallic surfaces during glow discharge nitriding. Various types of recesses and their geometric features are studied to evaluate their impact on electric field concentration, which in turn affects the uniformity of surface modification. A field concentration criterion is introduced to quantify these effects, and an analytical framework is developed to describe the relationship between surface geometry and electric field parameters. The influence of the dimensions of internal recesses on field concentration is examined using numerical simulations. The results provide a deeper understanding of the mechanisms leading to localized variations in current density distribution on nitrided surfaces. The developed analytical tools are applicable for predicting and controlling electric field concentration indicators in glow discharge processes used for the surface modification of metallic components, which is critical for ensuring optimal mechanical and tribological properties.

Keywords: local notches, nitriding, electric field, field concentration coefficient

Introduction

Glow discharge nitriding is a widely used surface modification technique for enhancing the mechanical and tribological properties of metallic components. One of the key factors influencing the effectiveness of this process is the distribution of current density over the treated surface, which directly affects the uniformity of nitrogen diffusion and, consequently, the formation of hard surface layers. The presence of internal local recesses such as grooves, holes, and notches—on functional surfaces leads to significant electric field concentration effects. These localized intensifications of the field can result in uneven heating, local overheating, and the formation of areas with inferior physical and mechanical properties, which compromise the overall performance of nitrided parts.

While the theoretical aspects of field concentration around external surface features have been extensively studied, there is limited understanding of the behavior of internal recesses, especially in the context of complex geometries found in real engineering components. Addressing this gap, this study focuses on developing an analytical foundation for describing and predicting electric field behavior in the vicinity of internal local recesses during glow discharge nitriding. A mathematical model is formulated to capture the interplay between surface geometry and field distribution, allowing the identification of critical parameters that influence current density concentration. The findings provide valuable insights for optimizing nitriding technologies for parts with complex geometries, ensuring a homogeneous and high-quality surface layer.

Literature review

The theoretical foundations of the interaction of the electric field with external local surface recesses are considered in [1-3]. Regarding issues related to the theory of internal local surface recesses and modeling of nitriding of complex surfaces, general information about them and the basic principles of solving the problem are given [4, 5-10].

The objective of the study [5] is to analyze the appearance, mechanisms, and processes responsible for the formation of the second plateau in the nitrogen penetration depth profile during thermal annealing after nitriding. The main hypothesis suggests that the second plateau arises due to the formation of nitrides, which is supported by X-ray diffraction spectra showing the presence of chromium nitride after annealing. A new mathematical model has been developed for nitriding, incorporating non-Fickian diffusion mechanisms and post-nitriding annealing. Simulations performed using the proposed model demonstrate that under certain conditions, a second plateau emerges, confirming the model's ability to reproduce nitrogen depth profiles with two plateaus. The paper provides a detailed analysis of these conditions and quantitatively investigates the influence of various parameters (diffusion coefficient, internal lattice stresses, processing time, etc.). Mathematical modeling of mass transport during gas nitriding was carried out in [6] through numerical calculations in the present study. The diffusion coefficient of nitrogen in 38CrMoAl steel and the mass transfer coefficient in the interfacial reaction were determined. Due to the significant difference between the nitrogen activity at the workpiece surface and the gas phase activity during the nitriding process, it is challenging to control the nitrogen potential and maintain a balanced nitrogen activity. To address this issue, a dynamic control of the nitrogen potential using a computer-based system is proposed. Under high nitriding rates, the computer-controlled technology applied in practical production demonstrates excellent reproducibility and enables precise regulation of the nitrogen potential, thereby reducing the brittleness of the nitrided layer. In [7], the relationships between process parameters and layer structure were established to support the development of software for a process control system aimed at achieving a complex layer structure and optimizing the kinetics of its formation and growth. A concept for a gas nitriding process control system was proposed, based on the synergistic integration of an experimental–theoretical process model and data from a magnetic sensor that detects the nucleation and growth of the layer. The article [8] focuses on the development of an advanced probabilistic model for the gas nitriding process of steel, utilizing a cellular automata framework. This model integrates two interconnected cellular automata that represent the two primary phenomena occurring during gas nitriding: the interstitial diffusion of nitrogen in iron and the structural-phase transformations within the nitride material. By adjusting parameter values, this approach enables the model to be adapted for describing various scenarios of the nitriding process. Low-temperature nitriding of steel or iron leads to the formation of expanded austenite,a solid solution with a high concentration of nitrogen interstitially dissolved in the fcc lattice. The nitrogen depth profiles in this phase typically exhibit plateau-like shapes, which cannot be described by standard diffusion models for semi-infinite solids, requiring a new approach. In [9], a model of interdiffusion in a viscoelastic solid, based on the Maxwell framework, is proposed. It combines mass conservation, Vegard's rule, and the Darken bi-velocity method. In the one-dimensional case, the original differential-algebraic system is reduced to a simpler differential system, facilitating analytical and numerical analysis. The resulting nonlinear coupled problem is solved numerically, and a series of simulations demonstrates its applicability. In [10], the coupled processes of burnishing and nitriding are analyzed. A mathematical model is developed to describe the evolution of stress and deformation states in the material under varying technological conditions. The proposed diffusion model for the nitriding process incorporates specific stages occurring in the surface layer of a complex material structure. Numerical simulations are presented, investigating how the initial deformation state influences nitrogen diffusion and the surface layer, as well as how diffusion processes affect the final residual stress distribution in the surface layer.

Despite significant progress in the study of glow discharge nitriding processes, several critical issues remain unresolved. Most existing studies focus on external surface features such as edges and protrusions. The influence of internal recesses (grooves, holes, slots) on electric field concentration and current density distribution remains insufficiently explored, especially for complex geometries typical of functional surfaces in engineering components. Theoretical approaches describing the interaction of electric fields with simple geometries cannot be directly applied to parts with intricate internal features. There is a need for analytical frameworks capable of predicting field concentration effects in such regions to avoid local overheating and degradation of mechanical properties. Although several mathematical models have been developed for nitriding processes, their validation under practical technological conditions, particularly for surfaces with complex internal recesses, is limited. This gap restricts their application in optimizing real-world processes.

The relevance of this research lies in addressing these gaps by developing an analytical and numerical framework to describe electric field concentration phenomena in internal local recesses during glow discharge nitriding. Solving this problem is essential for ensuring the uniformity and quality of surface modification in metallic components with complex geometries. The outcomes of this study can significantly contribute to advancing nitriding technologies and improving the functional performance and durability of engineering parts in various industries.

Objectives of the Study

The objectives of this study are as follows:

1. To develop an analytical model describing the interaction between the electric field and internal local recesses on metallic surfaces during glow discharge nitriding. The model should account for the geometrical features of surface recesses and enable the determination of electric field concentration in areas with complex configurations.

2. To conduct numerical simulations and analyze the impact of the size and shape of internal local recesses on the distribution of current density and electric field concentration, aiming to optimize nitriding process parameters and ensure uniform surface modification.

Purpose of work

Development of analytical foundations of the interaction of the electric field with internal local surface recesses.

Research results and discussion

The most general variant was chosen as a model – an internal local notch of a wedge-shaped shape (Fig. 1). The dimensions of the wedge-shaped groove, especially the width at the entrance, are comparable to the width of the cathode drop region (CDR). Depending on this ratio, the CDR inside the groove can partially or even completely (in the direction of the groove depth) overlap each other. Let us introduce the concepts of zones of complete (A), partial (B) overlap and the zone of ordinary discharge (C). The nature of the overlap, as will be shown below, plays a significant role in determining the trajectory of the electrons that have flown from the surface, since in zones A and B they are under the force influence of two fields from the two walls of the groove at the same time. Moving in the gap between these walls under the influence of a spatial system of forces, electrons can cross the line of symmetry of the groove, i.e. the trajectory of their movement corresponds to a certain extent to oscillatory motion, which significantly increases the length of the path that the electron will travel compared to the movement along the normal to the surface in the CDR of a conventional discharge. Accordingly, the probability of ionization processes increases, which in turn leads to a local increase in the discharge current.

It is obvious that the ratio of the lengths of the overlap zones varies significantly depending on the comparison of the groove width with the CDR width δ. The critical limit is the ratio of the equality of half the groove width b and the CDR width, at which the entire internal space of the groove is a zone of complete overlap.

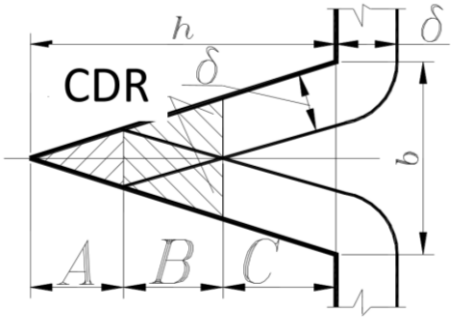

Fig. 1. Scheme of internal local surface recess (A - zone of complete discharge overlap, B - partial, C - ordinary discharge)

When moving to a rectangular groove or hole, the features of the CDR overlap should be taken into account, as well as the known fact of a discharge with a hollow cathode. That is, the field distribution to a depth of no more than double the width of the groove or two diameters of the hole has been experimentally established.

The design scheme of the internal local surface recess in the form of a wedge-shaped groove is shown in Fig. 2.

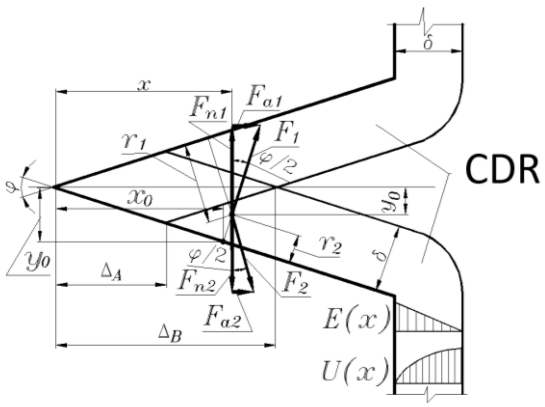

Fig. 2. Calculation diagram of the internal wedge-shaped groove

Groove size ratio (Fig. 1):

$$b/2h = tg\ \phi/2 \text{ from where } \quad \phi = 2arctg\ b/2h\,.$$

Changing the width of the upper edge of the groove: $y = x \cdot tg\ \phi/2$,

And the lower one: $y = x \cdot (-tg\ \phi/2) = x \cdot tg(-\phi/2)$.

In zones of complete or partial overlap of fields, an electron that has flown from any point on the face (for example, from the bottom) and whose initial coordinates are x0, y0, can be simultaneously affected by three electric fields: transverse from two faces E1 and E2 and longitudinal Ea. Taking into account the adopted linear law of distribution of transverse field intensity E(x) and the parabolic law of change of voltage drop in CDR – U(x), the field intensity values are:

$$E_1 = \frac{2U_K}{\delta}\left(1 - \frac{r_1}{\delta}\right), \tag{1}$$

$$E_2 = \frac{2U_K}{\delta}\left(1 - \frac{r_2}{\delta}\right), \tag{2}$$

$$E_a = \frac{2U_K}{\Delta_B}\left(1 - \frac{x}{\Delta_B}\right). \tag{3}$$

where UK is the cathode voltage drop; δ is the CDR width; r1, r2 are the current distances from the electron to the groove faces; ΔB is the distance from the groove top to the boundary of the partial overlap region:

$$\Delta_B = \frac{\delta}{\sin\left(arc\ tg(b/2h)\right)}\ .$$

Current distances of the electron to the faces:

$$r_1 = \frac{0{,}5bx + hy}{\sqrt{\frac{b^2}{4} + h^2}}\ , \quad r_2 = \frac{-0{,}5bx + hy}{\sqrt{\frac{b^2}{4} + h^2}}\ .$$

Longitudinal force acting on an electron:

$$F_a = q_e E_a\,,$$

where qe is the charge of the electron.

The resulting force acting on the electron in the transverse direction is:

$$F_n = F_{n1} - F_{n2} = F_1 \cos\frac{\phi}{2} - F_2 \cos\frac{\phi}{2} = q_e \cdot \cos\frac{\phi}{2}\left(\frac{2U_K}{\delta}\left(\frac{r_2}{\delta} - \frac{r_1}{\delta}\right)\right). \tag{4}$$

Resultant force in the longitudinal direction:

$$F_a = F_{a1} + F_{a2} + q_e E_a = F_{n1} \sin\frac{\varphi}{2} + F_{n2} \sin\frac{\varphi}{2} + q_e \frac{2U_K}{\Delta_B}\left(1 - \frac{x}{\Delta_B}\right). \tag{5}$$

The sum of the projections of all forces acting in the horizontal direction:

$$F_a = F_{a1} + F_{a2} + q_e E_a = F_{n1} \sin\frac{\varphi}{2} + F_{n2} \sin\frac{\varphi}{2} + q_e \frac{2U_k}{\Delta_B}\left(1 - \frac{x}{\Delta_B}\right). \tag{6}$$

The sum of the projections of all forces onto the horizontal axis:

$$\sum X_i = m_e \frac{d^2x}{dt^2} = F_a\,. \tag{7}$$

The sum of the projections of all forces onto the vertical axis:

$$\sum Y_i = m_e \frac{d^2 y}{dt^2} = F_n . \tag{8}$$

Integrating twice, we obtain for the horizontal axis:

$$\frac{d^2 x}{dt^2} = \frac{F_a}{m_e}; \qquad \frac{dx}{dt} = \frac{F_a}{m_e} t + C_1; \;\; x = \frac{F_a}{2m_e} t^2 + C_1 t + C_2 . \tag{9}$$

For the vertical axis:

$$\frac{d^2 y}{dt^2} = \frac{F_n}{m_e}; \qquad \frac{dy}{dt} = \frac{F_n}{m_e} t + C_3; \qquad y = \frac{F_n}{2m_e} t^2 + C_3 t + C_4 . \tag{10}$$

The integration constants are determined by taking into account that at t=0,

$$\frac{dx}{dt} = 0; \;\; x = x_0; \; C_2 = x_0; \; C_1 = 0; \; x = \frac{F_a t^2}{2m_e} + x_0 , \tag{11}$$

$$\frac{dy}{dt} = 0; \;\; y = y_0; \; C_4 = y_0; \; C_3 = 0; \; y = \frac{F_n t^2}{2m_e} + y_0 . \tag{12}$$

The field concentration coefficient is defined as the ratio of the total length of electron trajectories within the overlap zone to the total length of electron trajectories on a flat section of the face line, the length of which is $\frac{\delta}{tg(\phi/2)}$.

Considering that

$$t^2 = \frac{1}{\frac{F_a}{2m_e}}(x - x_0) = \frac{1}{\frac{F_n}{2m_e}}(y - y_0), \tag{13}$$

then

$$\frac{2m_e}{F_a}(x - x_0) = \frac{2m_e}{F_n}(y - y_0); \;\; \frac{(x - x_0)}{F_a} = \frac{(y - y_0)}{F_n}; \; \frac{y}{F_n} = \frac{(x - x_0)}{F_a} + \frac{y_0}{F_n} ,$$

where

$$y(x) = \frac{F_n}{F_a}(x - x_0) + y_0 .$$

Thus, the field concentration coefficient for internal local recesses in the form of a wedge-shaped groove:

$$K_E = \frac{1}{\delta} \int_0^{\delta/tg(\varphi/2)} \left(\int_{X_0}^{\Delta_B} \sqrt{1 + \left(\frac{d(y(x))}{dx} \right)^2} \, dx \right) dX . \tag{14}$$

Based on the obtained dependence, a computer program was created to determine the electric field concentration coefficients for local recesses of parts to prevent cases of arc discharge.

Conclusions

1. The study provides a detailed analysis of the influence of internal local recesses on the electric field concentration during glow discharge nitriding of metallic surfaces. The developed analytical model describes the

relationship between the geometry of internal recesses and the parameters of the electric field, enabling the prediction of field concentration effects in zones with complex configurations.

2. Numerical simulations performed within the proposed framework demonstrate how the dimensions and shapes of internal recesses affect current density distribution and electric field intensification. The results confirm that sharp-edged and narrow recesses significantly increase field concentration, potentially leading to localized overheating and non-uniform nitriding layers.

3. The introduced field concentration criterion and the analytical apparatus allow precise calculation of electric field concentration indicators, supporting the optimization of nitriding process parameters for components with complex geometries. This approach can help mitigate adverse effects such as local surface tempering and ensure homogeneous surface modification.

4. The developed methodology can be applied in industrial settings to predict critical areas susceptible to arc discharge and to design technological solutions that minimize these risks. By integrating the proposed analytical tools into process control systems, it is possible to enhance the reproducibility and quality of glow discharge nitriding for metallic parts with internal recesses.

References

1. Pastukh IM External local notches of metal surfaces and their influence on the parameters of the modification regime. Bulletin of TUP: Khmelnytskyi, 2001, No. 3, Part 1, Technical Sciences. P. 43-47.

2. Pastukh IM, Lukyaniuk MV, Kurskaya VO Initial provisions for determining electrical characteristics during nitriding in a glow discharge with non-stationary power supply. Bulletin of Khmelnytskyi National University. Technical Sciences. 2012. No. 1. P. 7-10.

3. Pastukh IM Theory and practice of hydrogen-free nitriding in a glow discharge. Kharkov: National Scientific Center "Kharkov Physical and Technical Institute", 2006. 364 p.

4.*Methodology*and results of the study of physical, mechanical and tribological characteristics of nitrided inner surfaces of long holes / M. Stechyshyn, O. Dykha, N. Stechyshyna, and D. Zdorenko // Problems of Tribology. -2024. – 29, No. 2/112. – P. 23–30.

5. Galdikas, A., Andriūnas, P., Czerwiec, T., Marcos, G., & Moskaliovienė, T. (2025). Modeling of Plasma Nitriding and Thermal Annealing Processes of Austenitic Stainless Steel. Physica B: Condensed Matter, 417487.

6.Hu M.-J., Pan J.-S., Li Y.-J., & Ruan, D. (2000). Mathematical modeling and computer simulation of nitriding. Materials science and technology, 16(5), 547-550.https://doi.org/10.1179/026708300101508054

7.Ratajski, J., & Suszko, T. (2008). Modeling of the nitriding process. Journal of materials processing technology, 195(1-3), 212-217.https://doi.org/10.1016/j.jmatprotec.2007.04.133

8.Ratajski, JZ, & Mydłowska, KA (2024). Mathematical modeling of gas nitriding process of steel using cellular automata. Journal of Achievements of Materials and Manufacturing Engineering, 125(2). https://orcid.org/0000-0001-8552-8266

9.Bożek, B., Sapa, L., Tkacz-Śmiech, K., Danielewski, M., & Rybak, J. (2022). A Mathematical Model and Simulations of Low Temperature Nitriding. CMES-Computer Modeling in Engineering & Sciences, 130(2).

10.Skalski, K., Wróblewski, G., & Piekarski, R. (2025). Modeling of residual stresses in surface layer treated by burnishing and nitriding. WIT Transactions on Engineering Sciences, 25.

Стечишин М.С., Диха О.В., Скиба М.Є., Здоренко Д. В., Люховець В.В. Теоретичні основи азотування у тліючому розряді внутрішніх локальних виїмок металевих поверхонь

Розглянуто типи локальних заглиблень поверхні, проаналізовано їхній вплив на концентрацію електричного поля та його зміну як чинник нерівномірності результатів модифікації. Запроваджено критерій концентрації поля, розв'язано аналітичну задачу щодо взаємозв'язків між геометрією поверхні та параметрами електричного поля. Досліджено вплив розмірів внутрішніх локальних заглиблень на концентрацію електричного поля. Отримані результати можуть бути використані для точного визначення розподілу щільності струму по азотованій поверхні. Розроблений аналітичний апарат може бути застосований для розрахунку показників концентрації електричного поля у тліючому розряді, що використовується для модифікації поверхонь металевих деталей.

Ключові слова: локальні виїмки, азотування, електричне поле, коефіцієнт концентрації поля

ISSN 2079-1372 Problems of Tribology, V. 30, No 3/117-2025, 13-20

Problems of Tribology
Website: http://tribology.khmu.km.ua/index.php/ProbTrib
E-mail: tribosenator@gmail.com

DOI: https://doi.org/10.31891/2079-1372-2025-117-3-13-20

Analysis of frictional stresses and wear in the contact pair of a vehicle current collector

O.S. Kovtun[0000-0002-1430-6479], **K.E. Holenko***[0000-0002-6140-4573], **A.L. Ganzyuk**[0000-0003-3767-9427], **M.O. Dykha**[0000-0003-3020-9625], **V.O. Dytyniuk**[0000-0001-6377-524X]

Khmelnytskyi national University, Ukraine
**E-mail: holenkoke@khmnu.edu.ua*

Received: 09 June 2025: Revised 20 June 2025: Accept: 18 July 2025

Abstract

The article presents the results of numerical modeling of the operation of the trolleybus current collector pair "contact insert - wire" using the Ansys software environment. The distribution of frictional stresses (Frictional Stress) and contact pressures for two types of insert materials is analyzed: electrographite (Electrographite, parallel to plane) and copper-graphite composite Cu–40%C(f) 0.90 laminate. It was established that the real area of the contact spot is smaller than the entire surface of the gutter, which significantly affects the calculated values of the average frictional stresses and, accordingly, the wear forecast. For the electrographite insert, the average value of Frictional Stress was 0.439 MPa, for the copper-graphite insert – 0.599 MPa. The calculations showed that at a mileage of 450 km, the wear of the electrographite insert exceeds the permissible value, while for the copper-graphite one it is 2.1564 mm and is within the normal range. However, due to the higher hardness of the copper-graphite material compared to the copper wire, the wire itself can become the main element of wear, which is undesirable. It was concluded that the optimal option may be to use a material with intermediate hardness, which will provide a balance between the wear resistance of the insert and the preservation of the contact wire resource.

Keywords: contact insert, contact wire, wear resistance, frictional stress, numerical modeling, Ansys, copper–graphite composite, electrographite

Introduction

The reliability and durability of trolleybus current collection systems are largely determined by the wear resistance of the friction pair “contact insert – contact wire”. Under conditions of prolonged operational load, changes occur in the geometry of the insert surface, which leads to deterioration of electrical contact, increased resistance and increased energy losses. Traditionally, electrographite inserts are used in structures, however, in order to increase the resource, composite materials, in particular copper-graphite, are increasingly used. To optimize the choice of material, it is necessary to model the stress-strain state and analyze friction parameters in conditions close to real ones. Numerical modeling in the Ansys environment allows you to determine the stress distribution, the area of the real contact spot and predict the amount of wear based on the tribological characteristics of materials. The relevance of the study is due to the need to increase the resource of contact inserts while maintaining the operational reliability of the contact wire, which directly affects the economic efficiency of urban electric transport.

Literature review

The dynamics of research indicates a transition from empirical and bench-top approaches to combined methods, where numerical modeling is combined with experiment and data-driven resource prediction. In the work [1], a physically based model of slider wear is proposed, which takes into account the triboelectric interaction and the features of the “slider–contact wire”; the work emphasizes the different role of the hardness of the wire and the insert and the sensitivity of the model to the contact load and current regime, which directly correlates with your calculations of the average friction stresses and the width of the real contact patch. In parallel, the emphasis

is increasing on the conditionally unsteady dynamics of the "pantograph–contact network" system, where fast interaction models show that the instability of the contact force leads to anomalous wear of both the insert and the wire; this emphasizes the importance of correctly setting the contact boundary conditions in numerical schemes, including the localization of the real contact patch. The influence of the environment and humidity on the conductive friction in carbon-copper pairs has been shown [2] in experimental studies: the water content in the carbon slider changes the friction coefficient, mass loss, contact resistance and arcing parameters, i.e. factors that in the practice of urban electric transport significantly affect the real intensity of wear and require scenario modeling. Materials science approaches [3] emphasize the microstructural parameters of composites: varying the graphite fraction and the orientation of its domains in copper-graphite composites allows you to control the current carrying capacity, flow stability and wear rate; non-monotonic dependences with wear minima have been established for a certain orientation of graphite plates and graphite content, which is consistent with the idea of selecting an "intermediate hardness" for the balance of the insert and wire resource. A separate line of work [4-7] is devoted to the force factor: increasing the normal load on the copper-graphite pair changes not only the friction level, but also the damage mechanisms (delamination, arc erosion), forming different wear transition modes; this is important for your scenarios of pressure changes from 0 to 0.5 MPa and extrapolation of wear to runs. At the level of system operational reliability, the application of AI methods for pantograph condition prediction is demonstrated [5]: building models based on neural networks allows for reducing failures through timely detection of degradation trends, which complements FEM-assessments of local stresses and wear with strategic condition-based maintenance tools. In [6], a study of tribocouples based on copper-graphite composites systematically shows the dependence of current-carrying triboproperties and wear mechanisms on contact load, highlighting the need to simultaneously limit slider wear and protect the wire - a key dilemma addressed in this study. Taken together, the results of [7] outline a framework for the approach: taking into account the real contact strip in the problem statement, parametric analysis of Frictional Stress taking into account load and current,and the selection of composites with a target microstructure/hardness as a means of balancing the life of the insert–wire pair.

Purpose of the work

To determine the influence of the area of the actual contact spot and the physical and mechanical properties of the insert material on the stress-strain state and predicted wear of the trolleybus insert-wire pair using numerical modeling in the Ansys environment in order to optimize the choice of material to increase the resource of the current collection system.

Research objectives

1. Develop a numerical model of the local contact of the "insert – wire" pair of a trolleybus, taking into account the actual area of the contact spot.
2. Calculate the distribution of friction stresses and contact pressures for electrographite and copper-graphite insert materials.
3. Determine the dependence of the predicted insert wear value on the average values of Frictional Stress and material hardness.
4. Compare the results obtained for different insert materials and evaluate their impact on the contact wire resource.
5. Formulate recommendations for selecting an insert material that provides a balance between insert wear resistance and maintaining wire durability.

Initial data for analysis

The boundary conditions of the first iteration of the contact modeling of the current-collecting contact pair of a trolleybus "insert – wire" in Ansys were based on the entire surface of the insert groove (Fig. 1).

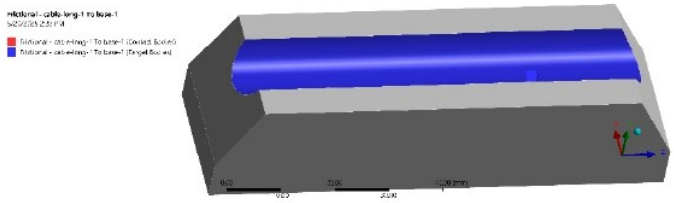

Fig. 1. Friction surface of trolleybus insert

This approach is correct and completely sufficient for determining the maximum pressure Pressure, von Misses Stress or friction (Frictional Stress), etc. However, based on the contact status map (Contact Tool > Status), it is clear that only the central dark yellow part of the trough participates in sliding (Fig. 2).

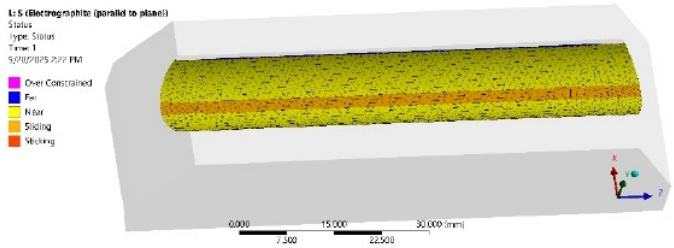

Fig. 2 Actual contact area of the insert with the wire

Since to calculate wear it is necessary to operate with the average Frictional Stress indicator, which is calculated by the integral method (depends on the number of measurement points), and therefore depends on the contact area, the boundary conditions were updated - a surface was distinguished on the surface of the gutter, the width of which corresponds to the sliding spot (Fig. 3).

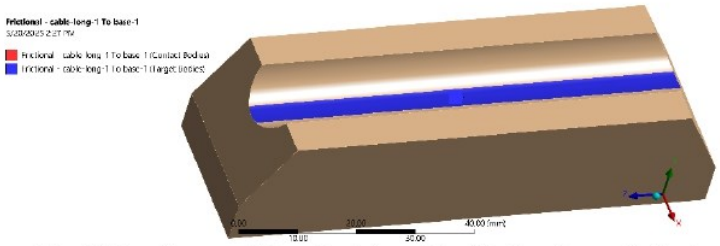

Fig. 3. Boundary conditions for determining friction stresses in the insert

Calculation results for Electrographite insert (parallel to plane)

Based on a comparison of the results of determining Frictional Stress for an insert with Electrographite (parallel to plane), we will illustrate the changes.

Full surface of the insert groove.

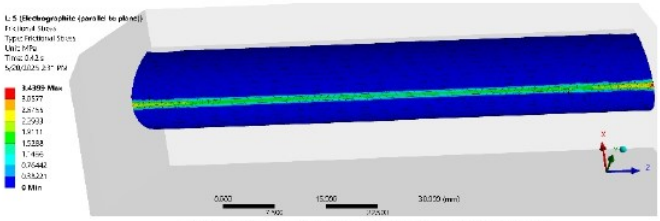

Fig. 4. Full surface of the insert groove

Full surface of the electrographite insert groove used in the numerical simulation. The geometry of the contact surface is modeled in its entirety, which makes it possible to determine the overall distribution of mechanical and frictional stresses before refining the analysis to the actual contact area.
The average value of Frictional Stress is 0.13901 MPa (Fig. 5).

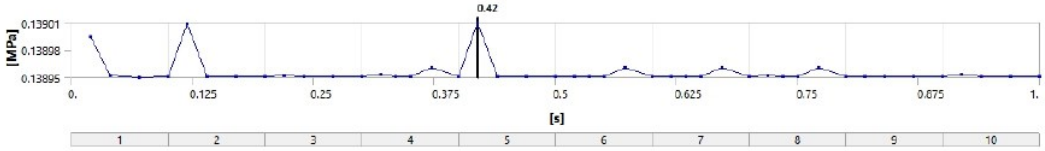

Fig. 5. Distribution of friction stresses over the entire surface of the insert

Distribution of frictional stresses (Frictional Stress) over the full surface of the electrographite insert groove obtained from numerical simulation. The highest values are concentrated in the central contact zone, indicating non-uniform loading and identifying local areas of potentially intensive wear, while the peripheral regions are characterized by significantly lower stresses.

The central part of the insert surface is highlighted: the maximum value of Frictional Stress is 3.3364 MPa (Fig. 6).

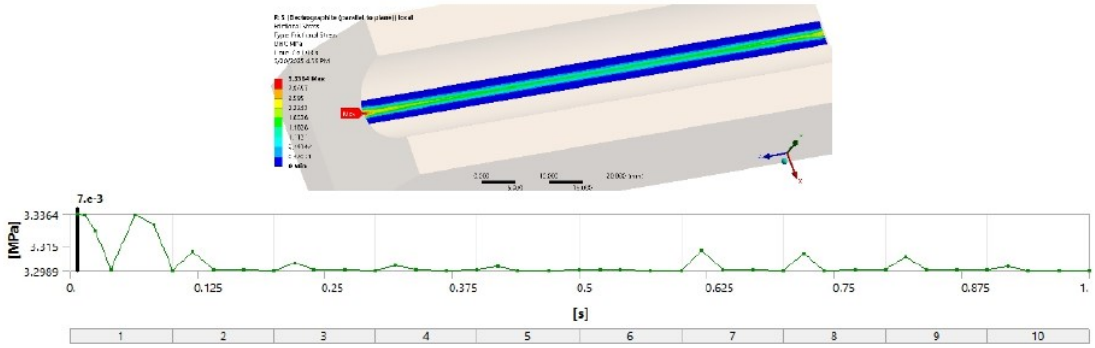

Fig. 6. Isolated part of the insert surface for friction stresses

Isolated central area of the electrographite insert surface for frictional stress analysis. The highest stress concentrations are observed within this zone, reflecting the actual contact patch during operation and indicating regions with the greatest potential wear intensity.

The average value of Frictional Stress is 0.439 MPa (Fig. 7).

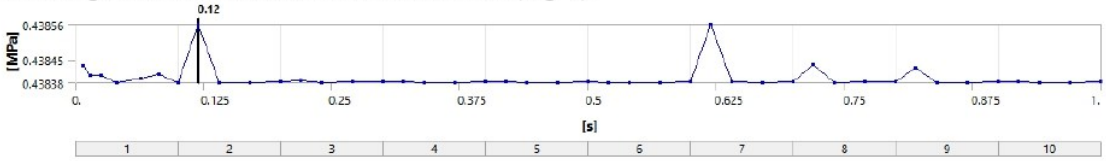

Fig. 7. Distribution of average stresses

Gap map (Fig. 8).

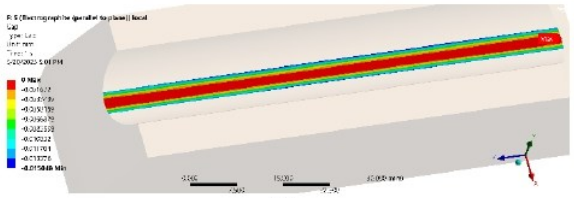

P

Fig. 8. Contact gap map

Contact gap map - visualization of the distribution of the clearance (gap) in the contact zone between the insert and the wire. The color gradient indicates areas of minimal and maximal separation, which directly characterizes the quality of the contact and the potential stability of current transfer.

Calculation results for insert with Cu-40%C(f) 0.90 laminate

To process this calculation case, it became necessary to reduce the size of the finite elements of the mesh and increase its density: the size of the finite elements of the wire bodies and the insert was set to 1 mm; the size in the contact area was 0.5 mm.

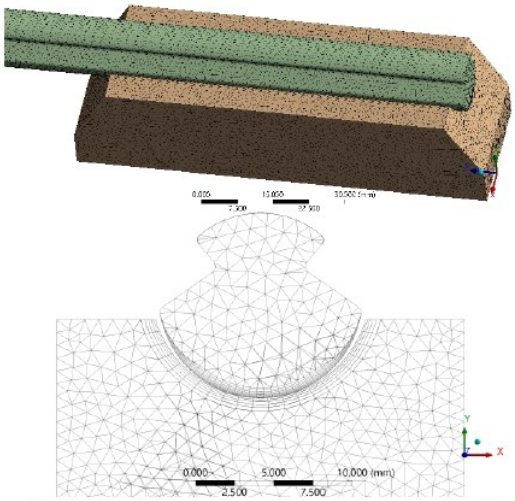

Fig. 9. Finite element mesh breakdown for Cu-C material.

The total number of elements is 1040866, and the number of nodes is 1900220.

The reason for this detailing is the higher hardness of the Cu-40%C(f) 0.90 laminate insert material and the correspondingly narrower contact spot compared to Electrographite (parallel to plane), which requires a smaller size of the end elements:

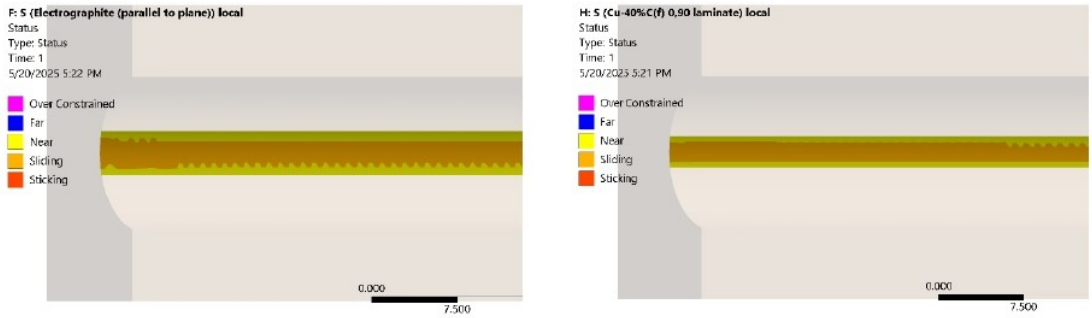

Fig. 10. Comparison of contact spots for electrographite material and copper-graphite material

The maximum value of Frictional Stress is 4.4242 MPa for the isolated central part of the insert surface (Fig. 11).

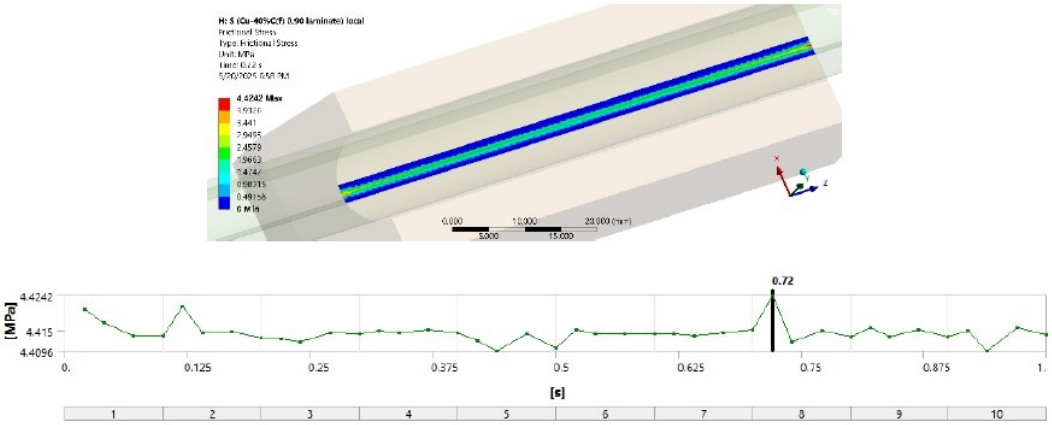

Fig. 11. Friction stress distribution for copper-graphite material

The average value of Frictional Stress is 0.599 MPa (Fig. 12).

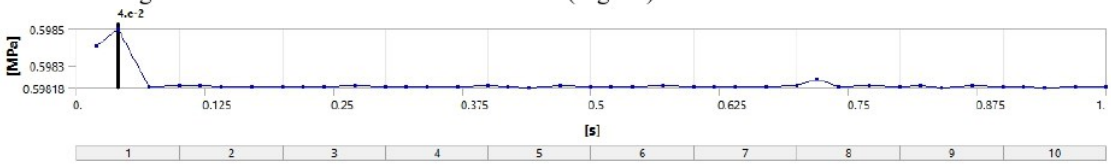

Fig. 12 Distribution of average friction stresses for copper-graphite material.

Distribution of average frictional stresses (Frictional Stress) for the copper–graphite insert obtained from numerical simulation. Elevated stress values are concentrated in the central contact zone, corresponding to the actual contact patch, while peripheral regions exhibit significantly lower stresses, indicating a non-uniform load distribution.

The Gap map is characterized by a decrease in the gap values for a given material (Fig. 13).

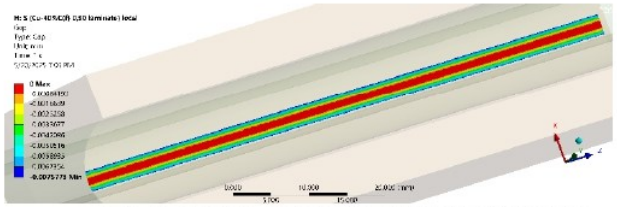

Fig. 13. Clearance map for copper-graphite insert

Calculation of insert wear

Common parameters:
- $\eta = 1 \cdot 10^{-5}$(local efficiency coefficient of energy conversion into wear)
- 1 HV ≈ 9.807 × 10⁶ Pa (Hardness – Vickers)
- $s_{total} = 0.2$m (path traveled by the insert)

Electrographite insert (parallel to plane)

Considering that the Vickers hardness (Hardness – Vickers) = 4.28 – 4.72 HV, the average hardness$H = 4.5 \cdot 9.807 \cdot 10^6 = 4.41 \cdot 10^7$Pa or 44.1 MPa.

If the average value of Frictional Stress is MPa, then the amount of wear will be:$\tau_{avg} = 0.439$

$$d = \frac{\eta \cdot \tau_{avg} \cdot s_{total}}{H} = \frac{1 \cdot 10^{-5} \cdot 0.439 \cdot 10^6 \cdot 0.2}{4.41 \cdot 10^7} \approx 1.99 \cdot 10^{-5}\text{mm}$$

Total wear per 100 km or 500 thousand cycles (100,000 m / 0.2 m = 500,000 cycles): mm$1.99 \cdot 10^{-5} \cdot 500000 = 9.95$

This means that over 450 km, the wear will be:$9.95 \cdot 4.5 = 44.775$mm, which exceeds the permissible limits. Let us recall that the requirements for the VKT insert state: "the warranty period of operation of the inserts is not less than 450 km in dry weather in the absence of eccentric displacement of the wires at the joints. The depth of the maximum wear of the inserts is 10 mm." It should be noted that the parameter was measured under the condition of applying the maximum permissible pressure of the insert on the wire, equal to 0.5 MPa. In real conditions of trolleybus movement, the pressure value will fluctuate in the range of 0–0.5 MPa. Taking into account the linear dependence of the value on the applied pressure (the graph for the full surface of the insert trough below), it is easy to model the approximate amount of wear, for example: under the condition of applying a pressure of 0.25 MPa, the value will be reduced by 2 times. In addition, the contact patch on the surface of the gutter also migrates during the movement of the trolleybus (turns, inclines, etc.), which distributes wear over a larger surface, reducing local wear.$\tau_{avg}\tau_{avg}d$

The approximate wear value is approximate, since the value of the coefficient can change as the insert pressure changes on the wire, and therefore change the nature of the contact. For example, the graph of the average values of Contact > Status (model with a full surface of the insert groove) is not linear.dη

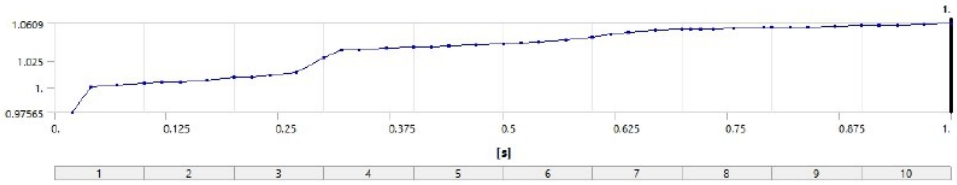

Fig. 14. Dependence for wear for full contact of the insert and wire

Conclusions on Electrographite (parallel to plane): provided the pressure of the insert on the wire is reduced and the real laboratory value of the coefficient is included in the calculation, it can theoretically be applied in inserts.η

Insert with Cu–40%C(f) laminate

Since the hardness is 120 - 135 HV, the average value$H = 127.5 \cdot 9.807 \cdot 10^6 = 1.25 \cdot 10^9$Pa or 1250 MPa. Assuming an average value of Frictional Stress$\tau_{avg} = 0.599$ MPa, the wear value will be:

$$d = \frac{\eta \cdot \tau_{avg} \cdot s_{total}}{H} = \frac{1 \cdot 10^{-5} \cdot 0.599 \cdot 10^6 \cdot 0.2}{1.25 \cdot 10^9} \approx 9.58 \cdot 10^{-7}\text{mm}$$

Total wear per 100 km or 500 thousand cycles: $9.58 \cdot 10^{-7} \cdot 500000 = 0.4792$mm

Over 450 km, the wear will be 2.1564 mm, which is quite within the normal range, but the hardness value of the wire materialCooper C10100(electrolytic tough-pitch hc copper) is lower than the composite insert material: Hardness - Vickers 80 - 115 HV. Thus, the wire will wear out first, which is not recommended.

It should be noted that the value did not change dramatically when going from Electrographite (parallel to plane) to Cu–40%C(f) laminate. In this case, it can be assumed that an intermediate hardness material will provide a value in the range between the measured 0.439 and 0.599 MPa.$\tau_{avg}\tau_{avg}$

Conclusions

The numerical simulation made it possible to specify the parameters of the local contact in the pair "insert - wire" of the trolleybus and to assess the influence of the area of the actual contact spot on the magnitude of the average friction stresses and the wear forecast. It was established that the use of electrographite inserts provides a lower level of wear of the contact wire, but their own resource under intensive operating conditions is limited. Copper-graphite inserts demonstrate higher wear resistance, but increase the risk of intensive wear of the copper wire due to a significant difference in hardness. To achieve optimal operational characteristics, it is advisable to select a material with intermediate hardness, which will balance the wear resistance of the insert and the durability of the contact wire. The results obtained can be used in the development of new insert materials and optimization of the designs of current collection systems of urban electric transport.

References

1. Dong, Y., Li, B., Chen, Z., Wang, H., & Zhang, H. (2025). A Study on the Pantograph Slide Wear Model Based on Energy Dissipation. Applied Sciences, 15(12), 6748. https://doi.org/10.3390/app15126748

2. Pan, L., Xu, Y., Liu, Z., Xiao, C., & Lei, J. (2024). A Fast Simulation Model of Pantograph–Stitched-Catenary Interaction in Long-Distance Travel. Applied Sciences, 14(22), 10160.https://doi.org/10.3390/app142210160

3. Wang, H., Gao, G., Deng, L., Li, X., Wang, X., Wang, Q., & Wu, G. (2023). Study on Current-Carrying Tribological Characteristics of C-Cu Sliding Electric Contacts under Different Water Content. Coatings, 13(1), 42.https://doi.org/10.3390/coatings13010042

4. Yang, Z., Li, W., Song, Y., Zheng, X., & Zhang, Y. (2025). The Influence of Graphite Orientation on the Current-Carrying Friction Performance of Copper–Graphite Composite Materials. Lubricants, 13(6), 238.https://doi.org/10.3390/lubricants13060238

5. Wang, N., Wang, C., Xu, W., Cheng, W., Wu, H., & Li, H. (2025). Friction and Wear Performances and Mechanisms of Graphite/Copper Composites Under Electrical Contact in Marine Environments. Materials, 18(7), 1516.https://doi.org/10.3390/ma18071516

6. Wang, N., Wang, C., Xu, W., Cheng, W., Wu, H., & Li, H. (2025). Friction and Wear Performances and Mechanisms of Graphite/Copper Composites Under Electrical Contact in Marine Environments. Materials, 18(7), 1516.https://doi.org/10.3390/ma18071516

7. Yang, Z., Zhao, M., Wang, X., Hu, K., Tian, X., & Zhang, Y. (2025). Effect of Normal Load on the Current-Carrying Friction Performance of Copper–10% Graphite Composites. Coatings, 15(6), 714.https://doi.org/10.3390/coatings15060714

Ковтун О.С., Голенко К.Е., Ганзюк А.Л., Диха М.О., Дитинюк В.О. Аналіз напружень тертя та зносу у контактній парі струмознімача транспортного засобу

У статті наведено результати чисельного моделювання роботи струмознімальної пари тролейбуса «контактна вставка – дріт» з використанням програмного середовища Ansys. Проаналізовано розподіл напружень тертя (Frictional Stress) та контактних тисків для двох типів матеріалів вставок: електрографітового (Electrographite, parallel to plane) та мідно-графітового композиту Cu–40%C(f) 0,90 laminate. Встановлено, що реальна площа плями контакту є меншою за всю поверхню жолоба, що суттєво впливає на розрахункові значення середніх напружень тертя та, відповідно, на прогноз зносу. Для електрографітової вставки середнє значення Frictional Stress становило 0.439 МПа, для мідно-графітової – 0.599 МПа. Проведені розрахунки показали, що при пробігу 450 км знос електрографітової вставки перевищує допустиме значення, тоді як для мідно-графітової він становить 2.1564 мм і знаходиться в межах норми. Проте через вищу твердість мідно-графітового матеріалу порівняно з мідним дротом основним елементом зносу може стати саме дріт, що є небажаним. Зроблено висновок, що оптимальним може бути використання матеріалу з проміжною твердістю, який забезпечить баланс між зносостійкістю вставки та збереженням ресурсу контактного дроту.

Ключьові слова: контактна вставка, контактний дріт, зносостійкість, напруження тертя, чисельне моделювання, Ansys, мідно-графітовий композит, електрографіт

ISSN 2079-1372 Problems of Tribology, V. 30, No 3/117-2025, 21-29

Problems of Tribology
Website: http://tribology.khnu.km.ua/index.php/ProbTrib
E-mail: tribosenator@gmail.com

DOI: https://doi.org/10.31891/2079-1372-2025-117-3-21-29

Research on the influence of rolling element geometry on the wear resistance of drilling equipment bearings

O. Makovkin[1]0000-0003-4487-7448, **O. Dykha**[1]*0000-0003-3020-9625, **I. Valchuk**[1],

T. Kalaczynski[2]0000-0001-7621-4505

[1]*Khmelnytskyi national University, Ukraine*
[2]*Politechnika Bydgoska im. Jana i Jędrzeja Śniadeckich, Poland*
**E-mail: tribosenator@gmail.com*

Received: 15 June 2025: Revised 20 July 2025: Accept: 20 July 2025

Abstract

The article presents the results of experimental studies of the influence of the geometric parameters of rollers and raceways on the resistance of roller bearings to rolling element rotation and jamming. Failure of bearing assemblies due to roller rotation is a common cause of emergency equipment shutdown, which is accompanied by expensive repairs. The aim of the work was to determine the optimal ratio of roller length to its diameter (l/d) and the influence of raceway diameter (D) on critical wear, which leads to loss of roller stability. The research methodology was based on mathematical experimental design with variation of parameters l, d and D in laboratory conditions when simulating misalignment of the bearing assembly. An empirical relationship was established that quantitatively describes the relationship between roller geometry, raceway diameter and critical wear. The results showed that increasing l/d increases the resistance of the rollers to turning, while an excessive increase in D contributes to the growth of backlash and distortions. The most effective configuration was found to be the one with the maximum length and minimum diameter of the roller at a small value of D. The results obtained can be used for the design improvement of bearing assemblies, in particular in drilling equipment, in order to increase the resource and reliability of their operation.

Keywords: roller bearings, rolling elements, wear resistance, drilling equipment, geometry optimization, roller skew, critical wear

Introduction

Roller bearings are an integral part of many mechanisms and machines, in particular in heavy machinery, metallurgy, automotive and drilling equipment. One of the common problems in their operation is the seizure of the bearing, which often causes the failure of the entire assembly. One of the critical scenarios is the reversal of the rolling elements, which is accompanied by a complete stop of the moving elements of the bearing. As a result, there is intensive wear of the raceways, the appearance of chips, cracks and even destruction of the working elements that are in contact with the rolling element.

Fig. 1 Appearance of worn rollers of the bearing assembly after operation

Particularly dangerous are cases when fragments of the bearing remain inside the mechanism. This can lead to secondary damage: damage to gears, shaft jamming, failure of gearboxes, the need to completely stop the equipment for dismantling.

During the operation of roller bearings, the main supporting element: the large-diameter rollers, bears the greatest load. This is especially true for bearings operating under high pressure or shock loads.

The main reason for the failure of a bearing assembly is the gradual wear of the rolling elements and raceways. As it is used: the diameter of the rollers decreases due to micro-cutting or fatigue fracture; the raceways (inner and outer) lose their geometric accuracy and hardness; the total weakening of the contact between the elements leads to an increase in the gaps. The critical point is when the free space in the assembly becomes sufficient for the rollers to turn under the influence of frictional forces and vibrations. This leads to jamming, temperature increase, loss of lubrication and subsequent destruction of the assembly.

When the wear level in a bearing assembly reaches a critical level, there is a risk of the rolling elements turning, which in turn can cause sudden jamming. This leads to an emergency stop of the equipment, breakage of structural elements and expensive repairs. Despite a large number of studies, there is still no consensus on the determining factor that most affects the bearing life. Various authors give preference to: the influence of dynamic loads, temperature conditions, fit stiffness, surface microgeometry, methods of thermal and chemical-thermal treatment of raceways.

This indicates the complexity of the task and the multifactorial nature of wear, which requires a comprehensive approach to improving the design and manufacturing technology of bearings. Based on studies of the kinematics of rolling element motion, the rotation of rollers in a bearing assembly a phenomenon that precedes jamming and complete failure of the assembly can be caused by a complex of factors. The main ones are:

1. Uneven load distributionon the rolling element along the length of the running track. This may be the result of misalignment, manufacturing inaccuracy or deformation of the housing.

2. Increase in the inter-roller clearance, which occurs due to wear of the rolling elements along the diameter. After the roller leaves the loaded zone, the clearance increases, which creates conditions for destabilization of its orientation.

3. Wear on the ends of the rollers and the sides of the running tracks, which weakens the guiding function of the structure.

4. Difference in angular velocities (or other moving part) and individual rollers. With significant wear or misalignment of the roller, the ends of the rollers may be subject to pinching, especially in the unloaded area.

5. Degradation of raceway geometry due to fatigue or abrasive wear. This leads to loss of stability of the rolling element trajectory.

These factors do not act in isolation; the mutual amplification of the negative impact leads to an avalanche-like deterioration of the unit's performance: first, micro-slippage occurs, then oscillations and reversals of the rollers, and ultimately complete destruction.

In general, failure of the friction unit in a roller bearing is caused by the total wear of the friction pair of rolling elements (rollers) and raceways. When, as a result of operational wear, a sufficient gap, i.e. free space in the contact, appears, the roller loses stability and can turn under the influence of forces arising between it and the sides of the track. This becomes the initial stage of jamming.

Prevent the rollers from turningpossibly in several ways, covering both constructive and tribological solutions:

1. Minimizing wear and tear by: optimizing load and speed modes; selecting appropriate materials and heat treatment; using wear-resistant coatings; improving the lubrication system.

2. Bearing geometry optimization, in particular the ratio of the roller length to its diameter. Proper design of the shape of the rolling elements and raceways contributes to better roller stability in contact.

All these measures are interrelated and effective only in combination with compliance with technological tolerances, manufacturing accuracy, high-quality assembly, and proper operating conditions.

Both tribological and design support for reliable operation of roller bearings are urgent tasks of modern mechanical engineering. Within the framework of this work, the main attention is paid to the design aspect, which consists in choosing the optimal geometric parameters of rolling elements.

Review and analysis of literary sources

The problem of increasing the wear resistance and durability of roller bearings is the subject of numerous studies. The scientific literature considers a wide variety of aspects: from the influence of operating conditions, friction materials and type of lubricant, to the design features of bearings and surface hardening methods.

In [1], it is shown that the service life of the roller bit mainly depends on the bearing. In order to find out the cause and mechanism of bearing failure, the mechanics and microstructure of the failed roller bit bearings are analyzed. The results show that the bearing failure mainly includes wear (including adhesive and abrasive wear), plastic deformation, cracks, fractures and burns. The main causes of these failures are: abrasive substances and temperature rise caused by chips and lubrication failure; stress concentration, shock and vibration due to uneven loading and fit clearance; and initial cracks or defects due to unqualified surface treatment.

References [2-4] provide an overview of bearing materials, bearing ratings, and studies of failed bearings. Rolling bearings are designed for rolling contact rather than sliding contact; friction effects, although low, are not negligible, and lubrication is important. The papers list typical characteristics and causes of several types of failure, describing wear failure, fretting failure, corrosion failure, plastic flow failure, rolling fatigue failure, and damage failure. The effect of roller profile was analyzed in [5[to determine the actual load-life relationship for modified roller profiles. For rollers without crowns (linear contact), the load-life degree is p = 4, which is consistent with the Lundberg-Palmgren value, but crowning reduces the degree p.

In [6], a multi-objective optimization method was proposed to improve the fatigue, wear, and thermal failure performance of roller bearings. The objective functions considered are: dynamic capacity (Cd), which is related to fatigue life, elastohydrodynamic minimum film thickness (hmin), which is related to wear life, and maximum bearing temperature (Tmax), which is related to lubricant life. This paper presents a nonlinear constrained optimization problem with three objectives with eleven design variables and twenty-eight constraints. These objectives were optimized separately (i.e., single-objective optimization) and simultaneously (i.e., multi-objective optimization) using a multi-objective evolutionary procedure called elitist non-dominated sorting genetic algorithm. In [7] it is stated that the optimization of the internal geometry of rolling bearings for specific applications is still a subject of research. Furthermore, in recent years, new rolling bearings have been developed based on existing geometries, which are still being developed. Many recent studies have focused on optimizing the contact between the roller end and the raceway rib surface. In contrast, this work focuses on the development of a new type of rolling bearing based on the existing CRO, but where the rib contact is no longer required. First of all, the geometric parameters defining the internal geometry of rolling bearings, more precisely the contact between the roller and the raceways, were investigated. In addition, several patents defining new rolling bearing geometries were analyzed. Thus, optimization of the geometric parameters of the rollers is one of the key areas for increasing the reliability of bearing assemblies operating under high loads and complex kinematic regimes. The authors note that as the length of the roller increases relative to the diameter, its diagonal also increases. Accordingly, in order for the roller to turn, significantly more wear of the end surfaces of the roller and the sides of the running track is required. This complicates the conditions for the occurrence of the rolling element turn and increases the stability of the bearing assembly.

Optimal l/d ratio of roller in cone bits.In the design of large-diameter three-cone drill bits, roller supports (bearings) are traditionally used instead of plain bearings. The domestic standard recommended taking the ratio of the length of the roller to its diameter (l/d) at approximately 1.5–2 (about 1.7–2.0). For American drill bits, it is characteristic to use even more “elongated” rollers - with a ratio of l/d even higher than 2, which approaches the area of needle bearings. In particular, needle bearings are roller bearings in which the length of the rollers exceeds the diameter by at least three times (l/d = 3…10). Thus, in American designs, the rollers of the bearings are often longer and thinner than was accepted according to Soviet standards.

Justification of the increased l/d ratio. The main reason for increasing l/d of rollers is to increase load capacity and wear resistance. A longer roller with the same diameter has a larger contact area with the raceways, which allows the load to be distributed over a larger surface. US engineers, seeking to increase the service life, made the rollers more elongated in order to place more rolling elements of smaller diameter in one row. This allows to reduce contact stresses and better withstand high radial loads.

In addition, modern designs use special measures to ensure the reliable operation of thin long rollers. For example, most modern cylindrical roller bearings have barrel-shaped (convex) rollers to prevent load concentration at the edges and premature failure from misalignment. The convex profile compensates for bending and small misalignments of the roller under load, distributing the stress more evenly along its length. Such solutions allow the use of increased l/d without a catastrophic increase in contact wear.

Limitations and disadvantages of overextended rollers. Despite the above advantages, an excessive increase in l/d can also have negative consequences. Long and thin rollers are more sensitive to manufacturing inaccuracies, deformations and misalignments. With a large l/d ratio, even a small angular misalignment of the roller in the bearing causes misalignment and uneven contact: the load is concentrated on the edges of the roller, which causes intense wear, heating and the risk of chipping of the tracks. Thus, excessively “needle” rollers can work worse without special design measures. It has also been observed that needle bearings are less suitable for high rotational speeds - their long thin rollers cause more friction and an increase in temperature, limiting the maximum speed. Standard needle bearings also have a limited permissible concentricity.

It is because of these factors that Soviet standards limited l/d to ≈1.5–2 as a compromise between engine life and bearing reliability. American manufacturers, while introducing higher ratios, simultaneously improved the design of the bearing assembly – they used sealing and continuous lubrication, precision tolerances, convex rollers, and even combined bearing schemes. Such engineering solutions allow for increased rigidity and uniformity of support operation even with longer rollers. A number of scientific and technical studies were aimed at determining the optimal l/d ratio. In particular, in tests with the participation of Ukrainian specialists, the geometry of the rollers was varied in laboratory conditions (diameter ~10–15 mm, different track lengths ~8–30 mm) at a load of 2000–3000 N and rotation ~150 rpm. The results showed that the optimal l/d ratio is about 1.0–1.5, i.e. somewhat less than that provided for by the standards (~1.7–2). The researchers note that at l/d≈1.0–1.5 the best balance between low contact stresses and resistance to roller misalignment is ensured. Further increase in the roller length beyond the optimum does not give a significant gain in load capacity, but leads to increased friction and the risk of

overheating/wearing of the roller edges. Thus, too high an l/d parameter can even reduce the bearing life if it is not structurally compensated.

Traditional standards were drawn up with a certain margin and allowed l/d≈2 precisely to maximize the load capacity. However, modern analysis shows that slightly smaller values contribute to greater reliability. American manufacturers, having experimentally increased l/d, were faced with the need to solve the problems of overheating of bearings. Therefore, in the designs of leading companies (Smith, Hughes/Baker, etc.) sealed bearing units with forced lubrication, heat-resistant materials and profiled rollers were introduced in order to realize the advantages of large l/d without premature failure of the unit. The recommended ratio of roller length to diameter in cone bits (≈1.5–2) has historically been chosen as a compromise between increasing the bearing load capacity and maintaining its reliability. Increasing l/d above 2 (practice in some Western designs) allows for more thin rollers to be placed and reduces the specific pressure, but requires more advanced implementation - high-precision tolerances, high-quality lubrication and constructive measures against skewing (for example, barrel-shaped rollers). Without these measures, excessively long rollers can overheat from friction and fail faster. Experimental data confirm that the optimum l/d lies within ~1.2±0.3, at which the bearing serves the longest. Thus, it was not for nothing that Soviet standards limited l/d to ~2: this value is close to the upper limit of the rational range. American engineers, going beyond this limit, gained a gain in load capacity at the cost of complicating the design of the bearing assembly. From the point of view of modern science, further increase in l/d gives decreasing returns and requires compensation for negative effects, while moderate l/d ≈1.3–1.5 seems to be the most balanced for roller bearings of tapered drill bits.

Research objective and problem statement

As noted earlier, the main causes of roller rotation in a bearing assembly are wear of the rolling elements and misalignment of the roller, which occurs due to uneven load distribution and increased axial/radial backlash due to degradation of the contact surfaces. In this regard, an urgent scientific and applied problem is to determine the critical conditions under which the roller turns, which leads to jamming of the assembly and failure of the assembly. The purpose of this workthere are:

1. Establishing the optimal ratio of the roller length to its diameter (l/d), which ensures resistance to turning under the influence of operational loads.
2. Detecting the effect of the diameter of the treadmills (D)on the probability of rolling body reversal.
3. Construction of a mathematical model that will allow quantitatively assessing the limit values of wear that lead to loss of roller stability and jamming of the assembly.

The research aims to establish a mathematical relationship between the total wear of the contact pair (roller - running track), the roller geometry (l/d), and the design parameters of the assembly, in particular the running track diameter (D). The resulting model will allow predicting the durability of the roller bearing based on its geometric parameters, initial tolerances, and wear intensity.

Experimental research methodology

During rotation, the bearing roller is constantly pressed against the peripheral shoulder of the outer ring, which leads to one-sided wear, the appearance of local gaps and a gradual increase in backlash in the support assembly. This phenomenon is the main cause of the rotation of the rollers and, as a result, misalignment, which only increases with operation. To simulate the real operating conditions of the bearing assembly in a laboratory environment, in particular to simulate the misalignment of the inner ring relative to the outer ring, an artificial angle α = 1…2° was set during the study. This allowed for a sufficiently accurate simulation of the geometric destabilization of the assembly, which occurs as a result of operational wear and causes the rollers to turn.

Fig. 2a and 2b present a general diagram of a laboratory setup for tribological research of friction pairs, which was used to study the influence of skew and load on the resistance of a roller to turning.

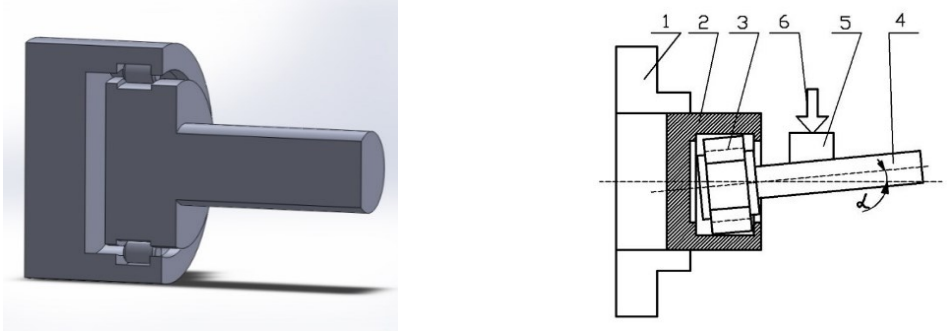

a b

Fig. 2. Scheme of tribological studies of friction pairs

As part of the study, the criterion for evaluating the results was the moment of the roller's turning, which occurred as a result of operational wear of the contact pair. The experiment was considered completed at the moment of fixing the roller's turning, after which precise measurements of the wear of the rolling elements and contact surfaces of the running tracks were carried out.

To identify the influence of design parameters on the development of wear and reversal, the mathematical design of experiments was used, which allowed to reduce the number of tests and at the same time provide statistically significant results.

Based on the preliminary analysis, an experimental plan was drawn up (Table 1) with variations in the main geometric parameters:

- roller diameter d = 10…20 mm;
- roller length l = 10…30 mm, which allows us to investigate the influence of the l/d ratio in the range from 1.0 to 3.0;
- treadmill diameter D = 100 and 200 mm— two levels of modeling of nodes with different dimensional bases.

Each combination of parameters was considered under constant conditions of load (2000…3000 N), rotation frequency (150 rpm), lubricant and ambient temperature. The experiment was carried out with fixing the time to the roller reversal and the wear values after stopping the test.

Table 1

Mathematical plan

Experiment No.	Factors			Roller length, l, mm	Roller diameter, d, mm	Diameter of the outer running track, D, mm
	A	B	C			
1	-1	-1	-1	10	10	100
2	1	-1	-1	30	10	100
3	-1	1	-1	10	20	100
4	1	1	-1	30	20	100
5	-1	-1	1	10	10	200
6	1	-1	1	30	10	200
7	-1	1	1	10	20	200
8	1	1	1	30	20	200

Research results and their discussion

To ensure the reliability of the results and the statistical stability of the estimates, each experimental point was carried out three times. Based on the results of the three repeated tests, the average value of the assessment criterion was determined - that is, the average moment of the roller's turn or the average amount of wear.

The results obtained were analyzed using mathematical statistics methods, after which generalized graphical relationships were constructed, reflecting the influence of the studied factors on the roller's resistance to turning.

In Fig. 3 presents a typical dependence of the critical wear value on the geometric parameters of the roller (l/d) and the diameter of the running track (D). The graph allows you to visually assess the influence of the main design parameters on the performance of the roller support and outline the areas of greatest sensitivity to wear.

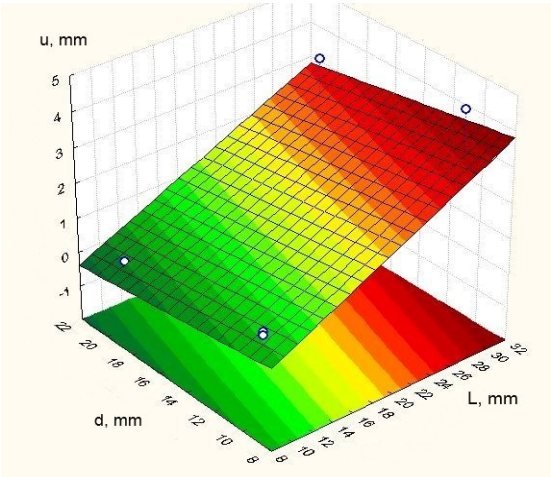

Fig. 3. Dependence of the critical value of roller wear, which leads to its reversal, on the geometric parameters: roller length l and its diameter d at variable values of the running track diameter D.

The color scale shows the zones of permissible (green), limiting (yellow) and emergency (red) wear. The graph shows that with the same roller diameter, increasing its length (i.e. increasing l/d) significantly reduces the

probability of turning - the area of permissible wear increases. Increasing the diameter of the running track D also has a positive effect on the resistance of the assembly to jamming.

Comparison with previous studies

The obtained experimental results are in good agreement with the conclusions of previous authors [1, 5, 6], who indicated the importance of the structural ratio l/d (length to roller diameter) as one of the key factors determining the resistance of the roller bearing to jamming.

The authors [1] theoretically substantiated, that increasing the length of the roller at a constant diameter reduces the probability of turning, since this requires more wear of the end surfaces and shoulders of the running track. It was also noted in [6] that American bits use an increased l/d value, which contributes to durability, although there was no quantitative justification for this choice.

Within the framework of this work, this assumption has been confirmed experimentally.The constructed dependence surface (Fig. 3) clearly demonstrates that:

- with increasing l/d ratio, critical wear, which leads to roller reversal, increases;
- The larger diameter of the raceway D also has a positive effect on the stability of the bearing assembly, reducing the likelihood of misalignment and backlash.

Thus, the previously put forward hypotheses have been experimentally confirmed, and the ranges of parameters that ensure optimal operation of the roller support have been quantitatively specified. This has important practical significance for the constructive improvement of the bits, increasing their resource and reducing the accident rate during deep drilling.

Mathematical dependence of critical roller wear

Based on the results of experimental studies, an empirical dependence of the critical value of linear wear of the roller, at which its reversal in the bearing assembly occurs, was established. The dependence takes into account the influence of the main geometric parameters - the roller length l, the diameter d and the diameter of the outer raceway D:

$$I=0.29\cdot l-0.093\cdot d-0.001\cdot l\cdot d-0.0009\cdot D\cdot l+0.0003\cdot D\cdot d-0.54 \quad (1)$$

where: I is the wear value at which the roller turned, mm;

l is the roller length, mm;

d is the roller diameter, mm;

D is the diameter of the outer running track, mm.

Analysis of the results shows that the greatest influence on the occurrence of a U-turn is the length of the roller. This is clearly visible both in the results of the experimental processing and in the coefficients of equation (1), where:

- the effect of the roller length is 0.29·l,
- influence of roller diameter — 0.093·d

That is, with increasing roller length l, the critical wear that is allowed to occur before the moment of turning increases much faster than with a change in diameter d. This statement is also illustrated graphically in Fig. 3, which shows the dependence of the wear value on l and d. The graph shows that increasing roller length significantly increases the bearing's resistance to turning, in contrast to diameter, the influence of which is less pronounced.

Assessment of the accuracy of the model and the influence of the l/d ratio on the resource of the unit. Comparison of the calculated and experimental data showed that the discrepancy between the results obtained using the proposed mathematical model (1) and the actual test results does not exceed 30%. This indicates sufficient accuracy of the model for practical application at the stage of engineering design.

The analysis of the experimental relationships shown in Fig. 3 indicates a clear trend: the greater the ratio of the roller length to its diameter (l/d), the higher the motor resource of the unit, i.e., the greater the amount of permissible wear until the moment of the roller turning. This allows us to conclude that increasing l/d is an effective design measure to preventjamming of roller bearings.

It should be noted that at large values of l/d = 2…3, in the course of the experiment, in some cases, the critical wear value was recorded at the level of 6…8.5 mm by the moment of the roller turning. This indicates the high stability of rollers with large l/d and the potential for a significant increase in the resource of the unit under conditions of rational selection of parameters.

The influence of treadmill geometry on roller stability

During the research, it was found by visual observations that the rollers during operation are inclined to the axis of rotation, and not placed strictly parallel to it. This phenomenon was observed regardless of the loading mode and design parameters, and is probably due to the presence of an axial component of the friction force and micro-warping of the supports.

In the scientific literature, the main attention is traditionally paid to the ratio of roller length to its diameter (l/d) as a key factor affecting the stability of the bearing assembly. At the same time, the influence of the geometry of the running tracks, in particular their diameter, is not sufficiently covered.

In this regard, a separate series of experimental studies was conducted aimed at assessing the influence of the diameter of the outer raceway (D) on the moment of roller reversal due to wear of the bearing assembly.

According to the results of the experiment, graphically presented in Fig. 4, it is established that:

- maximum service life of the roller bearingobserved at maximum roller length (30 mm);
- The best result is achieved with a minimum diameter of the treadmill (D = 100 mm).

This indicates that excessive increase in the diameter of the treadmill does not always improve the operating conditions of the roller, as it may reduce the support stiffness or worsen the balance of loads acting on the roller at an angle.

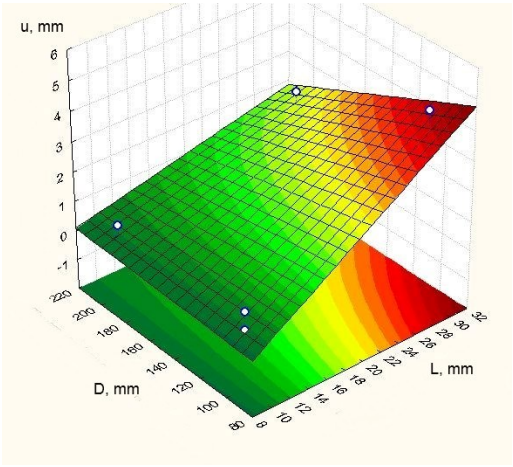

Fig. 4. Dependence of the linear wear value I, mm, on the roller length l, mm, and the outer diameter of the running track D, mm

The graph shows that the lowest wear before the roller turns is observed with a smaller diameter D (100 mm) and a longer roller length (30 mm). This once again confirms the effectiveness of increasing l while maintaining a moderate D as one of the key factors in increasing the wear resistance of the bearing assembly.

The color scale illustrates the wear gradient: the area of lowest values is shown in green, and critical values are shown in red.

The results of the conducted research indicate that to ensure maximum stability of the bearing assembly to the rotation of the rollers, it is advisable to use the minimum possible diameters of the raceways D and rollers of the maximum length l. This configuration reduces backlash, improves the direction of the roller movement and reduces the likelihood of its destabilization under load.

However, the probability of roller reversal increases significantly when large track diameters are used in combination with short rollers. It is with this geometry that the lowest critical wear value was observed before the roller lost stability. The conclusions drawn are fully consistent with the proposed mathematical model (1), which quantitatively reflects the dependence of the critical wear value I on the main geometric parameters of the node (l, d, D) and confirms experimental observations.

Fig. 5 presents the results of experimental studies of the dependence of the linear wear value*I,* mm, from the ratio of the roller diameter d, mm, to the outer diameter of the treadmill D, mm.

The graph illustrates how changing the geometric ratio d/D affects the ultimate wear of the bearing assembly before the moment of the roller turning. The obtained data allow us to draw a conclusion about the nature of the influence of the roller diameter in combination with the dimensions of the running track on the performance of the assembly.

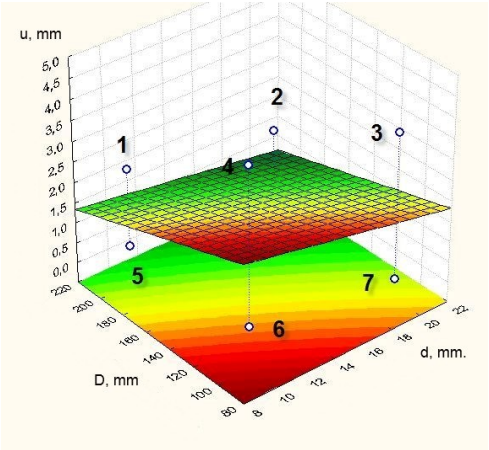

Fig. 5. Dependence of the linear wear value I, mm, on the roller diameter d, mm, and the outer diameter of the running track D, mm.

Based on the obtained experimental data, it was established that the probability of roller reversal is lowest at minimum values of roller diameter d and outer raceway diameter D. Such a geometric configuration provides greater stability of the contact pair and reduces the probability of roller orientation loss during wear.

As can be seen from Fig. 5 (points 1…4), with increasing roller length l, the critical value of linear wear I, at which reversal occurs, increases. This indicates an improvement in the stability of the assembly - the roller maintains the correct position for a longer time even under conditions of intensive wear.

On the other hand, when the roller length is reduced (points 5, 6, 7 in Fig. 5), the turn occurs much earlier - with lower wear values. This indicates a decrease in the resource of the unit due to the instability of short rollers.

The obtained results are consistent with the analytical model (1), which quantitatively takes into account the influence of the geometric parameters of the roller and the running track on critical wear, and once again confirm the feasibility of using long rollers of small diameter at small D to increase the reliability of the bearing assembly.

Table 2

The influence of the geometric parameters of the roller bearing on the wear and probability of the rollers turning

Parameter	Effect on wear	Impact on the probability of reversal	Comment
l	reduces	reduces	Most effectively
d	increases	Increases	Less favorable
D	increases	increases	Increases backlash and distortions

Conclusions

As a result of the research, key geometric factors influencing the occurrence of roller deflection in a bearing assembly have been identified. The ratio of roller length to diameter (l/d) and the diameter of the outer raceway D have the greatest influence.

The most resistant to reversal designs are provided by a combination of a large roller length (l = 30 mm), a small roller diameter (d = 10 mm) and a small running track diameter (D = 100 mm). This configuration provides maximum engine life by reducing backlash and distortion.

It has been experimentally established that with increasing l/d ratio, the probability of roller reversal decreases, and critical wear, which is allowed to lead to loss of stability, decreases. On the contrary, with short rollers (points 5–7 in Fig. 5), reversal occurs much earlier.

The results obtained are fully consistent with theoretical ideas about the nature of wear in rolling pairs, confirm the known provisions regarding the role of l/d, and at the same time expand existing knowledge by taking into account the influence of D, which is insufficiently covered in the scientific literature.

The practical value of the work lies in the possibility of using the results in design and modernization, in particular for selecting the optimal dimensions of the roller bearing, taking into account the maximum wear and service life.

References

1. Huang, Z., Li, G. Failure Analysis of Roller Cone Bit Bearing Based on Mechanics and Microstructure. J Fail. Anal. and Prevent. 18, 342–349 (2018).https://doi.org/10.1007/s11668-018-0419-3

2. Doll, GL (2022). Rolling bearing tribology: tribology and failure modes of rolling element bearings. Elsevier.https://books.google.com/books?hl=uk&lr=&id=w6RXEAAAQBAJ&oi=fnd&pg=PP1&dq=Influence+of+roller+bearing+geometry+on+failure+in+drilling+bits&ots=CrLshsco_E&sig=gIx_DCH1Nvxh952LtQ0R-wJnnVk

3. Widner, RL (2002). Failures of rolling-element bearings. In Failure Analysis and Prevention. ASM International.https://doi.org/10.31399/asm.hb.v11.a0001810

4. Hutchings, FR (2019). A survey of the causes of failure of rolling bearings.

5. Oswald, FB, Zaretsky, EV, & Poplawski, JV (2014). Effect of Roller Geometry on Roller Bearing Load–Life Relation. Tribology Transactions, 57(5), 928–938.https://doi.org/10.1080/10402004.2014.927545

6. Kalyan, M., Tiwari, R. & Ahmad, MS Multi-objective optimization in geometric design of tapered roller bearings based on fatigue, wear and thermal considerations through genetic algorithms. Sādhanā 45, 142 (2020).https://doi.org/10.1007/s12046-020-01385-3

7. Mármol, M. (2022). Development of a new bearing geometry to reduce friction losses. Technische Universität Kaiserslautern.https://kluedo.ub.rptu.de/frontdoor/index/index/docId/6986

Маковкін О.М., Диха О.В., Вальчук І.К., Калачинський Т. Дослідження впливу геометрії тіл кочення на зносостійкість підшипників бурового обладнання

У статті представлено результати експериментальних досліджень впливу геометричних параметрів роликів і бігових доріжок на стійкість роликових підшипників до розвороту тіл кочення та заклинювання. Вихід з ладу підшипникових вузлів унаслідок розвороту роликів є поширеною причиною аварійного зупинення обладнання, що супроводжується дороговартісним ремонтом. Метою роботи було визначення оптимального співвідношення довжини ролика до його діаметра (l/d) та впливу діаметра бігової доріжки (D) на критичне зношування, яке призводить до втрати стабільності ролика. Методика досліджень базувалася на математичному плануванні експерименту з варіацією параметрів l, d та D у лабораторних умовах при моделюванні перекосу підшипникового вузла. Встановлено емпіричну залежність, що кількісно описує взаємозв'язок між геометрією ролика, діаметром бігової доріжки та критичним зношуванням. Результати показали, що збільшення l/d підвищує стійкість роликів до розвороту, тоді як надмірне збільшення D сприяє зростанню люфтів і перекосів. Найбільш ефективною виявилась конфігурація з максимальною довжиною та мінімальним діаметром ролика при малому значенні D. Отримані результати можуть бути використані для конструкторського удосконалення підшипникових вузлів, зокрема в буровому обладнанні, з метою підвищення ресурсу та надійності їх роботи.

Ключові слова: роликові підшипники, тіла кочення, зносостійкість, бурове обладнання, оптимізація геометрії, розворот роликів, критичне зношування

ISSN 2079-1372 Problems of Tribology, V. 30, No 3/117-2025, 30-40

Problems of Tribology
Website: http://tribology.khnu.km.ua/index.php/ProbTrib
E-mail: tribosenator@gmail.com

DOI: https://doi.org/10.31891/2079-1372-2025-117-3-30-40

Analytical study of a hydraulic drive model for a municipal waste container overturning mechanism in a garbage truck considering the wear of friction pairs

O.V. Bereziuk[1*] 0000-0002-2747-2978, **V.I. Savulyak**[1] 0000-0002-4278-5155, **V.O. Kharzhevskyi**[2] 0000-0003-4816-2781, **S.Cv. Ivanov,** [3] 0000-0002-7719-6086**V.Ye. Yavorskyi**[1] 0009-0002-8724-3963

[1] *Vinnytsia National Technical University, Ukraine*
[2] *Khmelnytskyi National University, Ukraine*
[3] *Technical University Sofia, Branch Plovdiv, Bulgaria*
**E-mail: berezyukoleg@i.ua*

Received: 25 June 2025: Revised 28 July 2025: Accept: 05 August 2025

Abstract

The article is dedicated to the analytical study of the improved mathematical model of the hydraulic drive of the mechanism for overturning a container with municipal solid waste into a garbage truck, taking into account the wear of friction pairs. As a result of the analysis of the performed numerical studies of the nonlinear improved mathematical model of the hydraulic drive of the mechanism for overturning a container with municipal solid waste into a garbage truck, taking into account the wear of friction pairs, a linearized version of this model was developed in the form of a system of ordinary linear differential equations of the 2nd order. To carry out design calculations of new garbage truck designs, approximate analytical dependencies were obtained for the pressure in the hydraulic cylinder pressure line, the angular velocity and the angle of container overturning on time were obtained based on the proposed linearized mathematical model of the hydraulic drive of the container overturning mechanism in the technological operation of loading municipal solid waste into the garbage truck during the 1st phase – overturning the container to the equilibrium position, taking into account the wear of friction pairs. A regression equation was obtained, which allows to approximately determine the duration of the 1st phase – the rotation of the container to the equilibrium position during its overturning in the technological operation of loading municipal solid waste into a garbage truck, taking into account the wear of friction pairs, which can be used during design calculations of new garbage truck designs taking into account the wear of working bodies without the need to study the nonlinear mathematical model of the drive, as well as during optimization of the main parameters of the hydraulic drive. It was established that the analytical study of the linearized improved mathematical model of the hydraulic drive of the mechanism for loading municipal solid waste into a garbage truck, taking into account the wear of friction pairs during the 2nd phase – pouring waste from the container into the body of the garbage truck requires further research.

Keywords: linearized mathematical model, consideration of wear, Laplace transformation, hydraulic drive, wear, friction units, container overturning mechanism, garbage truck, solid waste.

Introduction

Among the current tasks facing modern municipal engineering in Ukraine, the improvement of mobile manipulator-type equipment, which includes garbage trucks, is particularly important [1]. In this field, ensuring increased wear resistance, reliability, and durability of machine parts is so important, since these characteristics directly affect the efficiency of equipment operation, reduce repair and maintenance costs, and increase the service life of equipment under conditions of intensive use [2, 3]. In Ukraine, the process of collecting and transporting municipal solid waste (MSW) to places of further processing or disposal is mainly carried out using body garbage trucks. The main working body of such machines is loading mechanisms designed in the form of hydraulically driven manipulators [4]. Currently, there are about 3700 garbage trucks in operation, which not only transport waste but also compact it. This significantly reduces transportation costs and the area of landfills required for waste

disposal, which is important both economically and environmentally. During the technological operation of MSW loading into the body of a garbage truck, friction components, in particular hinge joints and hydraulic cylinders of the manipulator, are subjected to significant loads. The intensive wear of these elements is due to a number of factors: the large weight of waste containers, which can reach 500 kg, the need for mechanisms to operate in reverse mode with reciprocating movements, and the high number of operating cycles performed during a single trip. An additional complicating factor is the operating conditions, which are characterized by significant fluctuations in relative humidity and temperature, as well as an increased level of dust in the environment. The combination of these factors leads to accelerated wear of working elements, which negatively affects the reliability and durability of garbage trucks. Deterioration of the operational characteristics of parts or insufficient lubrication leads to increased friction forces in the manipulator's hinge joints. This, in turn, causes an increase in the level of vibration in the system, which negatively affects its dynamic stability and reduces the mechanism's ability to withstand high loads under conditions of reversible friction. Accelerated wear of friction components not only reduces the efficiency of the garbage truck manipulator, but also creates potential risks for the safe operation of the equipment. This situation can lead to emergency operating modes that threaten the health of operators and can also have a negative impact on the environment in the event of uncontrolled spillage or leakage of solid waste. According to the Resolution No. 265 of the Cabinet of Ministers of Ukraine [5], one of the key areas of development of public utilities is the introduction of modern, highly efficient garbage trucks. Such vehicles are considered a central link in the system of technical means for the collection, transportation, and primary processing of solid waste. The use of the latest models of equipment not only optimizes logistics processes and reduces operating costs, but also contributes to the comprehensive solution of a number of pressing environmental problems related to waste management. In addition, the modernization of the garbage truck fleet ensures an increase in the overall reliability and efficiency of the country's public utilities, which is of strategic importance for the sustainable development of settlements. The planning of the renewal, maintenance, and repair of garbage trucks is facilitated by the determination of approximate analytical dependencies of the main power and kinematic characteristics of the hydraulic drive of the mechanism for overturning containers with solid household waste into a garbage truck, taking into account the wear of friction pair.

Analysis of recent research and publications

In the article [6], a structural analysis of the wear parts of a garbage truck is presented. The authors of the paper [7] proposed a method for diagnosing faults associated with the wear of the hydraulic cylinder seal and internal leaks of the working fluid, based on the fusion of energy characteristics. In the paper [8], a scheme of a robotic manipulator was developed, its 3D geometric model was created using SOLIDWORKS, and the motion analysis was performed. During the design of structural optimization, key parameters such as stress and deformation of the robotic manipulator were analyzed in detail, and objective functions and constraints were established for optimizing and improving its structure. This allows to reduce the failure rate of the manipulator during long-term high-intensity operation and better achieve joint operation with other systems of the garbage truck to increase the overall efficiency of MSW collection and transportation.

In the study [9], a method for optimizing the operation of a robotic cell is presented, which involves changing the position of the robot manipulator within the working area for programs with a fixed trajectory of the endpoint. The main goal was to reduce the total wear of the manipulator joints and prevent their uneven loading, when individual joints are subjected to greater stress compared to others. The assessment of wear was carried out by approximating the integral of the mechanical work of each joint along the entire trajectory, which is determined through angular velocities and applied torques. The proposed approach is based on the usage of dynamic modeling, which allows determining the torques and rotation speeds of the joints in different positions of the robot. The results of the study showed that the optimal location of the manipulator base allows reducing the overall level of wear of its joints by 22-53%, depending on the configuration of the trajectory of movement.

In the article [10], a mathematical model was developed that allows determining the optimal geometric parameters of the manipulator's structural elements, taking into account the maximum boom reach, load capacity and a number of other kinematic characteristics of the machine. Such a model is an important tool for design engineers, since it provides the possibility of rational selection of dimensional parameters of structural elements in order to increase the efficiency of the manipulator and ensure its reliability during operation. At the same time, special attention was paid to the peculiarities of the operation of articulated joints that operate in a cyclic mode, which is typical for manipulator-type machines. It was established that under such conditions, the formation of a complete hydrodynamic friction mode is impossible, since the lubrication process occurs mainly in the semi-dry and boundary friction modes. This leads to increased requirements for the properties of the materials of the parts, the quality of the surface finish and the efficiency of the lubrication system, since it is these factors that determine the wear resistance and durability of articulated joints in real operating conditions. Unlike the steady-state mode of hydrodynamic friction, the operation of sliding bearings in conditions of semi-dry or boundary friction is accompanied by more intense wear of the friction surfaces. This leads to a gradual loss of kinematic accuracy, the appearance of additional dynamic loads, impact loads and vibrations, which, in turn, cause the development of fretting corrosion and premature destruction of parts. To reduce the friction force, it is proposed to use special coatings of the conjugate elements of the manipulator hinges, in particular lead, phosphate and indium. It has been

proven that the intensity of contact wear can be significantly reduced by using lubricants based on oils and fats, as well as greases, which at a temperature of 25 °C acquire a thick, ointment-like consistency. In addition, the feasibility of using phosphate and anodic metal coatings has been determined, which contribute to better retention of lubricants on friction surfaces, increasing their efficiency and durability of components.

In the work [11], a detailed analysis of the main types of wear of hinged joints used in the structures of forest manipulators was carried out. The obtained research results made it possible to determine promising directions for increasing their wear resistance, which can be used by design engineers in order to extend the working life of the mentioned units depending on the specific operating conditions and requirements for the equipment. Particular attention is paid to the fact that manipulator machines mostly operate in difficult climatic conditions with sharp fluctuations in ambient temperature. Such factors significantly affect the stability of the properties of lubricants and the operational characteristics of the structural materials of the hinges, which ultimately causes accelerated wear and a decrease in the durability of the machines. Under conditions of reduced temperatures, the properties of the materials of friction pairs undergo significant changes. In particular, an increase in their fragility, a decrease in the yield point, and an increase in the rigidity of the working surfaces are observed. This leads to a complication of the processes of movement and annihilation of dislocations in the crystal lattice of the material, which is accompanied by the appearance of exoelectronic emission and a significant acceleration of the wear processes of friction surfaces. An additional negative factor is a change in the characteristics of lubricants: at low temperatures they can lose their fluidity, turn into a solid state or significantly increase their viscosity. As a result, the lubricant loses its ability to form a reliable film between the working surfaces, which sharply reduces its protective and antifriction properties and leads to an intensification of wear processes. In the summer, when the ambient temperature reaches high values, intensive heating of lubricants occurs, which leads to a decrease in their viscosity and subsequent spontaneous leakage from the friction zone. This negatively affects the processes of lubrication and cooling of working surfaces, since the ability of the lubricant to form a stable protective film decreases, and the risk of overheating of the contacting elements increases. As a result, wear processes are intensified and the durability of hinged units is reduced. To prevent such undesirable phenomena, it is proposed to use special sealing devices that are capable of simultaneously performing several important functions: to protect the hinged joints of manipulators from the penetration of dust, moisture and aggressive impurities that can cause corrosive destruction of surfaces; to keep the lubricant in the friction zone, preventing its premature leakage. The conducted studies have confirmed the feasibility of integrating contact and labyrinth sealing elements into the design of hinges, which, due to their design specifics, provide more reliable protection of units from the negative effects of the operating environment and increase the service life of manipulators.

In the article [12], the method of synthesis of the trajectory of the manipulation robot movement taking into account its degrees of mobility is considered. It is shown that the bending of the rod causes support reactions in the contact zone, similar to the beam on two supports. Based on the determined contact pressure, it is possible to estimate the potential wear processes of the surfaces of the hydraulic cylinder, rod and stuffing box. It is established that even in the conditions of complete absence of danger of loss of strength by the rod during bending, contact stresses, which reach approximately one third of the material strength limit, can significantly accelerate the wear of friction surfaces. This approach allows to more accurately explain the reasons for the formation of characteristic wear patterns and to determine the features of their identification.

In the paper [13], it is shown that when developing new promising designs of articulated joints, it is necessary to apply a comprehensive approach to the selection of scientific and technical solutions, since their performance is influenced by a significant number of parameters. Such an approach creates opportunities for the formation of new design solutions that can provide increased reliability and durability of articulated joints of manipulators of logging machines. The implementation of such solutions allows to significantly improve both mechanical and tribotechnical characteristics of joints, as well as to optimize the thermal mode of their operation, which is an important factor in increasing the efficiency of equipment operation.

The article [14] presents the results of the analysis of the design features of the grippers of the body garbage trucks and the study of their reliability. Based on the conducted research, a calculation model of the garbage truck was developed, which was considered as an oscillatory system. During the analysis process, the features of the oscillations of the garbage truck frame during operation were established, and the dependencies of the formation of forces in the interaction of the elements of the “grip – tank – gripper” system were also revealed. The research showed that the greatest loads correspond to the traction and rod of the hydraulic cylinder, and these loads increase with increasing of container mass. At the same time, a change in the mass of the garbage truck itself does not affect the magnitude or amplitude of the loads, but leads to a change in their frequency characteristic. During operational observations, it was established that the main cause of garbage truck failures is wear and corrosion of the working surfaces of the equipment parts. In particular, 32% of all failures in the hydraulic drive system occur on hydraulic cylinders. Failures of these units are associated with wear of the working surfaces of the mating parts, deformations of the rod and cylinder under the action of operational loads arising from uneven loading of the body, as well as abrasive wear in difficult operating conditions. The main factor in failures of the hydraulic drive is intensive wear of the working surfaces of key parts of its design, in particular spools and housings of hydraulic distributors, as well as hydraulic cylinder rods. An additional factor of degradation is hydroabrasive damage, which occurs as a result of untimely replacement of the working hydraulic fluid and the use of poor-quality or worn sealing elements, such as hydraulic cylinder seals. This leads to the penetration of dust particles and wear products into the sliding

zone, which significantly accelerates the destruction of the working surfaces. To increase the service life and restore the performance of parts, it is recommended to use the technology of chrome plating in cold self-regulating electrolyte, which ensures the production of chrome coatings with high quality of the deposit, increased wear resistance and sufficient productivity, which makes it one of the most promising methods of restoring worn elements of hydraulic drives.

Analytical study of the mathematical model of grinding of polymer waste in the grinding chamber of a rotary crusher with continuous classification of the finished product, carried out in [15], made it possible to determine with high accuracy the particle sizes of the final product, the crusher productivity, and energy consumption at different values of the rotor angular rotation speed, the initial waste sizes, the crusher design parameters, and the chamber loading modes.

In the article [16], an algorithm for numerical-analytical study of the dynamics of a planar six-bar linkage mechanism of a sewing machine thread take-up mechanism is proposed, which is based on the numerical solution of the differential equation of motion of the mechanism, and computer modeling of this mechanism is also carried out in Mathcad software.

In the paper [17], on the basis of analytical study of a mathematical model, the dependencies of the functioning of vibration and vibro-impact machines based on a hydropulse drive with a single-stage pulsator valve were determined.

In the materials of the article [18], an improved nonlinear mathematical model of the hydraulic drive operation of the mechanism for loading solid waste into a garbage truck during container overturning is proposed, which takes into account the wear of friction pairs and allowed to numerically study the dynamics of this drive during start-up and determine that taking into account the wear of friction pairs significantly affects the main parameters of the hydraulic drive for container overturning during MSW loading into a garbage truck. It was established that the duration of container overturning during MSW loading increases in a power-law dependence with increasing wear of the hydraulic cylinder.

The work [19] is dedicated to the determination of analytical dependencies that describe the quality indicators of transient processes of the hydraulic drive, which ensures the overturning of the container during the MSW loading into the garbage truck. In the article [20], a linearized mathematical model of the hydraulic drive for overturning the container during the technological operation of loading MSW into the garbage truck is proposed and analytically studied. However, this mathematical model does not take into account the wear of friction pairs.

However, in the process of analyzing known publications, authors did not find a linearized improved mathematical model of the hydraulic drive of the mechanism for overturning a MSW container into a garbage truck, taking into account the wear of friction pairs and the results of its analytical study.

Aims of the article

Analytical study of a linearized improved mathematical model of a hydraulic drive for a solid waste container overturning mechanism in garbage truck, taking into account the wear of friction pairs to obtain analytical dependencies of the main power and kinematic characteristics of this hydraulic drive in a steady-state mode of operation, which can be used when conducting design calculations of new garbage truck designs, taking into account the wear of the working bodies.

Methods

During the analytical study of the linearized improved mathematical model of the hydraulic drive of the mechanism for overturning a container with MSW in garbage truck, taking into account the wear of friction pairs, the following methods were used: operator calculus using the Laplace transformation to solve a system of ordinary linear differential equations, linearization of nonlinear dependencies, decomposition of complex expressions into simpler fractions, as well as computer modeling methods. To plot the graphs, the computer program "MatModel" described in [19] was used, which implements the 4th-order Runge-Kutta-Felberg numerical method with a variable integration step.

Results

Fig. 1 shows a calculation diagram of a linearized improved mathematical model of a hydraulic drive for overturning a container during the technological operation of MSW loading into a garbage truck, taking into account the wear of friction pairs when using the rear scheme of MSW loading. The diagram shows the following structural elements: C – container, G – gripper, L – lever, HC – hydraulic cylinder, HD – hydraulic distributor, P – hydraulic pump, SV – safety valve, F – filter, T – tank with working fluid, as well as the main geometric, kinematic and power parameters: p_1, p_2, p_3, p_4 – pressures at the pump outlet, at the hydraulic cylinder inlet, at the hydraulic cylinder outlet and at the filter inlet, respectively; W_1, W_2, W_3, W_4 – volumes of pipelines between the pump and the hydraulic distributor, the hydraulic distributor and the hydraulic cylinder inlet, the hydraulic cylinder outlet and the hydraulic distributor, the hydraulic distributor and the filter; Q_P –actual pump flow rate; S_P – cross-sectional area of the distributor opening; S_f – surface area of the filter element; D, d – piston and rod

diameters; J – moment of inertia of moving elements; G_C –container weight; R – radius of rotation of moving elements; l_P – distance between the centers of rotation of the gripper and the rod; h – the height of the container; α – angle between the axes of the lever and the cylinder arm, γ – angle that takes into account the deviation of the center of mass position; δ – angle between the gripping arm and the horizontal; λ – angle of inclination of the container wall; ψ – the angle between the axis of the cylinder arm and the axis passing between the centers of rotation of the gripper and the hydraulic cylinder; φ – grip rotation angle.

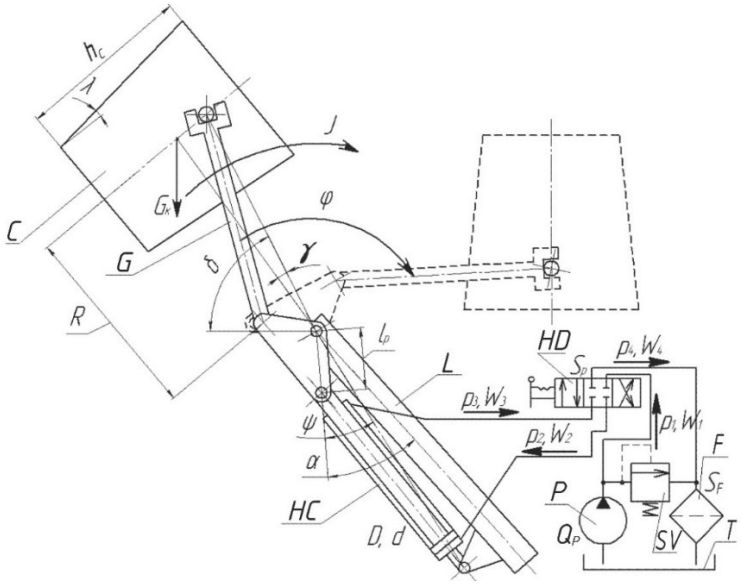

Fig. 1. Calculation scheme of the linearized improved mathematical model of the hydraulic drive for overturning the container during the technological operation of MSW loading, taking into account the wear of friction pairs

Analysis of the conducted studies of the nonlinear mathematical model [18] showed that $p_1 \approx p_2 \approx p_{12}$, and the influence of pressure in the drain lines and viscous friction forces on the operation of the hydraulic drive is insignificant. The process of overturning the container during the technological operation of MSW loading into a garbage truck can be divided into two phases:

1. The phase of overturning the container to the equilibrium position ($\delta+\varphi-\lambda \le \pi/2$).

2. Phase of pouring MSW from the container into the body of the garbage truck ($\delta+\varphi-\lambda > \pi/2$).

Thus, the system of differential equations of the nonlinear mathematical model is transformed into such systems of differential equations that correspond to the phases adopted above. The phase of rotation of the container to the equilibrium position can be described by a system of differential equations:

$$\begin{cases} Q_H = 2\dfrac{d\varphi}{dt} S_{Ц1} l_P \sin(\varphi+\psi) + \sigma_0 p_{12} + \alpha_\sigma\left(1-e^{-\beta_\sigma t}\right) + KW_{12}\dfrac{dp_{12}}{dt}; & (1) \\ p_{12} S_{Ц1} l_P \sin(\varphi+\alpha) = J\dfrac{d^2\varphi}{dt^2} + GR\cos(\varphi+\delta-\gamma), & (2) \end{cases}$$

where $W_{12} = W_1 + W_2$; σ_0 – coefficient of working fluid losses due to flow from the high-pressure region to the low-pressure region, m^5/(N·sec); α_σ, β_σ – coefficients of approximation of the dependence of working fluid losses on the duration of the friction pair wear process ($\alpha_\sigma = 4.054\cdot10^{-4}$; $\beta_\sigma = 128.1$).

In order to linearize the trigonometric functions of the system of differential equations, let's make the following substitutions:

$$\cos(\varphi+\delta-\gamma) \approx \cos(\omega_0 t+\delta-\gamma); \quad (3)$$

$$\sin(\varphi+\alpha) \approx \sin(\overline{\varphi}_1+\alpha); \quad (4)$$

$$\sin(\varphi+\psi) \approx \sin(\overline{\varphi}_1+\psi), \quad (5)$$

$$\omega_0 \approx \frac{Q_P}{2S_{C1}R} = const, \quad (6)$$

where ω_0 – the averaged value of the angular velocity of the container in the 1st approximation, rad/sec; $S_{C1} = \pi(D^2-d^2)/4$ – area of the rod cavity of the hydraulic cylinder, m^2; $\overline{\varphi}_1 = (\pi/2+\lambda-\delta)/2$ – averaged in the first approximation value of the container overturning angle for the first phase, rad.

Therefore, the linearized mathematical model of the hydraulic drive of the first phase of container overturning for the operation of MSW loading into a garbage truck has the following form:

$$\begin{cases} Q_H = 2\omega S_{C1} l_p \sin(\overline{\varphi}_1 + \psi) + \sigma_0 p_{12} + \alpha_\sigma (1 - e^{-\beta_\sigma t}) + KW_{12} \dfrac{dp_{12}}{dt}; & (7) \\ p_{12} S_{C1} l_p \sin(\overline{\varphi}_1 + \alpha) = J \dfrac{d\omega}{dt} + GR\cos(\omega_0 t)\cos(\delta - \gamma) - GR\sin(\omega_0 t)\sin(\delta - \gamma), & (8) \end{cases}$$

where $\omega = \dfrac{d\varphi}{dt} \neq const$ – instantaneous value of the angular velocity of container overturning, rad/sec.

For further study of the linearized mathematical model, we will use the Laplace transformation, according to which we obtain the following:

$$\begin{cases} \dfrac{Q_P}{s} = \Omega(s) 2 S_{C1} l_p \sin(\overline{\varphi}_1 + \psi) + P(s)\sigma_0 + \dfrac{\alpha_\sigma}{s} - \dfrac{\alpha_\sigma}{s + \beta_\sigma} + P(s) s K W_{12}; & (9) \\ P(s) S_{C1} l_p \sin(\overline{\varphi}_1 + \alpha) = \Omega(s) s J + \dfrac{sGR\cos(\delta - \gamma)}{s^2 + \omega_0^2} - \dfrac{\omega_0 GR\sin(\delta - \gamma)}{s^2 + \omega_0^2}. & (10) \end{cases}$$

Substituting equation (10) into equation (9), we obtain:

$$\Omega_1(s) = \frac{-b_4 s^4 + b_3 s^3 + b_2 s^2 + b_1 s + b_0}{s(s + \beta_\sigma)(s^2 + \omega_0^2)(a_2 s^2 + a_1 s + a_0)}, \tag{11}$$

where $a_2 = KW_{12} J$; $a_1 = \sigma_0 J$; $a_0 = 2 S_{C1}^2 l_p^2 \sin(\overline{\varphi}_1 + \alpha)\sin(\overline{\varphi}_1 + \psi)$; $b_4 = KW_{12} GR\cos(\delta - \gamma)$;

$b_3 = Q_P S_{C1} l_p \sin(\overline{\varphi}_1 + \alpha) - (KW_{12}\beta_\sigma + \sigma_0) GR\cos(\delta - \gamma) + KW_{12}\omega_0 GR\sin(\delta - \gamma)$;

$b_2 = (Q_P - \alpha_\sigma)\beta_\sigma S_{C1} l_p \sin(\overline{\varphi}_1 + \alpha) - \beta_\sigma \sigma_0 \omega_0 GR\sin(\delta - \gamma) + (KW_{12}\beta_\sigma + \sigma_0)\omega_0 GR\sin(\delta - \gamma)$;

$b_1 = Q_P \omega_0^2 S_{C1} l_p \sin(\overline{\varphi}_1 + \alpha) + \beta_\sigma \sigma_0 \omega_0 GR\sin(\delta - \gamma)$. $b_0 = (Q_P - \alpha_\sigma)\beta_\sigma \omega_0^2 S_{C1} l_p \sin(\overline{\varphi}_1 + \alpha)$ (12)

By the method of decomposing expression (11) into simpler fractions after reduction to the canonical form, we obtain

$$\begin{aligned} \Omega_1(s) = {} & A_1 \frac{1}{s} + F_1 \frac{1}{s + \beta_\sigma} + B_1 \frac{s}{s^2 + \omega_0^2} + \frac{D_1}{a_2} \frac{s + a_1/(2a_2)}{[s + a_1/(2a_2)]^2 + (4a_0 a_2 - a_1^2)/(4a_2^2)} + \\ & + \frac{C_1}{\omega_0} \frac{\omega_0}{s^2 + \omega_0^2} + \frac{4E_1 - D_1 a_1}{2\sqrt{4a_0 a_2 - a_1^2}} \frac{\sqrt{4a_0 a_2 - a_1^2}/(2a_2)}{[s + a_1/(2a_2)]^2 + (4a_0 a_2 - a_1^2)/(4a_2^2)}, \end{aligned} \tag{13}$$

where $A_1 = \dfrac{b_0}{\beta_\sigma a_0 \omega_0^2}$; $E_1 = -b_4 - (A_1 + B_1)a_1 + F_1(\beta_\sigma a_2 - a_1) - C_1 a_2$; $D_1 = -a_2(A_1 + F_1 + B_1)$;

$C_1 = \dfrac{J_1 - A_1 a_0 \omega_0^2 (a_0 + \beta_\sigma a_1 - a_2 \omega_0^2)}{G_1 \beta_\sigma} - F_1 \dfrac{\omega_0^2 (\beta_\sigma^2 a_1 a_2 - \beta_\sigma a_1^2 + a_0 a_1 + \beta_\sigma a_0 - \beta_\sigma a_2 \omega_0^2)}{G_1}$;

$B_1 = -\dfrac{b_1}{\beta_\sigma a_1 \omega_0^2} + A_1 \dfrac{a_0}{\beta_\sigma a_1} + C_1 \dfrac{a_0 - \omega_0^2 a_2}{\omega_0^2 a_1} + F_1 \dfrac{\beta_\sigma a_2}{a_1} - \dfrac{b_4}{a_1}$; $I_1 = \beta_\sigma a_0^2 - \omega_0^2(\beta_\sigma a_0^2 + a_1^2 - 2\beta_\sigma a_0 a_2)$;

$G_1 = a_1^2 \omega_0^2 + (a_0 - a_2 \omega_0^2)^2$; $H_1 = \beta_\sigma a_0 - \omega_0^2(\beta_\sigma a_2 + a_1)$; $J_1 = \beta_\sigma a_1 \omega_0^2 (b_3 + \beta_\sigma b_4) + (a_0 - a_2 \omega_0^2)(b_1 + \beta_\sigma \omega_0^2 b_4)$

$F_1 = \dfrac{I_1 J_1 - A_1 a_0 \omega_0^2 \{I_1(a_0 + \beta_\sigma a_1 - a_2 \omega_0^2) + G_1[\beta_\sigma(a_0 + \beta_\sigma a_1) - \omega_0^2(a_1 + \beta_\sigma a_2)]\} - \ldots \rightarrow}{\beta_\sigma \omega_0^2 \{H_1 G_1 \beta_\sigma a_2 - I_1[\beta_\sigma(\beta_\sigma a_1 a_2 - a_1^2 + a_0 - a_2 \omega_0^2) + a_0 a_1]\}}$ (14)

$\ldots \rightarrow \dfrac{- G_1 \{\beta_\sigma \omega_0^2 [a_1 b_2 - \beta_\sigma b_4 (a_0 - a_2 \omega_0^2)] + H_1 b_1\}}{}$.

Then we can find the original image of (13):

$$\omega_1(t) = A_1 + F_1 e^{-\beta_\sigma t} + B_1 \cos(\omega_0 t) + \frac{C_1}{\omega_0}\sin(\omega_0 t) + \frac{D_1}{a_2} e^{-\frac{a_1}{2a_2}t} \cos\left(\frac{\sqrt{4a_0a_2 - a_1^2}}{2a_2} t\right) + \\ + \frac{4E_1 - D_1a_1}{2\sqrt{4a_0a_2 - a_1^2}} e^{-\frac{a_1}{2a_2}t} \sin\left(\frac{\sqrt{4a_0a_2 - a_1^2}}{2a_2} t\right). \tag{15}$$

Excluding insignificant coefficients in expression (15), which have a higher order of smallness, and taking into account the accepted notations according to (6), (12), (14), the angular velocity of container overturning, taking into account the wear of friction pairs during the first phase, is described by the following equation:

$$\omega_1(t) \approx \frac{Q_н - \alpha_\sigma}{2S_{C1}^2 l_p^2 \sin(\overline{\varphi}_1 + \psi)}\left[1 + \frac{2S_{C1}^2 l_p^2 \sin(\overline{\varphi}_1 + \alpha)\sin(\overline{\varphi}_1 + \psi)}{\beta_\sigma \sigma_0 J}\right] \times \\ \times\left\{1 - e^{-\frac{\sigma_0}{2KW_{12}}t} \cos\left[S_{C1} l_p \sqrt{\frac{2\sin(\overline{\varphi}_1 + \alpha)\sin(\overline{\varphi}_1 + \psi)}{KW_{12}J}} t\right]\right\}. \tag{16}$$

After substituting the substitution $\sin(\overline{\varphi} + \alpha)\sin(\overline{\varphi} + \psi) \approx \sin^2[\overline{\varphi} + (\alpha + \psi)/2]$ into equation (16):

$$\omega_1(t) \approx \frac{Q_н - \alpha_\sigma}{2S_{C1}^2 l_p^2 \sin(\overline{\varphi}_1 + \psi)}\left[1 + \frac{2S_{C1}^2 l_p^2 \sin^2\left(\overline{\varphi}_1 + \frac{\alpha + \psi}{2}\right)}{\beta_\sigma \sigma_0 J}\right]\left\{1 - e^{-\frac{\sigma_0}{2KW_{12}}t} \cos\left[S_{C1} l_p \sin\left(\overline{\varphi}_1 + \frac{\alpha + \psi}{2}\right)\sqrt{\frac{2}{KW_{12}J}} t\right]\right\}. \tag{17}$$

To determine the container overturning angle, taking into account the wear of friction pairs during the first phase, we integrate equation (17) and, taking into account the initial conditions $\varphi(0) = 0$, we obtain the following:

$$\varphi_1(t) = \frac{Q_н - \alpha_\sigma}{2S_{C1}^2 l_p^2 \sin(\overline{\varphi}_1 + \psi)}\left[1 + \frac{2S_{C1}^2 l_p^2 \sin^2\left(\overline{\varphi}_1 + \frac{\alpha + \psi}{2}\right)}{\beta_\sigma \sigma_0 J}\right]\left\langle\left\{\frac{e^{-\frac{\sigma_0}{2KW_{12}}t}}{8KW_{12}S_{C1}^2 l_p^2 \sin^2[\overline{\varphi}_1 + (\alpha + \psi)/2] + J\sigma_0^2} \times\right.\right. \\ \times\left\{2KW_{12}J\sigma_0 \cos\left[S_{Ц1} l_p \sin\left(\overline{\varphi}_1 + \frac{\alpha + \psi}{2}\right)\sqrt{\frac{2}{KW_{12}J}} t\right] - 4K^{1,5}W_{12}^{1,5} S_{C1} l_p \sqrt{2J} \times\right. \\ \left.\left.\times \sin\left(\overline{\varphi}_1 + \frac{\alpha + \psi}{2}\right)\sin\left[S_{C1} l_p \sin\left(\overline{\varphi}_1 + \frac{\alpha + \psi}{2}\right)\sqrt{\frac{2}{KW_{12}J}} t\right]\right\} + t\right\rangle. \tag{18}$$

Excluding insignificant coefficients in expression (18), which have a higher order of smallness, we obtain a simplified equation for the change in the container overturning angle taking into account the wear of friction pairs during the first phase:

$$\varphi_1(t) \approx \frac{Q_н - \alpha_\sigma}{2S_{C1}^2 l_p^2 \sin(\overline{\varphi}_1 + \psi)}\left\{1 + \frac{2S_{C1}^2 l_p^2 \sin^2[\overline{\varphi}_1 + (\alpha + \psi)/2]}{\beta_\sigma \sigma_0 J}\right\} t. \tag{19}$$

From equation (19), we determine the duration of container overturning, taking into account the wear of friction pairs during the first phase:

$$t_1 \approx \frac{2S_{C1}^2 l_p^2 \beta_\sigma \sigma_0 J \sin(\overline{\varphi}_1 + \psi)}{(Q_P - \alpha_\sigma)\{\beta_\sigma \sigma_0 J + 2S_{C1}^2 l_p^2 \sin^2[\overline{\varphi}_1 + (\alpha + \psi)/2]\}} \varphi_1. \tag{20}$$

Solving the system of equations (9, 10) with respect to $P(s)$ after reduction to the canonical form, we obtain:

$$P_1(s) = A_{1p}\frac{1}{s} + I_{1p}\frac{1}{s+\beta_\sigma} + \frac{B_{1p}+J_{1p}-C_{1p}-F_{1p}}{KW_{12}}\frac{1}{s^2+\sigma_0/(KW_{12})} - D_{1p}\frac{s}{s^2+\omega_0^2} - \frac{E_{1p}}{\omega_0}\frac{\omega_0}{s^2+\omega_0^2} -$$
$$- \frac{G_{1p}}{a_2}\frac{s+a_1/(2a_2)}{\left[s+a_1/(2a_2)\right]^2+\left(4a_0a_2-a_1^2\right)/\left(4a_2^2\right)} - \frac{4H_{1p}-G_{1p}a_1}{2\sqrt{4a_0a_2-a_1^2}}\frac{\sqrt{4a_0a_2-a_1^2}/\left(2a_2\right)}{\left[s+a_1/(2a_2)\right]^2+\left(4a_0a_2-a_1^2\right)/\left(4a_2^2\right)}, \quad (21)$$

where $A_{1p} = \left[Q_P - \alpha_\sigma - 2A_1S_{C1}l_p\sin\left(\overline{\varphi}_1+\psi\right)\right]/\sigma_0$; $B_{1p} = -KW_{12}\left[Q_P - \alpha_\sigma - 2A_1S_{C1}l_p\sin\left(\overline{\varphi}_1+\psi\right)\right]/\sigma_0$;

$C_{1p} = -\dfrac{2S_{C1}l_pKW_{12}\left(B_1\sigma_0 - C_1KW_{12}\right)\sin\left(\overline{\varphi}_1+\psi\right)}{\sigma_0^2+K^2W_{12}^2\omega_0^2}$; $D_{1p} = \dfrac{2S_{C1}l_p\left(B_1\sigma_0 - C_1KW_{12}\right)\sin\left(\overline{\varphi}_1+\psi\right)}{\sigma_0^2+K^2W_{12}^2\omega_0^2}$;

$E_{1p} = \dfrac{2S_{C1}l_p\left(B_1KW_{12}\omega_0^2 + C_1\sigma_0\right)\sin\left(\overline{\varphi}_1+\psi\right)}{\sigma_0^2+K^2W_{12}^2\omega_0^2}$; $H_{1p} = \dfrac{2S_{C1}l_p\left(E_1\left(a_1KW_{12}-a_2\right) - D_1a_0KW_{12}\right)\sin\left(\overline{\varphi}_1+\psi\right)}{a_1KW_{12}\sigma_0 - a_2\sigma_0^2 - a_0K^2W_{12}^2}$;

$F_{1p} = \dfrac{2S_{C1}l_pKW_{12}\left(D_1\sigma_0 - E_1KW_{12}\right)\sin\left(\overline{\varphi}_1+\psi\right)}{a_1KW_{12}\sigma_0 - a_2\sigma_0^2 - a_0K^2W_{12}^2}$; $G_{1p} = -\dfrac{2S_{Д1}l_pa_2\left(D_1\sigma_0 - E_1KW_{12}\right)\sin\left(\overline{\varphi}_1+\psi\right)}{a_1KW_{12}\sigma_0 - a_2\sigma_0^2 - a_0K^2W_{12}^2}$;

$I_{1p} = \dfrac{\alpha_\sigma - 2F_1S_{C1}l_p\sin\left(\overline{\varphi}_1+\psi\right)}{\sigma_0 - KW_{12}\beta_\sigma}\cdot$ $J_{1p} = \dfrac{KW_{12}\left[\alpha_\sigma - 2F_1S_{C1}l_p\sin\left(\overline{\varphi}_1+\psi\right)\right]}{KW_{12}\beta_\sigma - \sigma_0}$ (22)

Next, we can find the original image of (21)

$$p_1(t) = A_{1p} + I_{1p}e^{-\beta_\sigma t} + \frac{B_{1p}+J_{1p}-C_{1p}-F_{1p}}{KW_{12}}e^{-\frac{\sigma_0}{KW_{12}}t} - D_{1p}\cos\left(\omega_0 t\right) - \frac{E_{1p}}{\omega_0}\sin\left(\omega_0 t\right) -$$
$$- \frac{G_{1p}}{a_2}e^{-\frac{a_1}{2a_2}t}\cos\left(\frac{\sqrt{4a_0a_2-a_1^2}}{2a_2}t\right) - \frac{4H_{1p}-G_{1p}a_1}{2\sqrt{4a_0a_2-a_1^2}}e^{-\frac{a_1}{2a_2}t}\sin\left(\frac{\sqrt{4a_0a_2-a_1^2}}{2a_2}t\right). \quad (23)$$

Neglecting the insignificant coefficients of equation (23), which have a higher order of smallness, and taking into account the notations according to (6), (12), (14), (22) and the initial conditions $p(0) = 0$, the pressure in the hydraulic cylinder pressure line, taking into account the wear of the friction pairs during the first phase, can be described by the following equation:

$$p_1(t) \approx \frac{\alpha_\sigma}{\sigma_0 - KW_{12}\beta_\sigma}e^{-\beta_\sigma t} + \frac{GR\cos\left(\delta-\gamma\right)}{S_{C1}l_p\sin\left(\overline{\varphi}_1+\alpha\right)} + \frac{Q_P}{S_{C1}l_p\sin\left(\overline{\varphi}_1+\frac{\alpha+\psi}{2}\right)}\sqrt{\frac{J}{2KW_{12}}}e^{-\frac{\sigma_0}{2KW_{12}}t}\sin\left\langle\sqrt{\frac{2}{KW_{12}J}}S_{C1}\times\right.$$
$$\left.\times l_p\sin\left(\overline{\varphi}_1+\frac{\alpha+\psi}{2}\right)t - \arcsin\left\{\left[\frac{\alpha_\sigma}{\sigma_0 - KW_{12}\beta_\sigma} + \frac{GR\cos\left(\delta-\gamma\right)}{S_{C1}l_p\sin\left(\overline{\varphi}_1+\alpha\right)}\right]\frac{S_{C1}l_p\sin\left[\overline{\varphi}_1+\left(\alpha+\psi\right)/2\right]}{Q_P}\sqrt{\frac{2KW_{12}}{J}}\right\}\right\rangle. \quad (24)$$

Comparison of the results obtained using nonlinear and linearized mathematical models of the hydraulic drive for overturning the container during the technological operation of loading MSW into a garbage truck, taking into account the wear in friction pairs, as well as using equations obtained as a result of the analytical solution of the linearized model, is shown in Fig. 2.

When comparing the characteristics of container overturning obtained using a nonlinear mathematical model and equations (16), (19), (24), as a result of analytical solution of the linearized mathematical model of the hydraulic drive for container overturning in the technological operation of MSW loading into a garbage truck, taking into account the wear of friction pairs, the error is about 10% at the beginning of the movement and decreases to 2-5% at the end of the movement compared to the nonlinear mathematical model, which is acceptable for performing preliminary design calculations. If necessary, the values of the main parameters can be specified at the final stage of design using a nonlinear mathematical model.

The obtained regression equation (20) allows to approximately determine the duration of the 1st phase – the rotation of the container to the equilibrium position during the container overturning during the technological operation of MSW loading into a garbage truck, taking into account the wear of friction pairs, which can be used when conducting design calculations of new garbage truck designs, taking into account the wear of working bodies without the need to study the nonlinear mathematical model of the drive, as well as when optimizing the main parameters of the hydraulic drive.

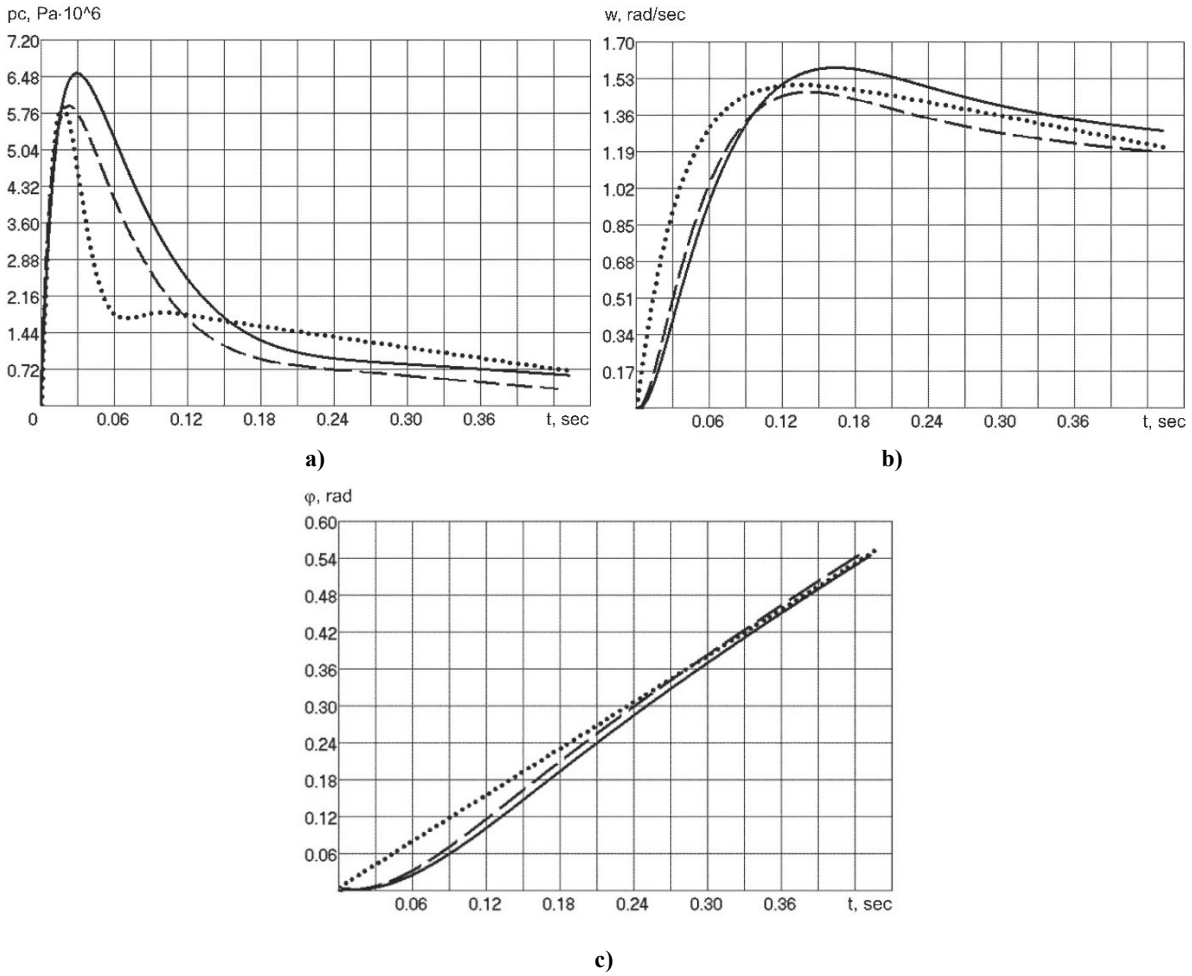

Fig. 2. Comparison of results obtained using nonlinear (——) and linearized (– – –) mathematical models of the hydraulic drive for overturning the container during the technological operation of MSW loading into a garbage truck, taking into account the wear of friction pairs, as well as using the equations obtained as a result of its analytical solution (···): a) –change in pressure in the hydraulic cylinder; b) –change in angular velocity; c) –angle of rotation

Analytical study of the linearized improved mathematical model of the hydraulic drive of the mechanism for MSW loading into a garbage truck, taking into account the wear of friction pairs during the 2nd phase – pouring solid waste from the container into the body of the garbage truck, requires further research.

Conclusions

To carry out design calculations of new garbage truck designs, approximate analytical dependences of the pressure in the hydraulic cylinder pressure line, the angular velocity and the angle of container overturning on time were obtained. It was based on the proposed linearized mathematical model of the hydraulic drive of the container overturning mechanism in the technological operation of loading municipal solid waste into the garbage truck during the 1st phase: overturning the container to the equilibrium position, taking into account the wear of friction pairs. A regression equation was obtained, which allows to approximately determine the duration of the 1st phase – the rotation of the container to the equilibrium position during its overturning during the technological operation of loading of municipal solid waste (MSW) into a garbage truck, taking into account the wear of friction pairs, which can be used during design calculations of new garbage truck designs taking into account the wear of working bodies without the need to study the nonlinear mathematical model of the drive, as well as during optimization of the main parameters of the hydraulic drive. It was established that the analytical study of the linearized improved mathematical model of the hydraulic drive of the mechanism for MSW loading into a garbage truck, taking into account the wear of friction pairs during the 2nd phase – pouring waste from the container into the body of the garbage truck, requires further research.

References

1. Holenko K., Dykha O., Koda E., Kernytskyy I., Horbay O., Royko Y., Fornalchyk Y., Berezovetska O., Rys V., Humenuyk R., Berezovetskyi S., Żółtowski M., Baryłka A., Markiewicz A., Wierzbicki T., Bayat H. (2024) Structure and strength optimization of the Bogdan ERCV27 electric garbage truck spatial frame under static loading. Applied Sciences, 14(23), 11012, https://doi.org/10.3390/app142311012

2. Kindrachuk M.V., Kharchenko V.V., Marchuk V.Y., Humeniuk I.A., Leusenko D.V. (2024) Methodology for Selecting Compatible Metal Materials for Friction Pairs During Fretting-Corrosion Wear. Metallophysics & Advanced Technologies, 46(7), 637-648, https://doi.org/10.15407/mfint.46.07.0637

3. Dykha A., Sorokatyi R., Pasichnyk O., Yaroshenko P., Skrypnyk T. (2020, December) Machine wear calculation module in computer-aided design systems. In IOP Conference Series: Materials Science and Engineering, 1001(1), 012040, https://doi.org/10.1088/1757-899X/1001/1/012040

4. Petrov O., Kozlov L., Lozinskiy D., Piontkevych O. (2019) Improvement of the hydraulic units design based on CFD modeling. Lecture Notes in Mechanical Engineering, 653-660, https://doi.org/10.1007/978-3-030-22365-6_65

5. The Cabinet of Ministers of Ukraine (2004) Resolution No. 265 "Pro zatverdzhennia Prohramy povodzhennia z tverdymy pobutovymy vidkhodamy" ["On Approval of the Program for Solid Waste Management"]. URL: http://zakon1.rada.gov.ua/laws/show/265-2004-%D0%BF.

6. Lazea M., Constantin G.A., Stoica D., Voicu G. (2020) Analiza structurala cu elemente finite a pieselor de uzura de pe placa de contrapresiune a unei autogunoiere. Revista Romana de Materiale, 50(2), 283-293.

7. Qiu Z., Min R., Wang D., Fan S. (2022) Energy features fusion based hydraulic cylinder seal wear and internal leakage fault diagnosis method. Measurement, 195, 111042, https://doi.org/10.1016/j.measurement.2022.111042

8. Li H., Li Y. (2025) Finite element analysis and structural optimization design of multifunctional robotic arm for garbage truck. Frontiers in Mechanical Engineering, 11, 1543967, https://doi.org/10.3389/fmech.2025.1543967

9. Kot T., Bobovský Z., Vysocký A., Krys V., Šafařík J., Ružarovský R. (2021) Method for robot manipulator joint wear reduction by finding the optimal robot placement in a robotic cell. Applied Sciences, 11(12), 5398, https://doi.org/10.3390/app11125398

10. Chernik D.V., Chernik K.N. (2020) Mathematical model of a combined manipulator of a forest machine. In IOP Conference Series: Materials Science and Engineering, 5(919), 052037, https://doi.org/10.1088/1757-899X/919/5/052037

11. Serebryanskii A. (2014) Except the negative reverse effect and automatically compensate for wear in the hinge manipulators. DOAJ – Lund University: Concept: Scientific and Methodological e-magazine, 4 (Collected works, Best Article).

12. Beisembayev A., Yerbossynova A., Pavlenko P., Baibatshayev M. (2023) Planning trajectories of a manipulation robot with a spherical coordinate system for removing oxide film in the production of commercial lead, zinc. Eastern-European Journal of Enterprise Technologies, 124(2), 80, https://doi.org/10.15587/1729-4061.2023.286463

13. Zadorozhnaya E., Levanov I., Kandeva M. (2018, May) Tribological research of biodegradable lubricants for friction units of machines and mechanisms: Current state of research. In International Conference on Industrial Engineering, 939-947, https://doi.org/10.1007/978-3-319-95630-5_98

14. Kargin R.V., Yakovlev I.A., Shemshura E.A. (2017) Modeling of workflow in the grip-container-grip system of body garbage trucks. Procedia Engineering, 206, 1535-1539, https://doi.org/10.1016/j.proeng.2017.10.727

15. Skyba M.E., Misyats O.V., Polishchuk A.O., Misyats V.P., Rubanka M.M. (2021) Systema adaptyvnoho chastotnoho keruvannia shvydkistiu obertannia asynkhronnoho tryfaznoho elektrodvyhuna pryvodu rotornoi drobarky [Adaptive frequency control system for the rotation speed of an asynchronous three-phase electric motor of a rotary crusher drive]. Herald of Khmelnytskyi National University. Technical sciences, 2(295), 139-146, https://doi.org/10.31891/2307-5732-2021-295-2-139-146

16. Manoilenko O., Dvorzhak V., Horobets V., Panasiuk I., Bezuhlyi D. (2024) Assessing the impact of sewing machine thread take-up mechanism parameters on the magnitude and nature of thread take-up. Eastern European Journal of Enterprise Technologies, 2024, 6(1(132)), 64-75, https://doi.org/10.15587/1729-4061.2024.315129

17. Iskovich-Lototsky R., Kots I., Ivanchuk Y., Ivashko Y., Gromaszek K., Mussabekova A., Kalimoldayev M. (2019). Terms of the stability for the control valve of the hydraulic impulse drive of vibrating and vibro-impact machines. Przeglad Elektrotechniczny, 4(19), 19-23, https://doi.org/10.15199/48.2019.04.04

18. Berezyuk O.V., Yavorskyi V.Ye. (2025) Udoskonalena matematychna model roboty hidropryvodu mekhanizmu zavantazhennia tverdykh pobutovykh vidkhodiv u smittievoz iz urakhuvanniam znosu par tertia [Improved mathematical model of the hydraulic drive of the mechanism for loading solid household waste into a garbage truck taking into account the wear of friction pairs]. Scientific Works of Vinnytsia National Technical University, 1, 154-164, https://doi.org/10.31649/2307-5376-2025-1-154-164

19. Bereziuk O., Petrov O., Lemeshev M., Slabkyi A., Sukhorukov S. (2023) Transient Processes Quality Indicators of the Rotation Lever Hydraulic Drive for the Dust-Cart Manipulator. Lecture Notes in Mechanical Engineering, 2, 3-12, https://doi.org/10.1007/978-3-031-32774-2_1

20. Berezyuk O., Savulyak V. (2017) Approximated mathematical model of hydraulic drive of container upturning during loading of solid domestic wastes into a dustcart. Technical Sciences, 20(3), 259-273, https://doi.org/10.31648/ts.5426

Березюк О.В., Савуляк В.І., Харжевський В.О., Іванов С.Ц., Яворський В.Є. Аналітичне дослідження моделі гідроприводу механізму перевертання контейнера з побутовими відходами у сміттєвоз із урахуванням зносу пар тертя.

Стаття присвячена аналітичному дослідженню удосконаленої математичної моделі гідроприводу механізму перевертання контейнера з твердими побутовими відходами у сміттєвоз із урахуванням зносу пар тертя. У результаті аналізу виконаних числових досліджень нелінійної удосконаленої математичної моделі гідроприводу механізму перевертання контейнера з твердими побутовими відходами у сміттєвоз із урахуванням зносу пар тертя, розроблено лінеаризовану версію цієї моделі у формі системи звичайних лінійних диференціальних рівнянь другого порядку. Для проведення проектних розрахунків нових конструкцій сміттєвозів отримано наближені аналітичні залежності тиску в напірній магістралі гідроциліндра, кутової швидкості та кута перевертання контейнера від часу на основі запропонованої лінеаризованої математичної моделі гідроприводу механізму перевертання контейнера на технологічній операції завантаження твердих побутових відходів у сміттєвоз під час 1-ї фази – повороту контейнера до положення рівноваги із урахуванням зносу пар тертя. Одержане рівняння регресії, яке дозволяє наближено визначити тривалість 1-ї фази – повороту контейнера до положення рівноваги під час його перевертання на технологічній операції завантаження твердих побутових відходів у сміттєвоз із урахуванням зносу пар тертя, що може бути використано під час проведення проектних розрахунків нових конструкцій сміттєвозів із урахуванням зносу виконавчих органів без необхідності дослідження нелінійної математичної моделі приводу його робочих органів, а також під час оптимізації основних параметрів гідроприводу. Встановлено, що аналітичне дослідження лінеаризованої удосконаленої математичної моделі гідроприводу механізму завантаження твердих побутових відходів у сміттєвоз із урахуванням зносу пар тертя під час 2-ї фази – висипання відходів із контейнера в кузов сміттєвоза вимагає проведення подальших досліджень.

Ключові слова: лінеаризована математична модель, урахування зносу, перетворення за Лапласом, гідропривод, знос, вузли тертя, механізм перевертання контейнера, сміттєвоз, тверді побутові відходи

ISSN 2079-1372 Problems of Tribology, V. 30, No 3/117-2025, 41-48

Problems of Tribology
Website: http://tribology.khnu.km.ua/index.php/ProbTrib
E-mail: tribosenator@gmail.com

DOI: https://doi.org/10.31891/2079-1372-2025-117-3-41-48

Dynamic processes in surface layers of parts as a source of their multicycle failure under friction and wear

Y. O. Malinovskyi[1]0000-0001-5980-0908, **O.O. Mikosianchyk[2]**0000-0002-2438-1333, **O. D. Uchytel[3]**0000-0001-6241-1786, **O. O. Skvortsov[2]**0009-0008-8778-6400, **D. P. Vlasenkov[1]**0009-0008-4202-1885, **S. O. Sytnyk[1]**, **S. Y. Oliinyk[4]**0000-0002-6169-8874

[1]Kryvyi Rih professional college of State University «Kyiv Aviation Institute», Ukraine
[2]State University «Kyiv Aviation Institute», Ukraine
[3]State University of Economics and Technology, Ukraine
[4]Krivyi Rih National University, Ukraine

E-mail: oksana.mikos@ukr.net

Received: 05 July 2025: Revised 30 July 2025: Accept: 15 August 2025

Abstract

During the operation of various machines and mechanisms, oscillatory movements may occur, excited by a non-stationary friction characteristic. These oscillations appear either at the contact area of two parts or in the zone located ahead of the moving part. In the contact area, a non-stationary friction force develops, leading to self-excited oscillations of the contact surface and to the occurrence of parametric oscillations in the area ahead of the active punch. At certain ratios of slip velocities and part movement speeds, self-excited and parametric motions may appear or disappear, as well as intensify or weaken. These oscillations are one of the causes of uncontrolled surface roughness (deformational), cracking, and spalling of interacting parts, as well as significant dynamic components during the loading of actuating, drive, and power mechanisms. Frictional and parametric oscillations in the surface layers of parts with deformation wave formation create residual plastic sinusoidal metal layers, which are sheared off during the interaction of parts. Due to the dynamic nature of interaction during friction, the forces acting in the contact plane (longitudinal) exceed the critical Euler force, which is a parametric load, and in some cases lead to dangerous parametric resonance. The work defines the frequency range near the parametric resonance, which is the area of dynamic instability ahead of the moving punch. The formulated and partially solved problem considers frictional and parametric oscillations during the interaction of parts, which lead to the formation of deformation waves, their partial or complete shearing, creating prerequisites for intensive wear and subsequent destruction of parts.

Key words: dynamic loads, friction, wear, frictional oscillations, self-oscillations, beam-strip, parametric oscillations, parametric resonance, primary instability zone, punch, elongated part, friction force, slip velocity, surface layers.

Introduction

Dynamic effects on frictional surfaces cause both elastic and non-elastic deformations in the contact zone. Elastic deformations are localized at discrete contact areas. In turn, impulse loads generate not only oscillations of the tribological pair but also surface waves in the contacting parts. Under certain friction conditions, a contact resonance mode arises, which abnormally increases the intensity of plastic deformation and damage accumulation. This accelerates diffusion processes, material transfer, and intensifies structural-energy phenomena in the surface layers of the material. Various processes occurring in the surface layers lead to the emergence of different types of material destruction during wear, since in the pre-destruction stage adsorption, physical, chemical, structural, and other transformations may occur. Under friction conditions, the influence of these processes is usually stronger than, for example, in contact or bulk fatigue. The shape, size, and surface texture of wear particles, as well as the degree of hardening/softening of the surface layers, are directly related to wear mechanisms and make

it possible to draw certain conclusions about the nature and characteristics of deformation processes in the friction zone, about structural changes in the near-surface layer of the material, and about wear mechanisms [1].

Modeling of friction and wear processes is an important tool across a wide range of engineering disciplines, including contact mechanics, fracture and fatigue, structural dynamics, and others. In work [2] , systems of classification of friction and wear processes and criteria for their identification are presented, covering the physical processes of friction associated with the mechanics of deformable bodies.

In the present study, the influence of parametric and self-oscillatory processes arising from the interaction of components under dynamic loading conditions on the durability of the surface layers of the material is examined.

Literature review

During various technological processes occurring in the contact zone of the parts of kinematic pairs, oscillatory movements may take place, leading to local failures due to the manifestation of plastic and sometimes brittle properties by the surface layers of the parts [3]. In some cases, these properties are caused by the non-stationary friction characteristic between the surface layers of the interacting parts as a function of slip velocity [4]. Such oscillations may intensify during machine operation and lead to the accumulation of surface fatigue in the metal and to local brittle and plastic fracture of the surface layers [5, 6]. Such destruction can be mathematically described, taking into account the components of continuum mechanics and dislocation theory [5]. Therefore, to solve such a problem, in addition to the deformation wave components, it is necessary to introduce into the equations of the surface layer terms that also describe brittle properties and include multi-cycle loading. For the reliable inclusion of such components into the dynamic equations, additional experimental and theoretical studies are required.

Purpose

The aim of the work is to study the conditions for the occurrence and stabilization of self-excited and parametric processes under dynamic loading of surface layers that occur in the interaction areas of parts during friction and wear when brittle and elastic-plastic properties are manifested in the surface layers.

Statement of the main material

Let us consider the mechanism of occurrence of frictional self-oscillations in the interaction zone of a punch with another part, as well as parametric oscillations in the zone ahead of the punch (Fig. 1).

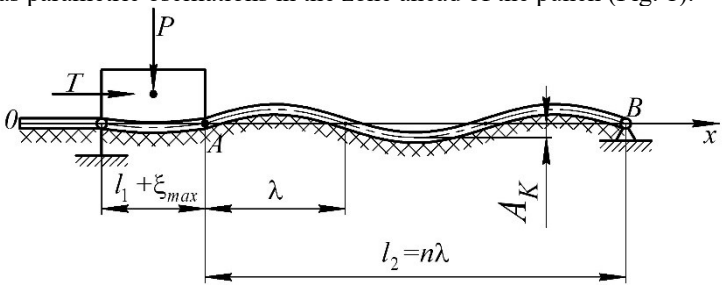

Fig. 1. Interaction of the punch with a half-space

The coefficient (force) of friction between two contacting parts can be approximated by a cubic function of slip velocity (Fig. 2). This friction characteristic has a decreasing section, which causes negative damping to appear in the oscillatory system, leading to self-excited oscillations that grow until the relative slip velocity of the parts reaches its critical value (Fig. 2).

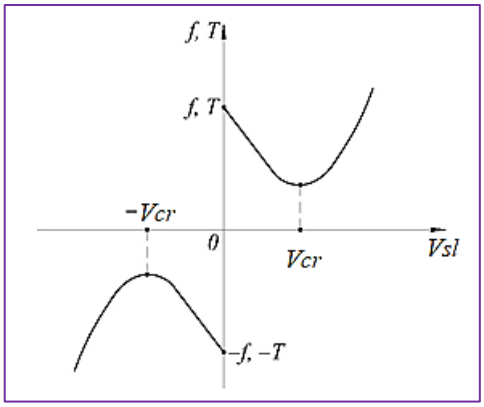

Fig. 2. Dependence of the coefficient (force) of friction on the slip velocity of parts

The presence of a nonlinear component in the friction characteristic indicates that after the slip velocity reaches its critical value, the influence of this component will increase, and the oscillation amplitudes will decrease. Thus, friction is accompanied by a self-oscillatory process that promotes additional frictional resistance and intensifies the fatigue wear of interacting surfaces.

Based on the conducted research, three problems of the theory of friction and wear concerning the rolls of rolling mills in the process of rolling sheets during metal processing or other similar processes were formulated:

1. Friction and wear of machined surfaces under the action of tangential forces suddenly applied to the outer layers of the machined part;

2. Friction and wear of machined surfaces under the action of periodic (impulse) forces applied to the outer layers of parts;

3. Friction and wear of machined surfaces as a result of the action of tangential loading caused by non-stationary friction between the forming tool and the part.

The formulated (and partially solved) problems are problems with phenomenological models for representing the processes of friction and wear.

Based on these three problems, it is highly likely that the sliding friction forces at the contact area, the resulting self-oscillations, and the parametric effects in the area in front of the punch are interrelated. Therefore, to describe the relationship between the processes at the contact area and ahead of the punch, let us consider these two adjacent sections on the beam-strip of the part's surface layer.

Let us distinguish two calculation schemes: the first within the framework of the contact area of the parts, where the tangential force T stretches the beam-strip of length l_1, and the second—where the tangential force T is applied to a beam-strip of length l_2 at the extreme point A, where the beam-strip (l_2) is in the compression zone (Fig. 1).

Considering the first calculation scheme, we can compose the equation of longitudinal displacements in the contact area of two parts of length l_1. If $q(x, t)$ can be defined as a function of oscillatory (or periodic) nature, then the variable $y(x, t)$ can be considered as the longitudinal displacement of the beam-strip during its oscillations.

Then the equation of longitudinal oscillations of a beam-strip loaded with distributed tangential loading along the Ox axis of the strip lying on an elastic foundation [4] takes the form:

$$\frac{\partial^2 y}{\partial t^2} = \frac{E_c F}{m} \cdot \frac{\partial^2 y}{\partial x^2} - \frac{\beta}{m} \cdot y + \frac{q}{m}, \tag{1}$$

where $y = y(x,t)$ – longitudinal displacement of the beam-strip during its deformation and oscillations; $E_c F$ – longitudinal stiffness of the beam-strip; m – distributed mass of the beam-strip; β – stiffness coefficient of the elastic foundation; $q = \frac{T}{bl_1}$ – intensity of the distributed load over the contact area of the surfaces; b – width of the contact area; l_1 – length of the contact area; P – external vertical load on the part; f_0 – static friction coefficient; $a = \frac{3(f_0 - f_{min})}{2V_{cr}}$ – linear coefficient of the friction characteristic; $\bar{b} = \frac{(f_0 - f_{min})}{2V_{cr}^2}$ – nonlinear coefficient of the friction characteristic; V_{cr} – critical relative velocity of the parts at which $f = f_{min}$; f – friction coefficient according to the cubic dependence on slip velocity [2]:

$$f = f_0 - \frac{3}{2} \cdot (f_0 - f_{min}) \cdot \frac{V_{\text{ск}}}{V_{\text{кр}}} + \frac{1}{2} \cdot (f_0 - f_{min}) \cdot \left(\frac{V_{sl}}{V_{cr}}\right)^3$$

V_{sl} – slip velocity of the parts.

Equation (1) is considered taking into account homogeneous boundary conditions:

$$\begin{cases} y|_{x=0} = 0 \\ \left.\frac{\partial y}{\partial x}\right|_{x=0} = 0 \end{cases}. \tag{2}$$

Expressions (2) represent the boundary conditions in the area of the beam-strip under the punch. Separately from conditions (2), we write the nonhomogeneous boundary condition (additional):

$$y|_{x=l_1} = \xi_{max}. \tag{3}$$

That is, at the right boundary of the contact area, we have the displacement value ξ_{max} (maximum).

Note that the value ξ_{max} is still undetermined

We take into account that the force $T = fP$. Then, considering the expression $f(V_{\text{ск}})$, and the coefficients a, $\bar{b}$ we solve equation (2) formally with respect to the function $y(x,t)$, and we consider this solution as approximate:

$$y(x,t) = -\frac{m}{\beta} \cdot \frac{\partial^2 y}{\partial t^2} + \frac{E_c F}{\beta} \cdot \frac{\partial^2 y}{\partial x^2} + \frac{mP}{bl_1\beta} \cdot \left[f_0 - a \cdot \frac{\partial y}{\partial t} + \bar{b} \cdot \left(\frac{\partial y}{\partial t}\right)^3\right]. \tag{4}$$

Then, into the right-hand side of (4) we substitute the approximate value $y_1(x,t)$, which we seek in the form:

$$y_1(x,t) = \sum_{i=1}^{n} Y_1(x) z_1(t) = (C_1 cosP_n x + C_2 sinP_n x) \cdot \frac{v_0}{P_0} sinP_0 t. \tag{5}$$

where $C_1 = 0$; $C_2 = \frac{\xi_{max}}{sin\sqrt{\frac{mP^2-\beta}{E_cF}}l_1}$ – arbitrary constants determined using (5) for the first natural mode of oscillations;

$z_i(t)$ – time-dependent component of the function $y_1(t)$ [5] ($i = 1, 2, 3, ...$).

For the first approximation $z_1(t) = \frac{v_0}{P_0} sinP_0t$

v_0 – initial slip velocity of the parts; P_0 – natural frequency of oscillations of one of the parts.

Then:

$$y_1(x,t) = \frac{\xi_{max}}{sin\sqrt{\frac{mP^2-\beta}{E_cF}}l_1} sin\sqrt{\frac{mP^2-\beta}{E_cF}} \cdot x \cdot \frac{v_0}{P_0} sinP_0t. \quad (6)$$

After substituting expression (5) into equation (4) and neglecting the transient components, we write the expression for the displacement ξ_{max}

$$\xi_{max} = \frac{mP}{bl_1\beta} \cdot \left[f_0 - \xi_{max} v_0 acosP_0t + \xi_{max}^3 v_0^3 \bar{b} cos^3 P_0t\right]. \quad (7)$$

We take $t = 0$ then the displacement ξ_{max} is determined from the cubic equation, which has three solutions, according to Cardano's formula; one of them has the largest real root – this will be the displacement ξ_{max}

$$\xi_{max}^3 - \xi_{max}\left(\frac{a}{\bar{b}v_0^2} + \frac{bl_1\beta}{mP\bar{b}v_0^3}\right) + \frac{f_0}{\bar{b}v_0^3} = 0. \quad (8)$$

The solution (8) has three real roots if $D < 0$, and one real root if $D > 0$. The discriminant is written as

$$D = \frac{f_0^2}{4\bar{b}^2 v_0^2} + \left(\frac{a}{3\bar{b}v_0^2} + \frac{bl_1\beta}{3mP\bar{b}v_0^2}\right)^3. \quad (9)$$

Thus, the maximum displacement of the beam-strip l_1 under the contact area during its deformation and oscillations is determined, we will consider that during longitudinal deformation of the beam-strip, the length of section l_1 increases to the value $l_1 + \xi_{max}$, and the length of section l_2 increases to the value $l_2 + \xi_{max}$, ξ_{max} is used for the increase of segment l_2, and for the development of a wave-shaped deformation of the strip l_2. The deformation of segmen l_2 will consist of n half-waves. Thus, in section l_2 the beam-strip becomes wavy, and the height of the corrugations will be considered as deformation micro-roughness. To determine the height of the corrugations of the deformed section l_2 it is necessary first to calculate the length and number of micro-waves of section l_2.

In order to determine the deflection arrow of section l_2 we assume that the beam-strip has lost its longitudinal stability. Therefore, as follows from [4], the length of the half-wave of the rod is equal to:

$$\lambda = \frac{\pi}{\alpha} = \pi \cdot \sqrt[3]{\frac{4E_cI}{E}}, \quad (10)$$

where α – number of half-waves of deformation of the section of the beam-strip of length π, that has lost longitudinal stability. as follows from [6], the length of the half-waves of deformation of the rod can be found through the modulus of elasticity of the surface and inner layers of the part, as well as the moment of inertia of the beam-strip; I – moment of inertia of the beam-strip cross section; E – modulus of elasticity of the inner layers of the part; E_c – modulus of elasticity of the surface layers of the part.

Then the flexibility coefficient of the rod on an elastic foundation according to [6] is equal to:

$$r = \frac{\beta}{EI} = \frac{E}{2}\alpha = \frac{1}{2l} \cdot \sqrt[3]{\frac{E}{4E_cI}}, \quad (11)$$

where: $l = l_2$ – unknown length of the beam-strip; β – stiffness of the elastic foundation of the beam-strip due to the elasticity of the inner layers of the part.

The flexibility coefficient of the rod on an elastic foundation can be related to the length of section l_2 and the number of half-waves n of the section when it loses its longitudinal stability, according to [6]:

$$r = \frac{\pi^4}{l^4} n^4 (n+1)^2, \quad (12)$$

or, taking into account expression (11), we obtain:

$$\frac{1}{2l_2} \cdot \sqrt[3]{\frac{E}{4E_cI}} = \frac{\pi^4}{l_2^4} n^4 (n+1)^2. \quad (13)$$

Expression (13) is transformed into a quadratic equation:

$$n^2\left(\frac{1}{2} - \frac{E}{4E_cI}\right) - 2n\frac{E}{4E_cI} - \frac{E}{4E_cI} = 0. \quad (14)$$

The solution of (14) has the form:

$$n = \frac{E}{4E_c I} \cdot \frac{1}{\left(\frac{1}{2} - \frac{E}{4E_c I}\right)} + \sqrt{\frac{E^2}{16E_c^2 I^2} \cdot \frac{1}{\left(\frac{1}{2} - \frac{E}{4E_c I}\right)^2} + \frac{E}{4E_c I} \cdot \frac{1}{\left(\frac{1}{2} - \frac{E}{4E_c I}\right)}}. \quad (15)$$

The deformed part of the beam-strip, ahead of the active punch, takes a sinusoidal shape and shifts in the direction of the punch movement in the form of a moving (deformation) wave of length l_2 with a speed v_0.

The shape of the wave is established after the beam-strip loses longitudinal stability.

Turning to the beam-strip before the punch enters section l_2 we see that this section is loaded with a tangential force T. The tangential force T stretches section l_1 of the beam-strip and compresses section l_2. As a result of the tangential force, section l_2 receives a longitudinal bend, and in some cases loses longitudinal stability. The longitudinal bend of the beam-strip is described using the following equation for the surface layer in partial derivatives [5]:

According to [3] $v(x,t) = \sum_{k=1}^{n} z_k(t) \sin\frac{k\pi x}{l_2}$ – transverse deflection of the beam-strip during longitudinal bending (for the case of hinged support of the beam-strip);

β – coefficient of restitution (stiffness) of the elastic foundation of the beam-strip due to the elasticity of the inner layers of the part;

I – moment of inertia of the cross section of the beam-strip;

$T(x,t) = T_A(x,t) = \frac{P}{bl_1} \cdot \left[f_0 - \xi_{max} a cos P_0 t + \xi_{max}^3 v_0^3 \bar{b} cos^3 P_0 t\right]$ – limit value of the tangential force of the beam-strip.

Substituting expressions $v(x,t)$ and $T(x,t)$ into the differential equation [5], we obtain a set of differential equations in simple derivatives:

$$\ddot{z}_k + \omega_{0k}^2[1 - \alpha_k \cos P_0 t + \beta_k \cos^3 P_0 t] z_k = 0. \quad (16)$$

where $k = 1, 2, 3, \ldots$ – simple integers;

$\omega_{0k}^2 = E_c I \cdot \left(\frac{\pi^4 k^4}{m l_2^4} + \frac{\beta}{m} - \frac{\pi^2 k^2}{m l_2^2} \cdot \frac{P}{bl_1} \cdot f_0\right)$ – square of the natural frequency of oscillations loaded with a constant value of tangential force;

α_k, β_k – constant coefficients of the friction characteristic:

$$\alpha_k = \frac{\pi^2 k^2}{m l_2^2} \cdot \frac{P}{bl_1} \cdot \xi_{max} v_0 a \cdot \frac{\beta m l_2^2 bl_1}{E_c I k^4 \pi^4 bl_1 + \beta l_2^4 bl_1 + \pi^2 k^2 P l_2^2 f_0}$$

$$\beta_k = \frac{\pi^2 k^2}{m l_2^2} \cdot \frac{P}{bl_1} \cdot \xi_{max}^3 v_0^3 \bar{b} \cdot \frac{\beta m l_2^2 bl_1}{E_c I k^4 \pi^4 bl_1 + \beta l_2^4 bl_1 + \pi^2 k^2 P l_2^2 f_0}$$

We denote the function $\varphi_k(t)$, which represents the parametric load on the oscillatory system, from equation (16):

$$\varphi_k(t) = \beta_k cos^3 Pt - \alpha_k cos Pt, \quad (17)$$

if the condition [7] is satisfied:

$$\left|\frac{\varphi'_k}{\varphi_k}\right| + \frac{\omega_{0k}}{2\pi} \ll 1. \quad (18)$$

Then we write equation (16) in the form:

$$\ddot{z}_k(t) + \omega_{0k}^2[1 + \mu\varphi_k(t)] z_k(t) = 0. \quad (19)$$

If condition (18) is not satisfied, then the function $\varphi_k(t)$ is determined according to [7] without the transformation effect, through direct integration. According to [5], the generating solution of (19) is represented in the form:

$$z_k(t) = A_k \cos\Psi_k. \quad (20)$$

where $\Psi_k = \omega_{0k} t + \Theta_k$ – time variable; A_k – amplitude of deformation waves for the k-th harmonic; Θ_k – initial phase for the k-th harmonic.

Then, taking into account the generating solution, according to [5], we have:

$$A_k(t) = B_k exp\left[-\frac{\mu_k}{4}\varphi_k(t)\right] \approx B_k\left[1 - \frac{\mu_k}{4}\varphi_k(t)\right], \quad (21)$$

where B_k – constant determined from initial conditions; μ_k – constant parameter set within the range $0 < \mu_k \leq 1$, we take $\mu_k = 1{,}3$ taking into account the value of B_k.

Next, using simple reasoning, we determine the condition under which parametric oscillations in the system will not occur. We consider the expression in square brackets of (21); if it is set to zero, we obtain the transcendental equation:

$$\beta_k cos^3 Pt - \alpha_k cos Pt + 1 = 0. \quad (22)$$

We solve (22) with respect to $\eta = cos Pt$, obtaining real values of the variable η, at which the functions $z_k(t)$ will equal zero.

We write instead of (22) the equation for the relative variable η:

$$\eta^3 - \frac{\alpha_k}{\beta_k}\eta + \frac{1}{\beta_k} = 0, \tag{23}$$

which has the solution:

$$\eta = \sqrt[3]{-\frac{1}{2\beta_k} + \sqrt{\frac{1}{4\beta_k^4} + \left(\frac{\alpha_k}{3\beta_k}\right)^3}} + \sqrt[3]{-\frac{1}{2\beta_k} - \sqrt{\frac{1}{4\beta_k^4} + \left(\frac{\alpha_k}{3\beta_k}\right)^3}}, \tag{24}$$

where $= 1, 2, 3, \ldots$ – mode number for which zones of absence of oscillatory motions are established.

When considering parametric oscillations, it remains important to determine the frequency range in which the unstable state of the systems develops, leading to parametric oscillations and, in some cases, to parametric resonance.

As follows from [9], the critical state occurs when the parametric load equation takes the form of the Mathieu function and, in magnitude, is equal to or exceeds the critical Euler force [9]. Since the second part of the parametric load in the Hill form does not affect the development of parametric oscillations and resonance, when determining the critical frequencies we focus on the solutions and results obtained in solving the Mathieu equation [8].

Thus, after the transformations performed in [9], we note that the regions of dynamic instability are located around the frequencies that are parametrically excited:

$$\Theta_{*k} = \frac{2\omega_{0k}}{k} \ (k = 1, 2, 3, \ldots), \tag{25}$$

where Θ_{*k} – natural frequency of the k-th mode of parametric oscillations during cutting; ω_{0k} – natural frequency of oscillations of the beam-strip for the mode with index k.

Thus, the main parametric resonance occurs when the frequency ratio is:

$$\Theta_* = 2\omega_0, \tag{26}$$

for $k = 1$ (if $k = 2, 3, 4, \ldots$ – then condition (25) applies).

It should be noted that under self-excited and parametric oscillations on the surface layers of parts, deformation-wave micro-roughness appears, which can be immediately sheared off by the moving punch. Therefore, deformation micro-roughness, even in the absence of parametric resonance and when operating in the elastic region, are subject to continuous alternating displacements; that is, the surface layers of the parts are in a state of multi-cycle fatigue loading. Moreover, the amplitudes of deformation wave oscillations in the surface layers exceed the corresponding oscillation amplitudes of the subsurface layers. Such deformations promote the separation of the outer layers of the parts from the inner layers.

The internal layers of the materials of the parts tolerate volumetric compression deformation well due to their elastic-plastic properties. However, in the outer layers, due to their brittle properties, critical crack formation and local destruction are observed, which leads to intensive wear of the outer layers of parts during frictional interaction.

Conclusions

1. Under dynamic loading of interacting parts, the role of parametric and self-excited processes in the development of multi-cycle stresses and deformations in the areas of beam-strips under the punch and ahead of the punch increases significantly, which leads to the intensification of wear and failure of the contacting surfaces.

2. To study non-stationary processes in the outer layers of interacting parts, a calculation scheme is applied in which the surface layers of the parts are represented as anisotropic plates on an elastic foundation and loaded with a tangential force determined by a variable friction coefficient, which in magnitude can exceed the critical Euler force.

3. The causes of the occurrence of dynamically unstable states of the beam-strip are identified, in which violations of the integrity of the surface layers of the workpiece and the tool are possible due to the manifestation of supercritical stresses and deformations in the material of the outer layers of the interacting parts.

4. The results of determining dangerous states of the surface layers of parts or workpieces under the action of non-stationary loads in the initial moments of interaction, as well as at the moments of the end of the slip effect or at the moments of speed equalization during oscillations, are obtained.

5. The third dynamic problem for the surface layers of the workpiece is formulated and solved. The layers are represented in the form of a brittle beam-strip on an elastic foundation, loaded with a tangential force caused by non-stationary friction in the contact zone of the parts (under the punch) and in the zone of interaction of the punch edge and the beam-strip, which leads to crack formation and premature wear of kinematic pairs.

6. The practical significance of the studies lies in the fact that for operating mining, metallurgical, and transport machines, the zones of unstable operation are calculated, where conditions may be obtained that do not ensure the high operational quality of such machines.

References

1. T. M.A. Al-Quraan, Ilina O., Kulyk M., Mnatsakanov R., Mikosianchyk O., Melnyk V. Dynamic processes of self-organization in non-stationary conditions of friction. *Advances in Tribology*. 2023. Vol. 2023. Article ID 6676706. P. 13. https://doi.org/10.1155/2023/6676706

2. Alexeyev N.M., Kuzmin N.N., Trankovskaya G.R., Shuvalova E.A. On the similarity of friction and wear processes at different scale levels. Wear. 1992. Vol. 156, Is. 2. P. 251-261 https://doi.org/10.1016/0043-1648(92)90221-S

3. Uchitel' O. D., Malinovs'kij Ju. O., Panchenko G. M. ta in. Intensifikacija procesiv mehanichnoï vzaєmodiï instrumentu z zagotovkoju pri vikonanni visokotochnih ta energoєmnih tehnologichnih operacij metodom tisku i rizannja. *Metalurgijna ta girnichorudna promislovist'.* 2019. № 5-6. C. 96-116. (In Ukrainian)

4. Smirnov V. V., Jakovlev R. A. Mehanika privodov prokatnyh stanov. M., «Metallurgija»,1977. 216 c.

5. Malinovs'kij Ju. O., Vlasenkov D. P., Sitnik S. A., Ter'oshina S. S., Olijnik S. Ju. Traktuvannja energetichnih metodiv u teoriï tertja ta znoshuvannja z pozicіï mehaniki sucil'nih seredovishh ta teoriï dislokacij. *Problemi tertja ta znoshuvannja*. 2023. № 4. C. 97-120. https://doi.org/10.18372/0370-2197.4(101).18083 (In Ukrainian)

6. Malinovs'kij Ju. O., Dubrovs'kij S. S., Malinovs'ka S. I. Deformacijno-hvil'ovi efekti pri terti ta znoshuvanni tverdih til. *Metalurgijna ta girnichorudna promislovist'*. 2017. № 2. C. 66-71. (In Ukrainian)

7. Cunningham W. J. Introduction to Nonlinear Analysis. New York : McGraw-Hill, 1958. 303 p.

8. Uchitel' O. D., Malinovs'kij Ju. O., Danilina G. V. ta in. Vpliv parametrichnogo rezonansu na mehanizm rujnuvannja kontaktujuchih poverhon' pri terti ta znoshuvanni. *Metalurgijna ta girnichorudna promislovist'.* 2018. № 4. C. 65-73. (In Ukrainian)

9. Uchitel' A. D., Malinovs'kij Ju. O., Panchenko A. N. ta in. Peredumovi viniknennja avtokolival'nih i hvil'ovih procesiv u formoutvorjuval'nih mashinah pid chas obrobki zagotovok i detalej metodom plastichnogo deformuvannja. *Metalurgijna ta girnichorudna promislovist'.* 2018. № 6. C. 21-29. (In Ukrainian).

Маліновський Ю. О. , Мікосянчик О. О., , Учитель О. Д. , Скворцов О.О., Власенков Д. П., Ситник С. О. , Олійник С.Ю. Динамічні процеси у поверхневих шарах деталей як джерело їх багатоциклічних руйнувань при терті і зношуванні

При роботі різноманітних машин і механізмів можуть мати місце прояви рухів коливального характеру, які збуджуються за нестаціонарної характеристики тертя. Ці коливання мають місце або на майданчику контакта двох деталей, або в зоні, розташованій попереду рухомої деталі. Так у зоні майданчику контакта розвиваються нестаціонарна сила тертя, яка приводить до автоколивань майданчику контакту, а також до виникнення параметричних коливань у зоні попереду діючого штампу. За певному співвідношенню швидкостей прослизання та швидкостей переміщення деталей, автоколивальні і параметричні рухи можуть проявитися, або зникнути, а також посилитись, чи послабитись. Ці коливання є однією з причин виникнення нерегламентованих шорсткостей (деформаційних), тріщинуватостей і лущення деталей, що взаємодіють, а також значних динамічних складових під час навантаження виконавчих, приводних та силових механізмів. Фрикційні та параметричні коливання в поверхневих шарах деталей з деформаційним хвилеутворенням формує залишкові пластичні синусоїдальні нашарування металу, які зрізаються під час взаємодії деталей. Через динамічний характер взаємодії деталей під час тертя, зусилля, що діють на площині контакту (поздовжні) перевищують критичне зусилля Ейлера, яке є параметричним навантаженням, у ряді випадків приводить до небезпечного параметричного резонансу. У роботі визначена область частот поблизу параметричного резонансу. Це є область динамічної нестійкості попереду рухомого штампу. У поставленій і частково вирішеній задачі розглянуті фрикційні та параметричні коливання при взаємодії деталей, які ведуть до утворення деформаційних хвиль, їх часткового, чи повного зрізання, що утворює передумови до інтенсивного зношування, та послідуючого руйнування деталей.

Ключові слова: динамічні навантаження, тертя, знос, фрикційні коливання, автоколивання, балка-смужка, параметричні коливання, параметричний резонанс, головна зона нестійкості, штамп, протяжна деталь, сила тертя, швидкість прослизання, поверхневі шари.

ISSN 2079-1372 Problems of Tribology, V. 30, No 3/117-2025, 49-61

Problems of Tribology
Website: http://tribology.khnu.km.ua/index.php/ProbTrib
E-mail: tribosenator@gmail.com

DOI: https://doi.org/10.31891/2079-1372-2025-117-3-49-61

Enhancing tribological system performance through intelligent data analysis and predictive modeling: A review

V.V. Aulin*[0000-0003-2737-120X], S.G. Kovalov[0009-0002-3922-8697], A.V. Hrynkiv[0000-0002-4478-1940], Yu.G. Kovalov[0000-0002-1729-2033], A.O. Holovaty[0000-0002-9552-0089], O.A. Kuzik[0000-0002-1729-2033], V.V. Slon[0000-0001-5535-0794]

Central Ukrainian National Technical University, Ukraine
E-mail: AulinVV@gmail.com

Received: 10 July 2025: Revised 10 August 2025: Accept: 30 August 2025

Abstract

The article presents a systematic analysis of the application of information technologies in tribology, including traditional methods, machine learning and artificial intelligence. The main goal of the study is to generalize and classify tribological informatics methods to improve the efficiency of tribological process analysis. The methodology is based on a review of key algorithms (ANN, support vector machines, K-nearest neighbors, random forest methods), determining their role in tribological research and analyzing information aimed at monitoring the technical condition, predicting behavior and optimizing tribological systems. It is determined that the use of artificial intelligence and machine learning algorithms significantly improves the accuracy of tribological system diagnostics, allows predicting their operational life and optimizing the operating parameters of tribological systems and machine mechanisms. A classification of tribological informatics methods is presented according to their functions: regression, classification, clustering, dimensionality reduction. This makes it possible to determine the most effective approaches for different types of tribological analysis. The practical focus of using intelligent modeling methods is the possibility of integrating the obtained results into production processes, which contributes to increasing the reliability of mechanical systems, reducing the costs of their maintenance and creating more accurate methods for predicting tribological characteristics, properties and tribological efficiency of the functioning of system components and assemblies of machines and mechanisms. It is shown that triboinformatics opens up new prospects for improving tribological research, providing more accurate monitoring, effective forecasting and optimization of tribological systems.

Key words: tribological system, technical condition monitoring, modeling and forecasting, friction, wear, artificial intelligence, machine learning.

Introduction

In the course of modern mechanical engineering development, the design of components, assemblies, and mechanisms has become increasingly complex. This trend leads to heightened requirements for their reliability, operational stability, and tribological efficiency. The achievement of enhanced reliability and efficiency in mechanical systems largely depends on tribological systems (TrBS), which integrate frictional components, lubricants, and technological media tailored to operational conditions (Fig. 1) [1-2].

Tribological systems are characterized by intricate dependencies that span subject-specific, temporal, and systemic dimensions. This complexity necessitates the expansion of relevant databases and the development of multi-component theoretical models capable of describing and predicting the behavior of tribological processes. The integration of existing theoretical concepts with experimental data enables the construction of predictive models aimed at optimizing tribological characteristics and enhancing the operational reliability of TrBS.

To improve the effectiveness of research and development, as well as to increase the reliability of tribological systems, it is essential to accelerate information exchange among their components. In this context, the application of modern information technologies is highly advisable, particularly data processing methods, machine learning (ML) techniques, and artificial intelligence (AI) algorithms [3-6]. By leveraging these strategies,

researchers can automate the evaluation of tribological data, uncover hidden regularities, and achieve higher fidelity in predictive modeling of wear and friction-related metrics.

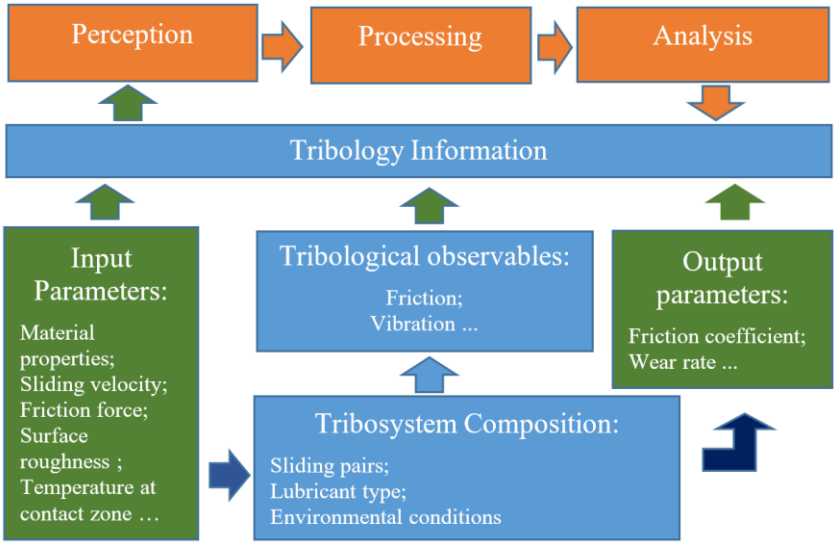

Fig. 1. Components of tribological systems [1]

The incorporation of artificial intelligence techniques alongside triboinformatics significantly enhances the effectiveness of evaluating tribological phenomena, forecasting component wear resistance, and fine-tuning the operational parameters of mechanical systems and assemblies. Advanced data analysis approaches enable the development of intelligent tribological systems with adaptive capabilities, including self-regulation, autonomous organization, and continuous improvement based on real-time wear diagnostics. Such functionality is critically important for ensuring the operational reliability of tribological systems [6]. Furthermore, the evolution of triboinformatics combined with AI-driven methodologies opens new avenues for improving the durability and performance of mechanical structures, which remains a key priority in modern engineering practice [7].

Literature review

Tribo-informatics has emerged as a pivotal interdisciplinary domain within tribology, aimed at formalizing research processes, constructing structured databases, and applying advanced information technologies for the acquisition, classification, storage, retrieval, analysis, and dissemination of tribological data [1]. This approach addresses the growing complexity and volume of tribological information, which often spans multiple disciplines and formats.

Modern tribo-informatics encompasses a broad spectrum of analytical functions, with regression modeling and classification techniques being among the most widely utilized [3]. The core objectives of this field include:

Condition monitoring: systematic collection of operational data related to wear, degradation, and performance of mechanical components [8]

Behavioral prediction: development of models capable of forecasting changes in tribological performance over time and under varying operational conditions [9];

System optimization: identification of parameter configurations that ensure maximal reliability and efficiency of tribological systems [10].

A critical challenge in tribo-informatics lies in establishing robust and time-sensitive correlations between tribological parameters and operational dynamics. This necessitates the integration of predictive modeling techniques and the deployment of intelligent monitoring algorithms [11].

Traditional data analysis methods in tribology often lack the flexibility and precision required to adapt to evolving operational environments. Consequently, the incorporation of AI and ML techniques is increasingly recognized as a promising strategy for enhancing the adaptability and predictive capabilities of tribological data systems [12].

The application of artificial intelligence technologies offers effective tools for addressing key challenges in tribological informatics [13–16]. Among the most promising directions are:

1. Optimization of tribological process dynamics in technical mechanical systems (TMS): Machine learning techniques enable the identification of optimal operating regimes and the selection of appropriate lubricants, which leads to reduced energy consumption and extended service life of mechanical components and assemblies.

2.- Intelligent processing and management of tribological data: AI-based systems facilitate the analysis of both structured and unstructured tribological datasets, support automated classification, and enhance the integrity and reliability of information repositories. These capabilities are essential for the development of advanced tribological materials and technologies.

3. Adaptive modeling and prediction of wear in tribological contacts (TC): The implementation of deep learning architectures allows for the simulation of wear behavior under variable operational conditions. This creates opportunities for dynamic adjustment of system parameters, contributing to improved performance and predictive maintenance of mechanical systems.

The contemporary evolution of tribology increasingly emphasizes the integration of information technologies, particularly AI algorithms, to enable joint management of databases and mathematical models of tribological processes [1-2]. This paradigm shift opens new avenues for predicting the behavior of TC and optimizing their performance. The inherent capabilities of AI systems – such as self-learning and real-time adaptation – facilitate the development of intelligent tribological solutions capable of responding dynamically to changing operational conditions [6-8].

A review of current literature reveals that the application of AI within tribo-informatics significantly enhances automation, improves data processing efficiency, and contributes to increased reliability and wear resistance of mechanical systems. Moreover, it enables cost-effective engineering design and accelerates the development of innovative solutions [3-5]. Despite these advancements, several unresolved challenges persist.

One of the primary difficulties lies in the fragmented and complex interdependencies among tribological parameters, material properties, loading conditions, and thermal regimes. These factors interact in a nonlinear manner, complicating the construction of accurate predictive models for tribosystem behavior [9-10]. Additionally, most existing diagnostic approaches rely heavily on empirical methods, which demand extensive experimental datasets. This reliance limits the adaptability of tribological solutions to novel operating environments and increases the overall cost of research and development [4, 17, 18].

To address these limitations, AI-driven modeling of tribological elements and systems presents a promising direction. One such approach involves the implementation of Digital Twins (DT) – virtual replicas of physical systems that simulate operational behavior under varying load conditions [19]. The integration of engineering simulation software (e.g., ANSYS) with machine learning algorithms enables predictive analysis of wear, load distribution, and structural optimization, thereby enhancing the functional efficiency of mechanical assemblies [20-21].

Another innovative strategy involves the use of generative adversarial networks (GANs), which can synthesize new operational scenarios by modeling the behavior of tribological materials under dynamic conditions. This technique is particularly valuable for the formulation of advanced lubricants and the determination of optimal operating regimes for machinery [5, 8, 22].

The Python programming language plays a pivotal role in the realization of such models, offering a robust ecosystem of libraries tailored for scientific computing and AI development [23]:

– TensorFlow and PyTorch are employed to construct neural networks that analyze extensive tribological datasets and forecast the behavior of components and assemblies [24-25].

– SciPy and NumPy support mathematical modeling, enabling the computation of complex relationships among system parameters and the optimization of operating conditions [26].

– Matplotlib and Seaborn facilitate the visualization of simulation results, thereby improving the interpretability of tribological analyses [22, 27].

The integration of these tools fosters the creation of adaptive tribological systems capable of autonomously adjusting their performance in response to real-time operational inputs. This advancement holds significant promise for mechanical engineering, production optimization, and the deployment of automated manufacturing lines [13-14,16, 23].

Purpose

The purpose of this work is to justify the choice of intelligent methods for modeling and adapting the functioning of the TrBS to changing environmental conditions using AI methods. To achieve the goal, the following tasks were used in the work:

1. To analyze current problems of tribology and triboinformatics:

- to outline the main unresolved issues in the field of tribology, in particular, modeling of friction, wear, and lubrication processes, optimization of triboelements and TrBS, and forecasting their technical condition;

- to consider the possibilities of using digital technologies for analyzing tribological data.

2. To clarify the conditions and effectiveness of implementing digital analogues of DT in tribological research:

- to analyze the concept of DT for simulating the operation of TrBS, machines, and mechanisms in various conditions;

- to determine the methods for modeling tribological processes in ANSYS and their combination with Python algorithms to improve analysis using AI methods.

Methods

TrBS embedded in machines, mechanisms, and production lines perform essential functions such as the transmission of motion, energy, and information, as well as the redistribution of stress and strain within

triboelement materials. These processes enhance the reliability of mechanical systems and facilitate effective interaction between components [1, 2, 21]. One of the primary objectives in managing tribological system databases is to enable predictive diagnostics and condition-based monitoring of assemblies and units, thereby supporting efficient control of tribological processes [3, 4, 13]. As a cybernetic system, TrBS have output factors and parameters that describe their technical condition and behavior. Such signals include tribological parameters that can act as target output data. For example, in the case of a bearing, the output signal is the moment of motion, and the input signals can be the characteristics of the material of its elements, lubrication modes, and methods of treating friction surfaces. The main parameters of the TrBS state include stress, friction, vibration, wear, and heat generated in the contact zone of parts in the friction zone [28-29]. Tribological informatics employs a diverse array of techniques for gathering, processing, and interpreting tribological data. Conventional methods include statistical tools such as Gaussian regression, linear regression, and the least squares approach [5–6]. However, modern technologies actively use machine learning algorithms, which significantly expand the possibilities of predicting the tribological behavior of machines and mechanisms and optimizing their characteristics [30-31]. It is worth noting that AI methods are products of machine learning and allow for accurate analysis of complex processes in the TrBS [32-33]. One of the key tasks of tribological informatics is to establish the relationship between the elements, factors and parameters of the TrBS. In this regard, such areas of research as monitoring the technical condition, predicting the behavior of the Tribological System and optimizing their operation are considered [34-35]. Monitoring involves the analysis of the current characteristics of the system, which can be both observable and hidden [36]. Forecasting allows you to determine the dependencies between the input parameters, their changes over time and possible future states of the TrBS [37]. Optimization of tribological processes, in turn, is aimed at finding the best operating conditions for machines and mechanisms to ensure their durability and efficiency [38].

In practice, the processing of tribological information should be based on physical models and fundamental principles of tribology. This provides a deep integration between computer science and tribology, allowing data analysis to be carried out on the basis of the constructed tribological models. It is important that each characteristic parameter has a physical meaning, and its processing is based on the principles of contact interaction mechanics [39]. To increase the efficiency of tribological research, modern data collection technologies are used. The use of sensor systems allows you to register key factors and parameters of the operation of tribological units, systems and assemblies, in particular, temperature, friction force, speed of movement and level of wear [40]. Integration of IoT technologies allows you to combine devices for registering tribological factors and parameters in real time[22-23]. In addition, optical analysis methods using high-precision cameras and microscopes allow you to obtain detailed images of the surface structure after the operation of Tribological Units, machines and mechanisms [24]. The processing of the obtained data is carried out using machine learning algorithms, such as neural networks and clustering. These methods contribute to structuring data, removing noise and identifying key factors that affect the efficiency of the operation of Tribological Units [25-26]. Identifying patterns in changes in factors and parameters of the technical condition helps to create accurate predictive models that provide prediction of the service life of system and assembly units and determine the optimal conditions for their operation [27, 35]. Modern methods of tribological data analysis can be classified according to their purpose. In this case, regression analysis allows to determine quantitative dependencies between the parameters of the TrBS [28, 30]. Database classification helps to identify characteristic types of tribological behavior [31, 36], and clustering groups similar tribological phenomena and helps to find new patterns [32, 33]. Methods of data dimensionality reduction are used to optimize the information array, which improves the accuracy of research [34]. The most effective methods of tribological database analysis include ANNs, which are able to process large amounts of information and increase the accuracy of prediction [29, 37]. Support vector machines (SVMs) are used for binary classification of tribological parameters [38], and the K-nearest neighbors (KNN) and random forest (Random Forest - RF) methods are effective for clustering tribological phenomena and analyzing their features [39, 40]. ANNs consist of a set of node connections and demonstrate high efficiency in the field of AI and tribology. Their structure includes three main blocks:

- input block, which receives data from the external environment;
- hidden block, which performs internal information processing;
- output block, which generates results based on the analysis of input data [28, 29].

In tribological studies, input parameters can be speed and load, and output parameters can be friction, wear and lubrication modes. In addition, easily observable signals, such as acoustic oscillations, electrical characteristics or vibrations, can be used to predict difficult-to-observe quantities, in particular the coefficient of friction (CoF) or the wear rate of the material [30, 31].

It is substantiated that the integration of machine learning methods and intelligent data analysis in triboinformatics significantly improves the accuracy of wear prediction, optimizes the operating parameters of the Tribological Devices and contributes to the development of new tribological models [32-33]. The use of modern data processing algorithms allows the creation of adaptive Tribological Devices capable of self-learning and automatic adjustment of operating parameters [34-35]. In many cases, it is quite difficult to determine the most significant characteristic parameters only on the basis of classical tribology models. Therefore, there is a need to analyze the relationships between several characteristic factors and parameters that affect the Tribology. For this, correlation methods are used that allow determining the optimal factors and parameters of tribological

characteristics and properties of triboelements and Tribology as a whole [36-37]. The obtained data can be used to create new tribological models or refine existing principles, which ensures more effective optimization of tribological processes and the functioning of components and assemblies of machines and mechanisms (Fig. 2).

Fig. 2. Classification of tribo-informatics technologies by purpose

Tribological informatics technologies can be classified according to their main purpose:

- regression analysis – used to establish quantitative relationships between parameters of tribological systems;
- classification – allows you to determine characteristic types of tribological behavior of mechanisms;
- clustering – helps group similar tribological phenomena and discover new patterns;
- dimensionality reduction methods – optimize the analysis of large data sets, increasing the accuracy of calculations.

In tribological studies, input factors and parameters can be speed of movement, load and lubrication modes, while output data are friction, wear, temperature and structural changes of surfaces. Additionally, easily observable signals, such as vibration, acoustic or electrical characteristics, can be used to estimate difficult-to-observe parameters, such as CoF or material wear rate

Results

Classification methods are essential components of tribo-informatics, enabling the identification of tribological states, prediction of system behavior, and optimization of operational parameters. Among the most widely used algorithms in tribological research are SVM, KNN, and RF, each offering distinct advantages in terms of accuracy, interpretability, and adaptability to nonlinear data. SVM is a supervised learning algorithm designed for binary classification tasks. Its core principle involves constructing a hyperplane that maximizes the margin between data points of different classes, thereby ensuring robust separation and generalization [30]. In tribological applications, SVM has been successfully used to classify wear regimes, friction states, and lubrication conditions based on acoustic, vibrational, and image-based features [31, 36]. When dealing with non-linearly separable data, SVM employs kernel functions to project input vectors into higher-dimensional spaces, enabling linear separation in transformed domains. This capability is particularly valuable in tribology, where system behavior often exhibits nonlinear dependencies among material properties, operating conditions, and surface interactions [2, 4]. KNN is a non-parametric classification method that assigns class labels based on the majority vote of the k closest training samples. Its simplicity and effectiveness make it a popular choice for tribological diagnostics, especially in scenarios involving limited data and low-dimensional feature spaces [30, 38]. The selection of the parameter k is critical: small values may lead to overfitting, while large values can cause underfitting. Empirical studies have shown that optimal k values vary depending on the complexity of the tribological system and the noise level in the dataset [38]. KNN has been applied to predict coefficients of friction (CoF), wear rates, and lubrication states by analyzing historical data on material composition, load, and sliding velocity [35].

RF is an ensemble learning method that constructs multiple decision trees using random subsets of data and features (Fig. 3). The final prediction is obtained through majority voting (classification) or averaging (regression), which enhances robustness and reduces overfitting [29].

In tribological informatics, RF has demonstrated high accuracy in predicting tool wear, classifying lubrication regimes, and estimating CoF under varying operational conditions. Hasan et al. [28] showed that RF outperformed other models in predicting wear behavior of aluminum–graphite composites. Wu et al. [29] applied RF to tool wear monitoring in manufacturing, achieving reliable classification based on vibration and force signals.

RF also facilitates feature importance analysis, allowing researchers to identify dominant tribological parameters such as reinforcement content, temperature, and surface roughness [39-42]. This interpretability is crucial for engineering decision-making and model validation.

Compared to SVM and KNN, RF offers superior performance in handling high-dimensional, noisy, and nonlinear tribological datasets (Fig. 4). Its ensemble structure mitigates the limitations of single-tree models and provides stable predictions across diverse tribological scenarios [3, 5].

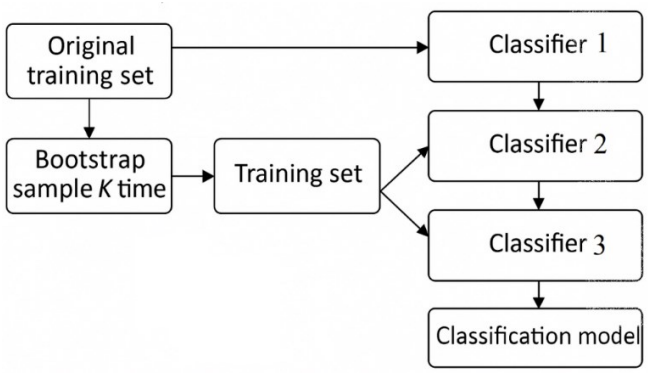

Fig. 3. Simplified diagram of the RF method as a classification algorithm

Algorithm	Task Type	Advantages	Limitations	Typical Use in Tribology
ANN	Regression, Classification	High accuracy, adaptability	Requires large datasets	Wear rate prediction, material optimization [15]
SVM	Classification	Effective with small datasets	Sensitive to kernel selection	Acoustic signal classification, wear stage detection [30]
RF	Classification, Regression	Robust to noise, interpretable	May be slow with large datasets	Friction state prediction, wear pattern analysis [29, 41]

Fig. 4. Comparative analysis of ML algorithms for wear prediction

According to the goals of tribological research, tribological informatics approaches can be classified into three main areas: monitoring the tribological state of the Tribological Functional Region (TFR); predicting the tribological behavior of the TFR; optimizing the TFR [2, 6, 40].

Tribological methods have a structured system and are not a simple adaptation of information technologies to tribological problems. They are based on data analysis and model building. The physical tribological model contributes to the accuracy and reliability of calculations, supporting computer science methods in creating more effective algorithms [1, 3, 8]. Monitoring the condition of friction involves the use of information about the accompanying friction processes to analyze the condition of components, systems, machine units and mechanisms [13, 14, 31]. Monitoring the technical condition of tribological units is an important aspect of real-time fault diagnosis and ensuring the stability of machines and mechanisms [36, 41]. Key parameters that can be observed to determine the condition of the Tribological Units include visual changes, sound pressure, temperature indicators, lubricant quality and vibration characteristics [22, 31, 32]. At the same time, advanced analytical models are used to monitor difficult-to-observe tribological variables, such as wear, friction and lubrication processes. [6, 36].

The use of AI methods in monitoring the technical condition of Tribological Units in real-time mode allows for continuous monitoring of the condition thanks to a set of sensors and data processing algorithms [13, 14, 36]. If the system detects an abnormal increase in temperature or an increase in the level of vibration, this may signal potential problems, such as wear or degradation of the elements of the unit, system or assembly of machines and mechanisms [31, 39]. AI systems provide operational decision-making, which allows preventing breakdowns, minimizing the risks of sudden equipment failure. Early warning systems based on data dynamics analysis predict possible failures or emergencies. This makes it possible to carry out preventive maintenance, which reduces equipment downtime and optimizes resource costs [4, 6, 41]. Research on tribological systems focuses on the analysis of damage to mechanical parts caused by friction, most of which is a consequence of wear processes [5, 10, 35]. Wear prediction can be divided into two main categories:

- quantitative wear analysis - estimates the speed and magnitude of wear [28, 38];
- classification of wear behavior - is used to determine the patterns of wear of machine parts and mechanisms [29, 42].

For quantitative prediction of wear of parts, a large database is first formed, after which the dependence between wear intensity and operating time is analyzed. At this stage, ANN, support vector regression, RF algorithm and adapted data mining methodology (DMME) are used [10, 15, 28, 29].

It should be noted that the gradient boosting algorithm is effective in applying machine learning methods to predict tribological behavior and efficiency of the TBR, while the RF method is more suitable for analyzing wear patterns.

Monitoring of friction processes can be divided into two main areas [38, 41]:

- analysis of the friction shape, which allows assessing geometric changes in surfaces [34, 36];
- control of tribological characteristics, such as friction force and friction torque [18, 20].

In modern research, a significant number of methods for monitoring the form of friction are used, but in-depth analysis of its technical condition remains limited [2, 5]. The assessment of the friction force and its moment is important for high-precision mechanical systems [36, 40].

The friction informatics method has some important applications in other scenarios: identification of damage to friction surfaces, material processing [2, 4]. A set of acoustic data was collected during the reciprocating motion of tribocouplings of parts, a bearing, and the use of RF methods to predict three friction states: running-in; steady state; wear stage [29, 41]. The ANN method was used to optimize the formula of the friction material [15], machine learning algorithms were used to quickly and accurately predict the width of the images of the zone of a given 2D material, which contributed to the application of materials in the field of semiconductor devices [35]. Monitoring the state of wear of machine parts and mechanisms is conventionally divided into:

- monitoring the wear of machined parts;
- monitoring the functional components of the system [13, 14].

Lubrication performance prediction involves analyzing the relationship between the state of the lubricating medium and surface characteristics, such as material roughness and texture. [9, 21]. It also covers the evolution of lubrication performance, which allows predicting the service life of lubricants and optimizing mechanical systems [6, 36]. Analysis of wear processes can be rationally carried out by the method of ferrography and ferrospectrometry. This is a new mechanical wear testing method that uses magnetic separation of metal particles in oil and their placement on a substrate according to particle size. This approach allows for the assessment of the particle concentration in the lubricating medium and the micromechanical properties of wear particles, which contributes to a deeper understanding of wear mechanisms [34]. This technology is an important tool for wear testing and analysis, allowing for detailed tribological studies. The application of triboinformatics approaches can improve the efficiency of particle detection, recognition and classification in ferrospectrometry [2, 10]. An algorithm model for automatic detection and classification of wear particles was developed, which improved the efficiency of ferrospectrometry analysis [6, 31]. ANN was used for particle detection and recognition, and SVM was used for particle classification [30, 32]. A CNN method was developed to classify seven types of ferrograph images. The proposed method can be used to determine the degree of wear with an accuracy of 90% [6, 42]. In the actual use of ferrographs, problems may arise such as fuzzy ferrograph images, which affects the accuracy and fairness, and low ferrograph data acquisition frequency, which affects the accuracy and performance of real-time

wear monitoring [42]. A CNN with a large convolution kernel was used to build a degradation model, which reduces the effect of blurring and defocusing in the ferrograph visualization process [6]. In order to realize real-time wear monitoring, the data volume of ferrograph images should be increased. A method based on Gaussian process regression approximation data was used [5]. For data analysis, it is reasonable to increase the sample size and predict wear based on a large sample size [38]. If it is possible to monitor the condition of parts and their mating parts in real time, then it is possible to accurately determine the moment of its replacement or repair. The main signals for such analysis are sound pressure, image and vibration characteristics [22, 31]. Machine learning methods, in particular SVM, are used to establish the relationship between sound signals and wear. Regularized particle filtering helps to reduce errors in the results, providing a more accurate determination of the degree of wear [40]. In this case, the wear behavior is considered as a complex dynamic process that depends on many factors:

- processing parameters of the materials of the mating parts;
- composition and structure of the material of the parts and the lubricating medium;
- operating conditions of the tribological mechanical component (TMC);
- lubrication modes of the TMC [6, 37].

To predict the wear behavior of the TMC, clustering, decision-making, fuzzy logic and neural networks methods are used, such as ANN, adaptive neural systems and fuzzy clustering [15, 40]. As a rule, determining the state of the TMC wear requires the use of physical laws [1, 9]. Combining ANN models, rule-based inference and logical reasoning models allows us to identify patterns in the occurrence of wear processes in the TMC [40]. CoF is a critical tribological characteristic of the TMC, which is used to assess the mechanical elements of the TMC and their shortcomings [18, 35]. The implementation of accurate CoF predictions allows us not only to determine the future state, but also to control the choice of methods for preliminary preparation, strengthening and modification of the TMC of the mating parts of the surfaces [5, 28]. The higher the accuracy and criticality of the design of systems of units and assemblies, the more important friction monitoring becomes, which affects the overall stability of machines and mechanisms [6, 36]. It is known that the process, lubrication, is a decisive factor affecting the processes of friction and wear [9, 21]. Lubrication monitoring systems usually assess both the state of friction and the state of the lubricating medium [6, 36]. ANN and Linear Discriminant Analysis (LDA) neural networks are used to classify the states of the lubrication system, which allows you to effectively determine deviations from the normal operating mode [15, 40]. It is known that lubricants significantly reduce friction and wear, so their correct choice is crucial for the efficiency of the operation of the Lubricating Medium [5, 21]. Optimization of the lubricating medium involves two main areas:

- development of new lubricants [5, 21];
- optimization of the proportions of the components of lubricating mixtures [6, 38].

In connection with the development of two-dimensional (2D) materials, screening of 2D materials has become a key aspect of optimizing the lubricating medium [35].

The application of tribological informatics in tribology significantly expands the possibilities of analyzing, monitoring and predicting the technical condition of the mechanical components of machines and mechanisms [1, 2, 4]. The use of AI and machine learning allows you to increase the accuracy of prediction, optimize the parameters of the mechanical components and prevent premature failure of mechanical components [3, 5, 6]. Thanks to modern technologies, it has become possible to perform real-time condition analysis, which contributes to increasing the efficiency of maintenance and extending the service life of the mechanical components of tribological systems [13, 14, 36]. Tribological condition monitoring systems play a key role in detecting faults in real time and ensuring stable operation of mechanisms [7, 31]. If the mechanical component is a bearing, its condition can be assessed by friction force and friction moment, using RF algorithms, gradient boosting classifier and additional tree classifier [29, 38, 42]. Among the most accessible parameters for analyzing the condition of the mechanism are visual changes, sound pressure, temperature indicators, quality of the lubricating medium and vibration [22, 31]. At the same time, tribological variables that are difficult to measure are often determined through the analysis of wear, friction, and lubrication processes [5, 33]. The introduction of AI into monitoring allows you to track changes in the technical condition of the machine and mechanism in real time thanks to sensors and data analysis algorithms [6, 13, 14]. If the system detects abnormal changes in temperature or vibration levels, this can signal the initial stages of wear or degradation of mechanical components [36, 41]. Such technologies provide efficiency in decision-making, which allows you to minimize the risks of equipment failure [4, 7]. The assessment of friction parameters is critically important for high-precision mechanical systems, such as adjusting mechanisms of car engines or impulse wheels of satellites [6, 20]. The higher the requirements for the accuracy of the mechanism, the greater the role played by monitoring friction characteristics, which affects the stability of the entire system [36]. Lubrication is also an important factor, which affects the efficiency of friction and wear processes [9, 21]. Monitoring of the lubricating medium is carried out through two key parameters:

- monitoring the state of friction;
- assessment of the state of the lubricant and its characteristics [32, 36].

Neural networks and linear discriminant analysis are used to classify the states of the tribological system, which provides an accurate assessment of the operation of the mechanism [15, 30, 40].

Thanks to the use of AI, machine learning algorithms and monitoring methods, it has become possible to analyze the state of the mechanism in real time, which allows preventing emergency situations and increasing the reliability of the operation of the tribological system [6, 7, 41].

This process is the result of the merger of information technology and tribology, which provides a comprehensive approach to the analysis of mechanical systems and their optimization [1, 2]. The method of deep neural networks plays an important role in predicting the coefficient of friction [9, 10, 20]. Optimization of TrBS is based on the prediction of tribological behavior, which allows improving the operational characteristics of mechanisms [5, 6, 38]. Optimization of the TrBS is based on the analysis of its components and can be implemented from three main aspects:

- optimization of materials of tribocoupling elements [35];
- optimization of the lubricating medium [21, 32];
- optimization of Tribological operating conditions [6, 37].

AI plays a crucial role in this direction, contributing to increasing the efficiency of design and reducing the costs of developing Tribological Systems [2, 4, 6]. It is worth noting that optimization of TrBS is a complex engineering task that requires an integrated approach taking into account three main factors: tribocoupling of parts; lubricants; operating conditions [5, 21, 40].

Optimization of the TrBS can be divided into three main areas: design of the texture of friction surfaces; development of materials for parts; selection of the most optimal materials [6, 9, 38].

Regarding optimization of the surface texture, measuring friction changes when modifying the surface structure allows us to assess the impact of production processes on tribological characteristics [6, 21]. AI methods contribute to the creation of optimal surface textures to achieve effective friction control [6, 38]. In the case when the process of preparation or formation of the surface texture does not meet the expected friction parameters, the tribological system must be optimized [40].

Optimization of friction materials is carried out through the development of composite materials, as well as control of the parameters of the cementation and nitriding technological processes. This can be implemented using ANN [15, 28].

When studying materials, two key aspects should be taken into account: material composition; structural properties of the material. Most often, such parameters change due to adjustments to production conditions [5, 35].

When optimizing materials of TC elements, machine learning algorithms make it possible to test numerous combinations of materials in digital models, which significantly reduces the cost of experimental research [4, 28, 38]. Machine learning methods are also used to analyze the chemical, physical and mechanical properties of new materials, which allows you to create components with specified characteristics, for example, materials with high wear resistance or low friction coefficient [5, 35, 38]. AI algorithms can predict the behavior of a material under different operating conditions, which reduces the time and cost of testing new technological solutions [6, 20, 28].

Input parameters of the TrBS, such as sliding speed, load, temperature and humidity, affect the processes of friction and wear [5, 6, 37]. To achieve optimal functioning of the Tribological System, adaptive operating conditions can be developed, which will ensure the effective operation of the tribological system [6, 40]. Since machine learning algorithms can analyze large amounts of data on operating conditions (temperature, humidity, load), it is possible to automatically select optimal settings, which ensures increased tribological efficiency [4, 6, 38]. The introduction of automation in tribology and tribotechnology not only saves operators' time, but also minimizes the likelihood of human errors in the effective functioning of the TrBS [7, 40]. Equipping the TrBS with production robots requires the provision of algorithms AI. This provides high accuracy and efficiency in performing complex tasks, such as coating or precision grinding of TC [6, 20]. In addition, such machines can operate in harsh conditions (for example, at high temperatures or pressure loads), where the use of human labor can be dangerous [6, 7]. Analysis of the results of experiments in TC using AI allows you to identify hidden patterns that are not always obvious with traditional analysis methods [2, 5]. AI helps automate data comparisons, establish relationships between parameters, and optimize the process of further experimental research [4, 6, 40]. Modern tribological informatics methods enable the prediction of the service life of TC, facilitate real-time monitoring of their condition, and uncover previously unknown correlations between physical parameters in tribolog [6, 28, 38]. Triboinformatics represents a comprehensive scientific discipline rather than merely the application of computer science techniques to isolated tribological challenges [1, 2, 5, 7]. When implementing computational tribology methods, the Tribological Model is taken into account - this model reflects a multidisciplinary, time-dependent system that defines the interaction between two specific physical variables [1, 2]. Architectural frameworks for triboinformatics have been proposed, emphasizing that practical applications must consider input/output data, tribological states, and the operational rules of TrBS [2, 6, 7].

Selecting the most appropriate computational method for a given tribological issue remains a complex task. Currently, triboinformatics research typically involves applying a chosen information technology to address specific problems [2, 5]. This approach relies on extensive input data, necessitating standardized tribological testing protocols to enable the reuse and integration of diverse datasets.

Tailored solutions must be developed to suit the unique characteristics of each process or enterprise. Artificial intelligence can incorporate the specific parameters of TC, offering customized strategies for their maintenance and operation. Such advancements highlight the importance of tribological data structures. Enhanced circulation, reuse, and sharing of tribological data will significantly boost research efficiency [2, 5, 7].

A robust foundation of tribological data is essential. Cutting-edge sensing technologies play a vital role in data acquisition. Among these, electrical signals are among the easiest to measure and interpret. Autonomous sensors—utilizing triboelectric effects, nanogenerators, and intelligent coatings—are emerging as key tools in active tribology for efficient data collection [6, 7]. If environmental and material factors influencing triboelectric signals (e.g., temperature, humidity, vibration frequency, and material properties) are properly addressed, autonomous sensors could become highly practical instruments for gathering tribological data [6, 7].

The application of triboinformatics approaches significantly improves the efficiency of particle detection, recognition and classification in ferrospectrometry. An algorithmic model was developed that automatically identifies and classifies wear particles, ensuring higher accuracy of analysis of ferrospectrometric studies [31, 34].

ANN was used for the particle recognition process, and particle classification was performed using the SVM method [30, 31]. In addition, a CNN method was created to classify seven types of ferrographic images. The proposed algorithm allows determining the degree of wear with an accuracy of up to 90% [6, 42].

The actual use of ferrographs can be complicated by the inconsistency of the obtained images, which negatively affects the accuracy of the analysis [31]. Also, the low data collection frequency affects the efficiency of real-time wear monitoring [42].

To solve these problems, a CNN with a large convolution kernel was used, which allows reducing the blurring effect due to defocusing during the acquisition of ferrographic images [42].

To implement reliable real-time wear monitoring, it is necessary to increase the volume of received ferrograph images. The Gaussian process regression approximation method was used, which provides an expansion of the data sample and wear prediction based on a large array of images [7].

Triboinformatics methods can be effective for solving other problems, in particular:

- identification of damage to friction surfaces [2, 5];
- optimization of the materials processing process [6, 28].

A set of acoustic data was collected during the reciprocating motion of tribocoupled parts, including bearings. The use of the RF method made it possible to identify three key stages of friction:

1. Initial running-in.
2. Stable operational state.
3. Active wear stage [36, 41].

Machine learning was used to optimize the friction material formula. And machine learning algorithms were used to quickly predict the width of the zone images of 2D materials, which facilitates the implementation of such materials in semiconductor devices.

Triboinformatics approaches can be applied in various aspects of tribology, such as:

- manufacturing processes [6, 10];
- development and optimization of lubricants [21, 32];
- materials processing technologies [5, 38];
- surface engineering [9, 40];
- applied tribotechnologies [6, 7].

To solve tribological problems, it is necessary to implement information solutions that include:

- monitoring of the condition of the friction material [13, 14];
- prediction of the behavior of the TrBS [6, 28];
- optimization of tribological parameters [5, 38].

To increase the efficiency of the TrBS, optimization algorithms are being developed, such as genetic algorithms and Bayesian optimization, which provide automatic adjustment of the TrBS parameters [40].

Thanks to machine learning algorithms, it is possible to analyze large volumes of operational data (temperature, humidity, load) and automatically determine the optimal settings, increasing the efficiency of the TrBS [37].

Automation in tribology and tribotechnology not only saves operators' time, but also minimizes the risk of human errors, ensuring stable operation of the mechanism [40].

The introduction of production robots into tribological systems requires providing them with AI algorithms, which allows achieving high accuracy and efficiency when performing complex tasks, such as:

- coating application [20];
- precise grinding of mechanical components [20].

The robots can also operate in extreme conditions, such as high temperature or elevated pressure, which makes them an ideal solution for hazardous production environments.

Integrating production process data into digital platforms helps minimize downtime and optimize resource management. These platforms, driven by AI algorithms, are able to predict production performance and adapt tribological processes in real time, which allows to compensate for the shortcomings of existing approaches [6, 7].

Conclusions

1. It was found that to implement effective monitoring of the state of friction, lubricating medium of tribological wear systems in real time, it is necessary to increase the amount of information received from sensors.

The method of Gaussian process regression approximation is used, which provides an expansion of the data sample and improves forecasting.

2. It is substantiated that triboinformatics approaches can be applied in various areas of tribology, such as production, development of innovative materials for tribological system parts, machine parts and mechanisms, lubricants, surface treatment and engineering of tribological systems. It is important to implement information solutions for monitoring the technical condition, predicting the behavior of innovative machines and mechanisms and optimizing the parameters of tribological systems.

3. It was found that optimization algorithms, including genetic algorithms and Bayesian optimization, allow you to automatically adjust the parameters of tribological systems, increasing their accuracy and efficiency. Thanks to artificial intelligence methods, it is possible to analyze large amounts of data on the operating conditions of machines and mechanisms of production systems and lines to determine the best settings.

4. It was determined that the introduction of digital platforms into production processes with increased tribological efficiency of tribo-coupled parts minimizes downtime of machines and mechanisms of elements and ensures effective resource management. Artificial intelligence allows you to predict production indicators and adapt processes in real time, which improves the performance of existing tribological systems.

5. Prospective developments in triboinformatics are anticipated to integrate methodologies such as regression analysis, classification algorithms, dimensional analysis, and predictive modeling. This convergence is expected to establish a cohesive framework that combines advanced tribological techniques with artificial intelligence-driven information technologies, thereby enhancing the precision of monitoring, forecasting, and optimization processes.

References

1. Zhang Z N, Yin N, Chen S, Liu C L. Tribo-informatics: Concept, architecture, and case study. *Friction* 9(3): 642-655 (2021)

2. Yin N, Xing Z, He K, Zhang Z. Tribo-informatics approaches in tribology research: A review. *Friction* 11(1): 1–22 (2023)

3. Marian M, Tremmel S. Current trends and applications of machine learning in tribology—A review. *Lubricants* 9(9): 86 (2021)

4. Paturi U M R, Palakurthy S T, Reddy N S. The role of machine learning in tribology: A systematic review. *Arch Comput Methods Eng* 30: 1345–1397 (2023)

5. Sose A T, Joshi S Y, Kunche L K, Wang F, Deshmukh S A. A review of recent advances and applications of machine learning in tribology. *Phys Chem Chem Phys* 25(3): 456–472 (2023)

6. Yin N, Yang P, Liu S, Pan S, Zhang Z. AI for tribology: Present and future. Friction 12: 1060–1097 (2024)

7. Rosenkranz A, Marian M, Profito F J, Aragon N, Shah R. The use of artificial intelligence in tribology—A perspective. Lubricants 9(1): 2 (2021)

8. Profito F J, Rosenkranz A. Artificial intelligence in tribology: Current status and future perspectives. Tribology International 174: 107005 (2022)

9. Gropper D, Wang L, Harvey T J. Hydrodynamic lubrication of textured surfaces: A review of modeling techniques and key findings. Tribology International 94: 509–529 (2016)

10. Bitrus S, Velkavrh I, Rigger E. Applying an adapted data mining methodology (DMME) to a tribological optimisation problem. Data Science – Analytics and Applications: 38–43 (2021)

11. Berman D, Deshmukh S A, Erdemir A, Sumant A V. Macroscale superlubricity enabled by graphene nanoscroll formation. Science 348(6239): 1118–1122 (2015)

12. Hölscher H, Ebeling D, Schwarz U D. Friction at atomic-scale surface steps: Experiment and theory. Phys Rev Lett 101(24): 246105 (2008)

13. Aulin V V, Kovalov S G, Hrynkiv A V, Varvarov V V. Algorithm for optimizing the reliability of functioning and efficiency of the use of production equipment using artificial intelligence methods. *Central Ukrainian Scientific Bulletin. Technical Sciences* 10(41), Part I: 60–67 (2024) [in Ukrainian]

14. Aulin V V, Kovalov S G, Hrynkiv A V, Varvarov V V. Increasing the reliability and efficiency of production lines using artificial intelligence methods, using acoustic signal monitoring. *Central Ukrainian Scientific Bulletin. Technical Sciences* 10(41), Part II: 142–151 (2024) [in Ukrainian]

15. Kovalov S G, Kovalov Yu G. Features of the implementation of the artificial neural network model by hardware means. *Science and Technology Today* 6(34): 1131 (2024) [in Ukrainian]

16. Kovalov S G. Optimization of production time using the reinforcement learning method as a particular case of improving the efficiency of automated production lines. *Central Ukrainian Scientific Bulletin. Technical Sciences* 11(42), Part I: 198–205 (2025) [in Ukrainian]

17. Jia D, Duan H T, Zhan S P, Jin Y L, Cheng B X, Li J. Design and development of lubricating material database and research on performance prediction method of machine learning. *Sci Rep* 9(1): 20277 (2019)

18. Xie H B, Wang Z J, Qin N, Du W H, Qian L M. Prediction of friction coefficients during scratch based on an integrated finite element and artificial neural network method. *J Tribol* 142(2): 021703 (2020)

19. Liu X, David I. AI Simulation by Digital Twins: Systematic Survey, Reference Framework, and Mapping to a Standardized Architecture. *J Softw Syst Model* (2025)

20. Chang H C, Borghesani P, Peng Z X. Automated assessment of gear wear mechanism and severity using mould images and convolutional neural networks. Tribology International 147: 106280 (2020)

21. Luo D B, Fridrici V, Kapsa P. A systematic approach for the selection of tribological coatings. *Wear* 271(9–10): 2132–2143 (2011)

22. Šabanovič E, Žuraulis V, Prentkovskis O, Skrickij V. Identification of road-surface type using deep neural networks for friction coefficient estimation. *Sensors* 20(3): 612 (2020)

23. Van Rossum G, Drake F L. *Python 3 Reference Manual*. Python Software Foundation (2009)

24. Abadi M et al. TensorFlow: Large-scale machine learning on heterogeneous systems. *arXiv* preprint *arXiv*:1603.04467 (2016)

25. Paszke A et al. PyTorch: An imperative style, high-performance deep learning library. *NeurIPS* 32: 8024–8035 (2019)

26. Virtanen P et al. SciPy 1.0: Fundamental algorithms for scientific computing in Python. *Nat Methods* 17: 261–272 (2020)

27. Hunter J D. Matplotlib: A 2D graphics environment. *Comput Sci Eng* 9(3): 90–95 (2007)

28. Hasan M S, Kordijazi A, Rohatgi P K, Nosonovsky M. Triboinformatic modeling of dry friction and wear of aluminum base alloys using machine learning algorithms. *Tribol Int* 161: 107065 (2021)

29. Wu D Z, Jennings C, Terpenny J, Gao R X, Kumara S. Tool wear prediction using random forests. *J Manuf Sci Eng* 139(7): 071018 (2017)

30. Zhang Z H. Introduction to machine learning: k-nearest neighbors. *Ann Transl Med* 4(11): 218 (2016)

31. König F, Sous C, Chaib A O, Jacobs G. Machine learning based anomaly detection and classification of acoustic emission events for wear monitoring in sliding bearing systems. *Tribol Int* 155: 106811 (2021)

32. Chimeno-Trinchet C, Murru C, Díaz-García M E, Fernández-González A, Badía-Laíño R. AI and FTIR spectroscopy for evaluating lubricant degradation. *Talanta* 219: 121312 (2020)

33. Kilundu B, Dehombreux P, Chiementin X. Tool wear monitoring by machine learning techniques and singular spectrum analysis. *Mech Syst Signal Process* 25(1): 400–415 (2011)

34. Yuan W, Chin K S, Hua M, Dong G N, Wang C H. Shape classification of wear particles by image boundary analysis using machine learning algorithms. *Mech Syst Signal Process* 72–73: 346–358 (2016)

35. Borjali A, Monson K, Raeymaekers B. Predicting the polyethylene wear rate in pin-on-disc experiments in the context of prosthetic hip implants: Deriving a data-driven model using machine learning methods. *Tribol Int* 133: 101–110 (2019)

36. Moder J, Bergmann P, Grün F. Lubrication regime classification of hydrodynamic journal bearings by machine learning using torque data. *Lubricants* 6(4): 108 (2018)

37. Zhang H, Nguyen H, Bui X N, Pradhan B, Asteris P G, Costache R, Aryal J. A generalized artificial intelligence model for estimating the friction angle of clays in evaluating slope stability using a deep neural network and Harris Hawks optimization algorithm. *Eng Comput*: 1–14 (2021)

38. Thankachan T, Soorya Prakash K, Kavimani V, Silambarasan S R. Machine learning and statistical approach to predict and analyze wear rates in copper surface composites. *Met Mater Int* 27(2): 220–234 (2021)

39. Bellotti M, Wu M, Qian J, Reynaerts D. Tool wear and material removal predictions in micro-EDM drilling: Advantages of data-driven approaches. *Appl Sci* 10(18): 6357 (2020)

40. Kronberger G, Kommenda M, Lughofer E, Saminger-Platz S, Promberger A, Nickel F, Winkler S, Affenzeller M. Using robust generalized fuzzy modeling and enhanced symbolic regression to model tribological systems. *Appl Soft Comput* 69: 610–624 (2018)

41. Hamrol A, Tabaszewski M, Kujawińska A, Czyżycki J. Tool Wear Prediction in Machining of Aluminum Matrix Composites with the Use of Machine Learning Models. *Materials* 2024, 17(23): 5783.\

42. Cardoz B et al. Tool wear classification using vibration signals and RF. *Int J Adv Manuf Technol* 126: 3069–3081 (2023)

Аулін В.В. , Ковальов С.Г., Гриньків А.В., Ковальов Ю.Г., Головатий А.О., Кузик О.В., Слонь В.В. Підвищення ефективності трибологічних систем за допомогою інтелектуального аналізу даних та прогностичного моделювання

У статті проведено систематизований аналіз застосування інформаційних технологій у трибології, включаючи традиційні методи, машинне навчання та штучний інтелект. Основною метою дослідження є узагальнення та класифікація методів трибоінформатики для підвищення ефективності аналізу трибологічних процесів. Методика ґрунтується на огляді ключових алгоритмів (ANN, опорні векторні машини, методи K – найближчих сусідів, метод випадкового лісу), визначенні їх ролі у трибологічних дослідженнях та аналізі інформації, спрямованої на моніторинг технічного стану, прогнозування поведінки та оптимізацію трибологічних систем. Визначено, що застосування алгоритмів штучного інтелекту та машинного навчання суттєво покращує точність діагностики трибологічних систем, дозволяє прогнозувати їхній експлуатаційний ресурс та оптимізувати робочі параметри трибологічних систем та механізмів машин. Наведено класифікацію методів трибоінформатики відповідно до їх функцій: регресія, класифікація, кластеризація, зниження розмірності. Це дає змогу визначити найбільш ефективні підходи для різних типів трибологічного аналізу. Практична спрямованість використання інтелектуальних методів моделювання полягає у можливості інтеграції отриманих результатів у виробничі процеси, що сприяє підвищенню надійності механічних систем, скороченню витрат на їх обслуговування та створенню більш точних методів прогнозування трибологічних характеристик, властивостей та трибологічної ефективності функціонування вузлів систем і агрегатів машин та механізмів. Показано, що, трибоінформатика відкриває нові перспективи для вдосконалення трибологічних досліджень, забезпечуючи більш точний моніторинг, ефективне прогнозування та оптимізацію трибологічних систем.

Ключові слова: трибологічна система, моніторинг технічного стану, моделювання та прогнозування, тертя, зношування, штучний інтелект, машинне навчання.

ISSN 2079-1372 Problems of Tribology, V. 30, No 3/117-2025, 62-68

Problems of Tribology
Website: http://tribology.khnu.km.ua/index.php/ProbTrib
E-mail: tribosenator@gmail.com

DOI: https://doi.org/10.31891/2079-1372-2025-117-3-62-68

Self-lubricating glass composite magnesium carbide nanocoating

V.V. Shchepetov[1] 0000-0002-8352-8307, **N.M. Fialko**[1] 0000-0003-0116-7673, **S.S. Bys**[2] 0000-0002-7518-3310

[1] *Institute of Technical Thermophysics of the National Academy of Sciences of Ukraine, Kyiv*
[2] *Khmelnytskyi National University, Khmelnytskyi*
**E- mail : serhiibys@gmail.com*

Received: 05 August 2025: Revised 30 August 2025: Accept: 10 September 2025

Abstract

The results of the study of the friction and wear characteristics of the developed nanostructured glass composite self-lubricating coatings are presented, the structural components which through magnesium carbide have a qualitative effect on the graphitization process due to the formation of a surface layer of carbide α-graphite, which, when combined with surface oxides characterized by low shear resistance, performs the role of solid lubricants under friction conditions. The positive role of the glass phase in the form of aluminoborosilicate, which affects the tribotechnical properties of coatings, has been established. It has been determined that the increase in adhesion strength is achieved by forming a surface layer of vitreous sodium silicate during spraying. It has been found that the intercalation of the graphite layer with dispersed particles of the surface structure does not significantly affect the tribotechnical characteristics. The developed nanostructured glass composite coatings showed high antifriction characteristics.

Keywords: wear intensity, glass composite, nanostructure, wear, glass phase.

Introduction

Preservation of operational characteristics limited by friction and wear, both of individual components and of technical systems as a whole, can be ensured by modern surface engineering tools that implement the basic principle of minimum costs for maximum results. Structural engineering methods that use modification through the use of solid lubricants have achieved significant success in recent years in ensuring antifriction properties of contact joints. Coatings containing solid lubricants are among the innovative and most promising antifriction materials, the high quality of which is especially noticeable in conditions operation where traditional liquid lubricants are not very effective [1,2]. They are used in various fields of engineering from lubricating precision aircraft mechanisms to preventing seizure of threaded joints [3,4].

Development of anti-friction nanostructured glass composite coatings, having self-lubricating properties due to solid lubricating compounds based on graphite, meets modern priorities of tribotechnical materials science, aimed at increasing the wear resistance of moving joints and development scientific and applied solutions in the interests of improving the efficiency of the application of high-quality production technologies [5,6].

The purpose of the work

Research on the structural-phase composition and surface secondary structures of glass composite nanocoatings and their effect on the self-lubrication process under friction conditions.

Materials and research methods

As is known from the comparative characteristics of gas-thermal coatings, similar in structural and phase composition, the maximum operational properties are possessed by detonation-gas coatings [7]. Therefore, for spraying the studied coatings, the technology of detonation-gas spraying of nanostructured powders of the SiC-Ni-Cu-Al-Si-C composition with a uniform distribution of the aluminoborosilicate glass phase (SiO_2-Al_2O_3-B_2O_3) was used. Structurally free magnesium carbide (MgC_2) was added to the nanoglass composition obtained by the mechanical method, after which it was mixed, ensuring its uniform distribution in the resulting powder mixture

ready for spraying. All components of the powder materials used in the work were taken from the mineral raw material base of Ukraine.

The self-lubricating properties of the coatings were evaluated when rubbing ring samples according to the end scheme under conditions of distributed contact in a continuous sliding mode at a constant load of 10.0 MPa. The influence of the environment, speed, and load implemented during the tests were selected taking into account the maximum approximation of the processes of physicochemical mechanics of friction to real conditions of contact interaction. In addition, the research program of nanostructured glass composite coatings with magnesium carbide provided for a comparative analysis of their parameters with similar values obtained during tests of coatings of the WK15 type and coatings sprayed with doped nichrome powder.

The study of contact joints, in which the processes of activation occur during friction, which determine the intensity of surface heterophase configuration reactions and tribochemical phenomena, was carried out by modern methods of physical analysis, which include metallography (optical microscope type Neophot-32 with a prefix), X-ray electron micro analyzer type "Camscan 4DW" with a program for the distribution of chemical elements. Determination of the phase composition of surface layers was carried out on a general-purpose X-ray diffractometer type DRON-3 with monochromatized CuKα radiation.

The increase in adhesion strength, as a criterion for the performance of glass composite coatings, was carried out by preliminary application of a sub layer of vitreous sodium silicate $Na_2O(SiO_2)_2$ to the working surface. The exclusion of unproductive losses and compliance with the measurement technology [8] determined the correctness of the obtained adhesion strength results, which amounted to 140-145 MPa.

Research results and their discussion

The contact interaction of surfaces is a complex sequence of mutual influence of both external factors and internal transformations, the qualitative coordination of which reflects the commonality of quantitative patterns and determines their ordered causal relationship. According to the results of the interaction of coatings under friction loading, fig. 1 gives experimental values that reflect the averaged functional dependences of the wear intensity and friction coefficients, which change in time and stabilize after running-in, in the field of sliding speeds at a constant load equal to 10.0 MPa. As can be seen from the graph, in the entire range of tests at a monotonically increasing sliding speed, the minimum parameters of wear intensities and the corresponding friction coefficients are characteristic of glass-composite nano coatings (curves 1 and 1'). The structure of the glass composition, which determines their properties, consists of a finely dispersed mixture, which represents solid solutions and, mainly, intermetallic compounds in the presence of a glass phase. The constancy of the chemical composition and the constancy of the properties of technological spraying determine the stability of the structure of the coatings, the relative density of which reaches 98%. The cross-section of the glass composite nanocoating is presented in fig. 2. Metallographic analysis has established that the sprayed layer has a quasi-ordered lamellar appearance and fits tightly to the base material, completely copying the surface relief, while the accumulation of component oxides, as well as slag contamination, are virtually absent, and defects in the form of pores and cracks are not detected.

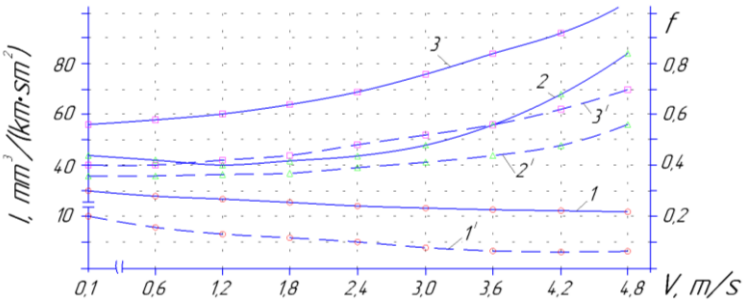

Fig. 1. Dependence of wear intensity (1, 2, 3) and friction coefficient (1', 2', 3') on the sliding speed of SiC-Ni-Cu-Al-Si-C+glass phase+MgC2 coatings (1,1'), WC-Co (2,2') and Ni-Cr-Al-B (3,3') on the sliding speed (P=10.0MPa).

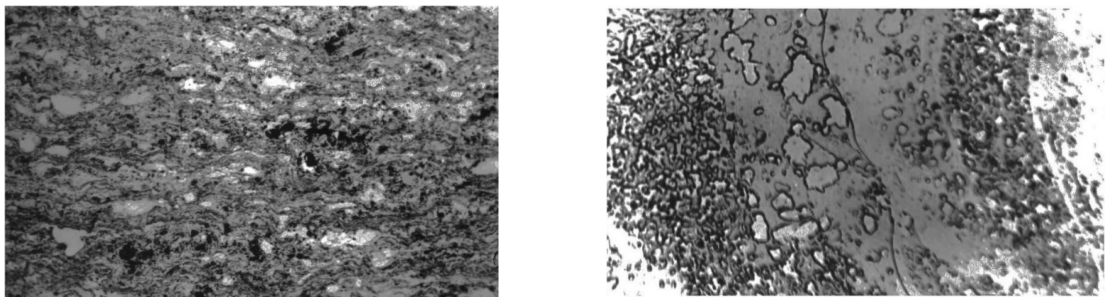

a **b**

Fig. 2. Coating structure: a x 320; b x 5000

The micro geometry of the working surface of the nanocoatings under study, in combination with their physical and mechanical properties, determines their operational state. Studies have shown that during the running-in process, the initial technological relief disappears, the chemical composition, structure of the surface layer and its geometry radically change. It is possible to determine that running-in is one of the manifestations of the self-organization process, in which the quasi-relaxation of the surface structure from the equilibrium state will pass to a stable state. At the same time, a new surface quality is formed, characterized by the formation of balanced roughness, which is not only optimal for specific friction conditions, but also ensures stable wear in the entire range of tests.

The problem of coating performance is related to the quality of reproducibility and optimization of the spraying process. Changing the technological modes leads to changes in the properties of the coatings. To obtain high-quality coatings by optimizing the technological process, processing of technological parameters, such as particle size distribution, loading depth, barrel filling degree, working gas ratio, spraying distance [9], is implemented.

Synthesis and research of solid solutions based on refractory compounds, in particular silicon carbide, are being carried out quite intensively, however, the capabilities of the latter and its complex of tribotechnical properties are far from the expected results [10]. Thus, by controlling the technological process of forming glass composite nanocoatings, it was possible to implement not only the desired chemical composition, but also to obtain the predicted stable structure. Which optimizes the complex of properties that determine the manifestation of structural adaptability. At the same time, the possibility of obtaining constant quality was achieved, namely, the variation of strength and plastic properties in samples of one batch was stably 5-10%.

The developed glass composite is an antifriction material with a finely dispersed structure. It is generally accepted that elastic-plastic deformation is the main factor determining the development of the external friction process, and in addition, in our opinion, the formation of a gradient structure is a derivative of it. It can be said that the evolution of the structure during contact interactions has pronounced scale levels, and the processes occurring at different scale levels are mutually dependent. The layer-by-layer picture of plastic deformation, obtained by the diffraction method, reveals the main patterns of the formation of a scale structure and allows us to establish uniform transitions from a dispersed polycrystalline fragmented structure on the surface through intermediate textured layers to the initial crystalline structure inherent in the deep material. In the studied coating, as the friction surface approaches and the contact pressure and deformation intensity increase, the structure gradually changes to an ultra disperse one. At the same time, high contact compressive and shear stresses create conditions for the realization of significant plastic deformations in the surface layer of the coating material, which lead to the formation of ultra disperse structures.

This gives grounds to distinguish in the structure subjected to tribotechnical loads, a near-surface zone in which deformation processes developing in micro volumes in homogeneously form a specific layer at the near-surface level, in which structural-thermal activation causes a complex of physicochemical interactions that determine the accompanying and dominant type of wear. The near-surface zone has a structurally inhomogeneous fine-dispersed composition.

As shown by the results of micro-X-ray spectral analysis (MRSA) performed on the CamebaxSX installation, the basis of the nanoglass composition is silicon carbide of non-stoichiometric composition, along the grain boundaries of which silicate compounds are located, among which inclusions corresponding to the composition of silicon dioxide predominate, also in the carbide structure the role of dispersedly strengthened components is performed by Al_2O_3 oxides distributed along the boundaries and intermetallic inclusions in the form of spherical nanograins. But the high thermo mechanical properties of SiC carbide are discredited by significant fragility. We have noted that the solid substitution solution formed by Al and SiC causes a slight distortion of the crystal lattice of the carbide, since the differences in the masses of Al and Si atoms are extremely small, as a result of which the micro hardness does not change, and the plasticity increases. Cu and Ni have a similar effect on the composition of SiC, which form solid substitution solutions by replacing Si atoms. The formation of phases in the coating, as shown by the tests, is determined not only by the ratio of components, temperature, dispersion, but also depends on their defectivity and external conditions. It is undeniable that tribochemical interaction occurs when molecules receive the necessary activation energy. Endothermic reactions do not occur without activation at all. The interaction of SiC with Mg, which is formed during the thermal decomposition of structurally free magnesium carbide under running-in conditions and depends on the process temperature, is accompanied by the formation of magnesium silicide and magnesium acetylide, the latter under the influence of thermo mechanical interactions promotes the formation of graphite through the intermediate dimagnesium tricarbide ($2SiC+5Mg \rightarrow 2Mg_2Si+MgC_2$, $MgC_2 \rightarrow Mg_2C_3 \rightarrow Mg+C$). It should be noted that under thermodynamic action, the presence of a catalyst in the form of Al in the structure promotes the decomposition of magnesium carbide. The basis of physical phenomena that initiate the mechanism of decomposition of carbide graphite are structural transformations in the solid phase caused by thermal influences. The factors that determine the quality level of thermo mechanical carbide graphitization, in our opinion, include the degree of dispersion of structural components, specific pressure, operating temperature, and temperature in the contact zone, the presence of elements that initiate decomposition processes, as well as the influence of the environment (in a vacuum, the probability of the amount of graphite increases), in addition, internal factors related to the composition of the

material, its structure, the presence of defects, etc. In fig. 3 the topography of the friction surfaces obtained at sliding speeds of 0.5 m/s and 0.17 m/s is given. The antifriction layer of graphite, as can be seen, covers almost the entire working surface with all its capacity, ensuring an increase in the actual contact area, contributing to a decrease in the specific load due to an increase in the support length due to filling and leveling micro-irregularities and fixing graphite micro particles in micro-cavities. The contact zone, which is the surface layer (initial scale level), which separates the coating material from the antifriction film consisting of polydisperse graphite particles, represents a deformed zone, which, according to the results of micro-X-ray spectral analysis performed on MAP-3 (probe diameter 1 μm), represents finely dispersed heterogeneous structural-phase compounds of the components. Among which the presence of Ni as a structural component is due to its specific properties, namely, at the spots of actual contact when the temperature reaches 450-500°C depending on the dispersion and external influences in the conditions of a local high-temperature field, Ni interacts with SiC, forming metal-enriched nickel silicides (Ni_2Si). As a result, carbon is reduced, which is transformed into a solid phase of elementary polydisperse graphite colonies, combined into surface structures.

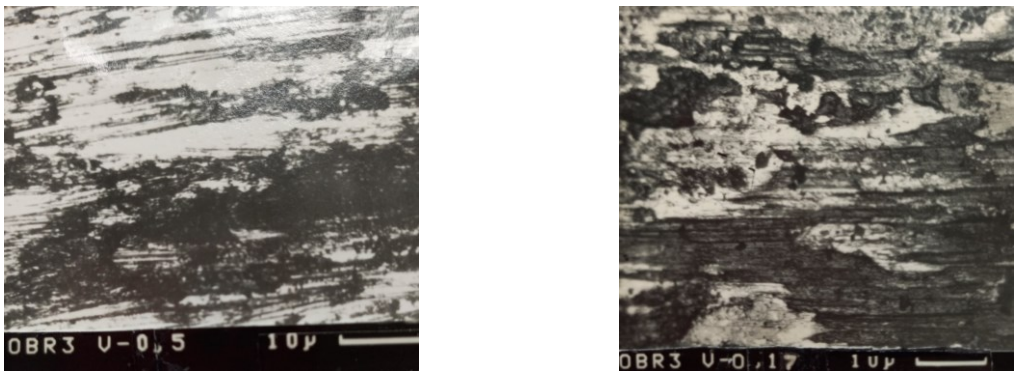

a **b**

Fig. 3. Friction surface topography at formation of graphite film: a – V=0.5 m/s; b – V=1.7 m/s

But the dominant component of the formation of the antifriction surface layer, consisting of a carbon product - graphite, remains magnesium carbide. The value of the specific work of wear, characteristic of the initial moment of running-in, as calculations have shown, is up to 10 kJ/mm^3, which is both a necessary and sufficient condition for the initiation of thermal decomposition of MgC_2, which leads to the formation of carbon in the form of a solid phase.

Using the natural ability of chemical elements to graphitize through the formation of carbide graphite, we obtained a high-quality, anti-friction layer that determines the operational properties of the coatings.

In the structural-phase study of glass composite coatings, the presence of intermetallic compounds based on Al and Ni of the NiAl and Ni_2Al_3 type was noted, while monoaluminide, which is a high-temperature phase, has significant hardness, as measurements showed, most likely close to 3.8 GPa. The presence of an ordered solid solution based on nickel monoaluminide was also established, which has an Al content of ~ 20-25 wt. %, which causes increased plasticity. According to the results of elemental and X-ray phase analyses, the presence of a solid solution of Ni in Cu was noted, but their compounds were not detected. Solid solutions of Ni in Si and Si in Ni, as well as their intermetallics Ni_2Si, Ni_3Si_2, $NiSi_2$ were established. In addition, the presence of small quantities of colonies of solid solutions of Si in Cu has been proven, and the formation of their chemical compounds such as copper silicates is also likely, since the structural micro hardness is significantly increased, but identifying them presented significant difficulties.

Aluminoborosilicate glass powders, the dispersion of which was 25-30 microns, in the process of mechanochemical treatment and thermo mechanical impact, as products of inorganic synthesis, caused, as was determined, along with the preservation of the initial components, the formation of new stable compounds from solid solutions of Al_2O_3 and SiO_2 with an orthorhombic syngony, which is close to the structure of sillimanite, most likely this is lower mullite, obtained by a reaction as a result of the interaction of oxidation products of the initial components. From the point of view of glass-ceramic technologies, the greatest interest, in our opinion, is the presence of components that form refractory metal oxides and primarily Al and Si oxides. The presence of B_2O_3, which, as a result of partial oxidation, became part of the solid solution Al_2O_3-B_2O_3, was also established.

From the perspective of condensed matter physics, the addition of a glassy component affects the quality of the coating material through the structural state and, as practice shows, interest in these technical products is steadily growing. When studying glass compositions, their optimal composition was established experimentally, in which the rational use of glass structures contributes to increased heat resistance and chemical stability, in addition, the manifestation of high cohesive strength, increased density of nanocomposites, crack resistance and, with significant corrosion resistance, ensures high adhesion (more than 127 MPa) with materials of different chemical nature, in addition, the formation of a silicate barrier layer prevents mutual diffusion of structure-forming particles of the coating and the substrate.

The surface zone, directly adjacent to the friction surface and separating the coating material from the antifriction layer, consisting of polydisperse graphite particles, is the thinnest film with a thickness of several micrometers. Studies have shown that the pressure in it is uneven, and the areas of tensile and compressive stresses, which are inevitable under conditions of deformation of heterogeneous phases, are close in structure to a conglomerate of finely dispersed (quasi-amorphous) structures, having dimensions in the range of 5-15 nm, and are mechanical mixtures, without oxygen and oxide compounds of the structure-forming components. The effect of plastic deformation is associated not only with the dispersion of the surface zone, but also with the accumulation of defects that change its physicochemical properties, including reactivity, and affect the intensity of chemical reactions in the solid phase.

At the same time, the thermal conductivity of the finely dispersed conglomerate has increased porosity and forms a lower near-surface zone than that of the solid material, therefore the heating temperature of the finely dispersed fragments of the zone is higher than the temperature of the surface areas.

The temperature factor stimulates physicochemical processes, in particular, the reactive diffusion of structure-forming particles at the atomic-molecular level, which promotes the penetration of kinetically active components of the dispersed zone due to the weakening of the bond between polyarene planes into the interlayer space of graphite and, thus, the formation of intercalated graphite.

By the method of X-ray phase analysis, it was established that the intercalating elements in the subsurface zone-graphite system, at the initial stage of the process, appeared ions Mg_2+, Al_3+, Cu_2+, which randomly penetrate into the interlayer space of the graphite matrix. At sliding speeds of more than 3.0 m/s, intercalates of binary molecular compounds of these elements with oxygen were found in the layered graphite system. Their intercalation is accompanied by a sequence of repeating stages, which, when changing the tribotechnical parameters, are reversible and are characterized by a specific transformation of the structure and, first of all, an increase in the distance between the layers due to the influence of various types of interlayer defects and the penetration of intercalants. It should be noted that today there is no general model of intercalation that explains the electrochemical mechanism of the synthesis of layered systems. From an energetic point of view, the intercalation process, which represents reversible topotaxis chemical reactions, can be considered as an adequate mechanism for the self-organization of surface layers in the process of structural adaptability of the friction system.

We have established that the level of quantitative changes during the intercalation of the graphite layer, which determines the high level of antifriction, does not affect the qualitative values of tribotechnical parameters during the testing process to the expected extent.

Antifriction nanostructure glass-ceramic self-lubricating coatings have been developed, which contain magnesium carbide and structural components that promote surface graphitization, do not contain expensive and scarce components, meet environmental safety requirements, and provide high performance properties. From our considerations, the developed and researched self-lubricating glass composite nanocoatings can be considered as an alternative to other promising materials for operation in modern designs of tribotechnical systems..Their application most effectively for increasing the operational reliability of friction units, for example, moving parts of control mechanisms, cams, pairs with reciprocating movement, sliding supports, lever parts, high-speed and thermally loaded couplings, in which the use of traditional lubricants is undesirable.

The development of nanostructured glass-ceramic antifriction self-lubricating coatings, the justification of their structural components, the results of applied tests, and the ability to work in production conditions allows us to significantly expand the arsenal of achievements in modern tribotechnical materials science.

It should be noted that a nanostructured glass composite powder has been developed, which contains magnesium carbide, can be used to strengthen and restore worn parts of any shape and design, using any technological methods that use powder materials.

Conclusions

1. The developed and investigated glass composite nanocoatings, which are characterized by stable and minimal values of friction coefficients and wear intensities under test conditions at a sliding speed of up to 5.0 m/s and a load of 12.5 MPa, have friction parameters significantly lower than those for control coatings by almost 3.5-8.0 times.

2. Through theoretical and experimental studies, the optimal structural-phase composition of nanostructured coatings of the SiC-Ni-Cu-Al-Si-C system, containing a glass phase of the SiO_2-Al_2O_3-B_2O_3 type and structurally free magnesium carbide, was implemented. At the same time, to improve the adhesion strength, a sublayer of vitreous sodium silicate was applied to the substrate. At the same time, the role of the glass phase in the formation of glass compositions was studied, which contributes to an increase in the cohesive component, continuity and strength of the nanostructure, and increased chemical resistance.

3. It is noted that the assessment of the quality of the studied coatings is associated with the problem of reproducibility of the technological process. By controlling the spraying of glass composite powders, it turned out to be possible to provide not only the required chemical composition, but also to obtain a given nanostructure that optimizes the complex of properties that contribute to the stable manifestation of the minimization of tribotechnical

parameters in conditions of structural adaptability. It is also noted that the variation of strength and plastic properties in the sprayed samples was stable and amounted to 5-10%.

4. The physical mechanism and main factors determining the level of thermo mechanical graphitization are considered. The nature and regularities that determine the tendency of coatings to passivation are studied. It is noted that its implementation is carried out both due to solid-phase tribochemical reactions, which cause the formation of quasi-spherical polydisperse surface films integrated on the basis of carbide graphite and dispersed oxide compounds.

5. The structural and phase composition of glass composite nanocoatings was investigated by means of physicochemical analysis, their fine-dispersed structure was established, while it was emphasized that the components of the composite particles are solid solutions based on binary oxides and inclusions of chemical compounds of simple and complex carbides and intermetallics, as well as mechanical mixtures of component compounds. These components have increased temperature stability, significant hardness and strength, and chemical inertness.

6. Fundamental ideas about the formation and structure of antifriction surface structures based on dispersed carbide graphite have been supplemented, which has allowed us to expand the arsenal of achievements in modern tribotechnical materials science.

References

1. Mayur A. Makhesana, KM Patel Performance assessment of CaF_2 solid lubricant assisted minimum quantity lubrication in turning. // Procedia Manufacturing 33 (2019) 43–50. doi.org/10.1016/j.promfg.2019.04.007.

2. I. Justin Antonyraj D. Lenin Singaravelu Tribological characterization of various solid lubricants based on copper-free brake friction materials – A comprehensive study. Materials today.Volume 27, Part 3, 2020, Pages 2650-2656.doi.org/10.1016/j.matpr.2019.11.088.

3. Qunfeng Z., Lili Z. Improving the Antifriction Behaviors of Steel by Hybrid Treatments of MoS_2 and Surface Texture \\ Journal of Modern Mechanical Engineering and Technology, v. 10, 2023.- pp. 21-25.

4. Maciej Matuszewski, Małgorzata Słomion, Adam Mazurkiewicz and Andrzej Wojciechowski Mass wear application of cooperated elements for evaluation of friction pair components condition. Mechanical Engineering. MATEC Web of Conferences 351, 01006 (2021). doi.org/10.1051/matecconf/202135101006.

5. Wear of Composite Materials. DE Gruyter, Berlin, 2018. ISBN 978-3-11-035298-63.

6. Kostornov V.G. Tribotechnical materials science. - Luhansk: "Knowledge", 2012.-701 p.

7. Vilhena, L.; Ferreira, F.; Oliveira, JC; Ramalho, A. Rapid and Easy Assessment of Friction and Load-Bearing Capacity in Thin Coatings. Electronics 2022, 11, 296. doi.org/10.3390/electronics11030296.

8. Zaytsev A.N., Aleksandrova YP, Yagopolskiy AG Comparative Analysis of Methods for Assessing Adhesion Strength of Thermal Spray Coatings. BMSTU Journal of Mechanical Engineering.5(734)/2021-p48-59. DOI:10.18698/0536-1044-2021-5-48-59.

9. Trefilov V.Y., Kadyrov V.Kh. Operational properties of detonation coatings. K.: Znanie, 1981.-29p.

10. Pogrebnjak AD, Beresnev VM Hard Nanocomposite Coatings Their Structure and Properties\\ Nanocomposites: New Trends and Developments.-2012.- Ch.6.-p. 123-160.

Щепетов В.В. , Фіалко Н.М. , Бись С.С. Самозмащувальні склокомпозиційні нанопокриття з карбідом магнію.

Наведено результати дослідження характеристик тертя та зношування розроблених наноструктурних склокомпозиційних самозмащувальних покриттів, структурні складові яких через карбід магнію мають якісний вплив на процес графітизації за рахунок утворення поверхневого шару карбідного α-графіту, який при спільній дії з поверхневими оксидами, що визначаються низьким зсувним опором, виконують в умовах тертя роль твердих мастил. Встановлено позитивну роль склофази у вигляді алюмоборосилікату, що впливає на триботехнічні властивості покриттів. Визначено, що підвищення адгезійної міцності досягається за рахунок формування при напилюванні поверхневого шару зі склоподібного силікату натрію. З'ясовано, що інтеркаляція графітового шару дисперсними частинками поверхневої структури суттєво не впливає на триботехнічні характеристики. Розроблені наноструктурні склокомпозиційні покриття показали високі антифрикційні характеристики.

Ключові слова: інтенсивність зношування, склокомпозит, наноструктура, знос, скло фаза.

ISSN 2079-1372 Problems of Tribology, V. 30, No 3/117-2025, 69-75

Problems of Tribology
Website: http://tribology.khnu.km.ua/index.php/ProbTrib
E-mail: tribosenator@gmail.com

DOI: https://doi.org/10.31891/2079-1372-2025-117-3-69-75

The effect of polyimide fibre on the tribological properties of polytetrafluoroethylene

A.-M.V. Tomina[1]0000-0001-5354-0674, **K.R. Voloshina**[1]0009-0007-8929-2191, **Predrag Dašić**[2]0000-0002-9242-274X, **Yu.E. Hranitskyi**[1]0009-0000-2338-624X

[1]*Dniprovsk State Technical University, Kamyanske, Ukraine*
[2]*Academy of Professional Studies Šumadija – Department in Trstenik, Trstenik, Serbia*
E-mail: an.mtomina@gmail.com

Received: 15 August 2025: Revised 10 September 2025: Accept: 20 September 2025

Abstract

The article investigates the effect of discrete polyimide fibre on the tribological properties of polytetrafluoroethylene under friction conditions without lubrication, using the "disk-pad" scheme. It was found that the introduction of 2.5-12.5 vol% filler contributes to a significant increase in the wear resistance of polytetrafluoroethylene, up to 370 times. At the same time, the friction coefficient increases slightly, reaching a maximum value at a fibre content of 7.5 vol%. The decrease in the linear wear intensity of polytetrafluoroethylene is due to an almost twofold increase in hardness. We can explain the improvement in wear resistance by the formation of strong intermolecular bonds at the "matrix-fibre" interface, increased structural uniformity, and the formation of a stable transfer film during friction. Morphological analysis of the friction surfaces confirmed a reduction in the intensity of damage for the filled composites. On the surface of pure polytetrafluoroethylene, traces of plastic deformation, numerous plowing grooves, and signs of micro-cutting were observed, indicating the prevalence of the adhesive-fatigue wear mechanism. In contrast, the composite surfaces are characterized by a smaller number and depth of defects, which suggests a reduced influence of the adhesive component of the friction force and a transition to a pseudo-elastic wear mechanism. However, when the fiber content exceeds 10 vol.%, the material properties deteriorate due to the non-uniform distribution of the filler and the formation of structural defects. For polymer composite materials with an effective fibre content of 7.5 vol%, a set of tribological tests was conducted to determine the critical values of sliding speed and load that affect the linear wear intensity.

Keywords: polytetrafluoroethylene, polyimide fibre, volume percentage, linear wear intensity, friction coefficient, hardness

Introduction

Modern agricultural, metallurgical, and machine-building industries face an acute shortage of tribotechnical materials capable of operating effectively under conditions of high loads, sliding speeds, temperatures, and especially limited or complete absence of lubrication. Such materials must be manufactured using accessible and economically feasible technologies, cheap and environmentally safe raw materials, and meet safety requirements for human health and the environment. In this regard, the development of new tribotechnical materials that meet the specified criteria is an extremely urgent scientific and technical task. One of the promising areas in this field is the use of polymer composite materials (PCMs). Depending on the type of polymer matrix, shape, nature, content, and arrangement of the filler (Fl), such materials can provide the necessary functional properties. When creating tribotechnical materials with high tribological properties, polytetrafluoroethylene (PTFE) is often used as a polymer matrix [1–3].

In its pure form, PTFE usually does not provide a sufficient level of functional properties, so various dispersed (for example, graphite, molybdenum disulfide, boron nitride, shungite) and fibrous (for example, fibreglass, carbon and organic fibres) Fls are introduced into its composition. These materials are characterised by high wear resistance under friction conditions without lubrication, a low coefficient of thermal linear expansion, resistance to the influence of many aggressive environments, as well as stable operation in a wide temperature range (from 203 to 543 K). Experience proves that replacing serial materials with composites based on

polytetrafluoroethylene allows increasing the resource of effective operation and reliability of operation of tribological connections of the agricultural, metallurgical, and machine-building equipment. Therefore, the search for new PCMs based on polytetrafluoroethylene is relevant and promising [4-6].

The purpose of the work

Considering the above, the purpose of this work is to study the effect of the percentage of fibrous filler – polyimide fibre – on the tribotechnical characteristics of polytetrafluoroethylene under friction conditions without lubrication.

Objects and methods of research

PTFE manufactured by Shandong Dongyue Polymer Material Co., Ltd (China) was chosen as a polymer matrix for the PCM. PTFE is obtained by polymerisation of tetrafluoroethylene ($C2F_4$) – a colourless, odourless gas [7], which is formed when chlorodifluoromethane ($CHClF_2$) is heated in the temperature range of 873–973 K. Chlorodifluoromethane, in turn, is synthesised by the reaction of hydrogen fluoride (HF) with chloroform ($CHCl_3$). The resulting tetrafluoroethylene monomers (small monoatomic molecules) are suspended or emulsified in water, and then polymerised – connected into high-molecular chains – under high pressure in the presence of free radical reagents. The main chain of PTFE consists of carbon atoms (C), each of which is connected to two fluorine atoms (F). Fluorine atoms, surrounding the carbon chain, act as a membrane, forming a chemically inert and relatively dense molecule with very strong C-F bonds [8].

A discrete (3 mm) polyimide (PI) fibre was chosen as a filler. It has excellent mechanical and thermal properties (see Table 1), and it is resistant to corrosion and ultraviolet radiation. Due to this, PI fibres have advantages over other high-quality polymer fibres in harsh operating conditions and have broad prospects for application in the aerospace field, environmental protection, and other industries [9, 10].

Table 1

Properties of polyimide fibre

Index	Value
Density, g/cm^3	1,3
Melting, inflection, decomposition or chemical transformation temperature, K	873
Elongation during stretching, %	6-8
Tensile strength, GPa	0,62-2,0
Tensile modulus, GPa	9-20

The production of samples of pure polytetrafluoroethylene and PCMs based on it, containing 2.5-12.5 vol% PI fibres, was carried out by compression moulding [11]. The study of the tribological properties of PTFE and PCMs based on it under friction conditions without lubrication was studied in rotational motion (v=580 rpm) using a “disk-pad” scheme in a pair with a steel cylindrical counterbody (steel 45, ø25 mm, hardness 45-48 HRC, and surface roughness R_a=0.32 μm) at a constant sliding speed of 1.5 m/s and a load of 1.5 MPa on the SMC-2 friction machine. The determination of the actual density of PTFE and PCMs based on it was carried out by the hydrostatic weighing method, which is based on the principle of liquid displacement by an immersed body according to Archimedes’ law. We chose this method because the measurement error is ±1.5%. We studied the morphology of the friction surfaces of PTFE and PTFE-based PCMs using a BIOLAM-M microscope. The hardness of PTFE and PTFE-based PCMs samples was determined using a dynamic hardness tester of the TD-42 modification on the Rockwell scale (HRC).

Results analysis and discussion

From the data presented in Fig. 1, it is clear that the introduction of 2.5–12.5 vol% PI fibre leads to a decrease in the wear intensity of polytetrafluoroethylene by almost 370 times, reaching a minimum value at 7.5 vol%. The increase in wear resistance of PTFE is due to the increase in the resistance of the friction surface to deformation because of the increase in the hardness of PCMs by almost 2 times (see Fig. 2). The improvement of these indicators at a fibre content of 2.5-7.5 vol% is due to the formation of strong intermolecular bonds at the " polytetrafluoroethylene -PI fiber" interface, which contributes to an increase in the structural uniformity of the composition and, accordingly, a decrease in local stress concentrators. In addition, polymer composite materials during friction on a steel counterbody form a stable transfer film (so-called antifriction layer), formed from finely dispersed wear products, which performs the function of a natural dry lubricating layer [12].

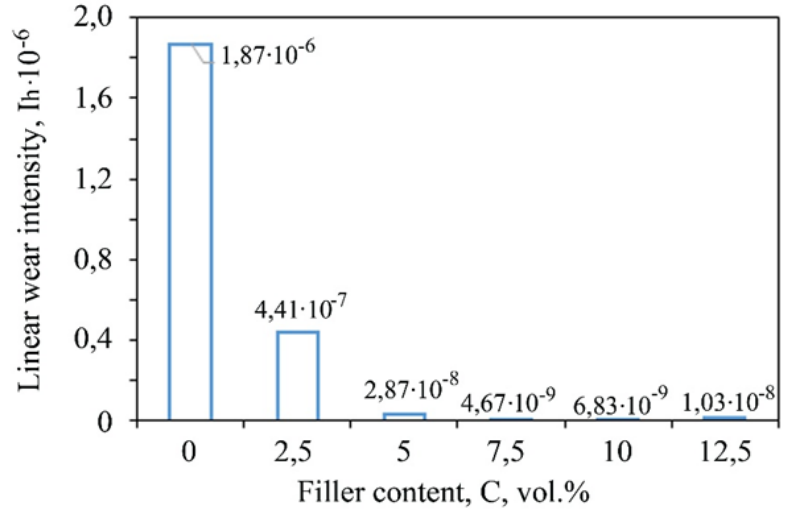

Fig. 1. Dependence of the polytetrafluoroethylene linear wear intensity (I_h) on the volume content of polyimide fibre (C, vol%)

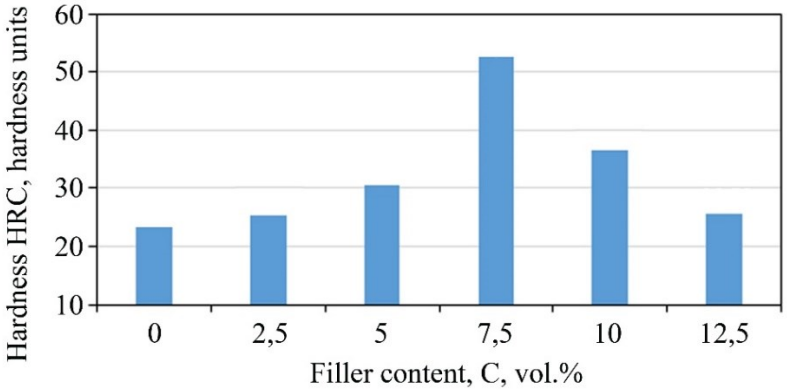

Fig. 2. Dependence of hardness (HRC, hardness units) of polytetrafluoroethylene on the volume content of polyimide fibre (C, vol%)

Morphological analysis of the friction surfaces of the samples after testing confirmed the increase in wear resistance. Comparing the obtained micrographs (Fig. 3), we can see a significant difference in the pattern of surface damage of pure polytetrafluoroethylene and PCMs filled with PI fibre. Thus, we observe signs of plastic deformation, multiple furrows, and traces of microcutting (Fig. 3, a) on the friction surface of pure PTFE. This indicates the predominance of the adhesive-fatigue wear mechanism. In contrast, the friction surfaces of PCMs (Fig. 3, b-e) are characterised by a smaller number of defects, a reduced depth of damage, and a more homogeneous microstructure. This indicates a decrease in the adhesive component of the friction force and a transition to a predominantly pseudoelastic wear mechanism [11].

We investigated the influence of the formation of a transfer film on the linear wear intensity for PCMs with an effective filler content (7.5 vol%). It can be seen from the data presented in Fig. 4 that the wear resistance of PCMs increases by almost 1.5 times with an increase in the test path. This can be explained by the fact that during the friction process, a stable transfer film forms on the surface of the counterbody, reducing the contact between it and the test sample [13]. Additionally, we observe an increase in the friction coefficient (Fig. 5), reaching a maximum value of ~0.135 at a filler content of 7.5 vol%. This can be explained by the fact that the polyimide fibre is characterised by high mechanical rigidity, which results in a more microrough friction surface. The latter contributes to an increase in mechanical adhesion between the contact surfaces during sliding. This, accordingly, increases the friction force. On the other hand, the increase in the friction coefficient of PCMs can also occur due to the low thermal conductivity of the PI fibre (0.1–0.35 W/m K), which leads to insufficient heat removal from the contact zone. The accumulation of heat in the friction zone contributes to a local increase in temperature, which causes an increase in the friction force [8].

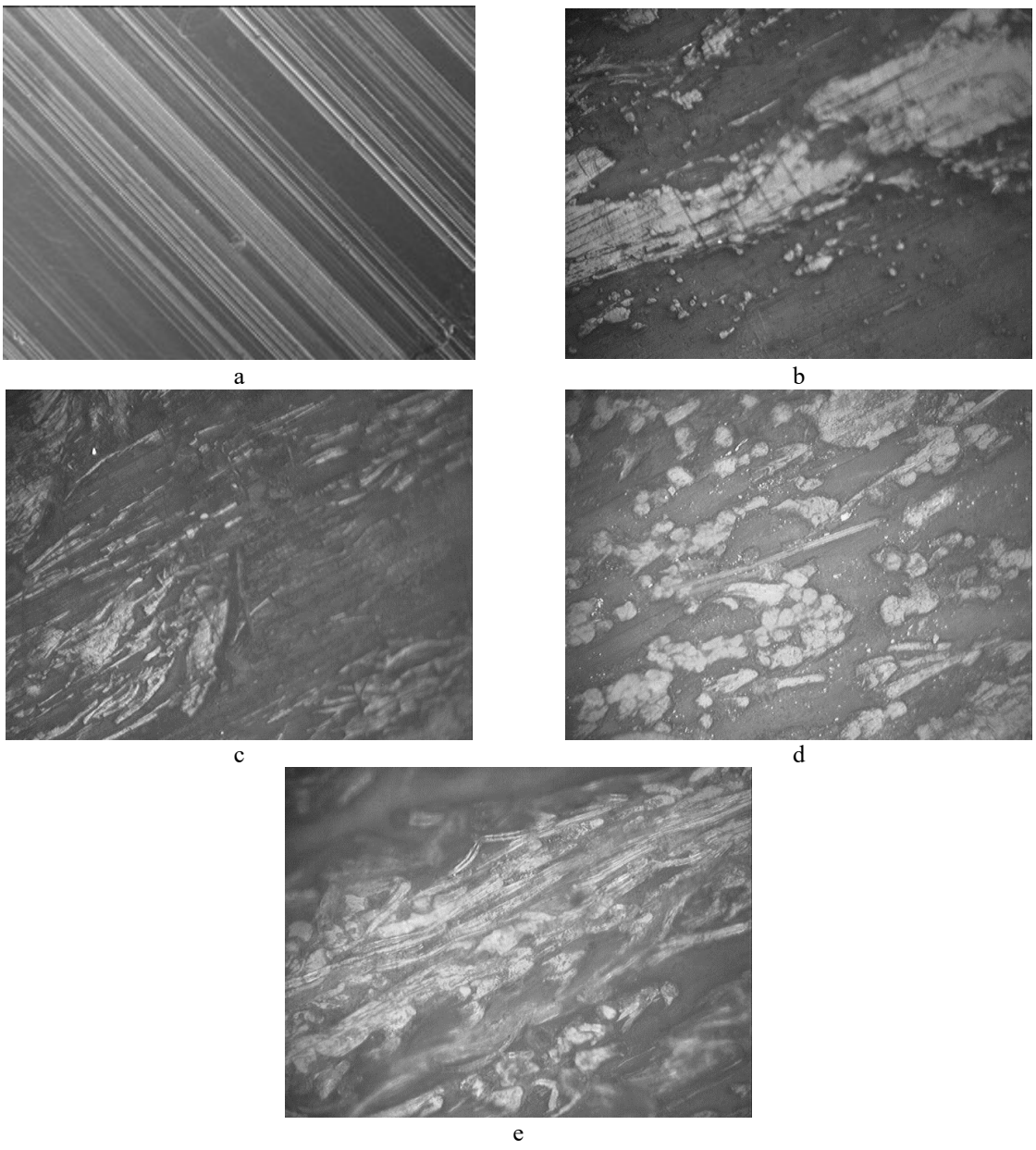

Fig. 3. Friction surfaces of pure PTFE (a) and composites based on it containing 5 (b), 7.5 (c), 10 (d), 12.5 (e) vol% polyimide fibre

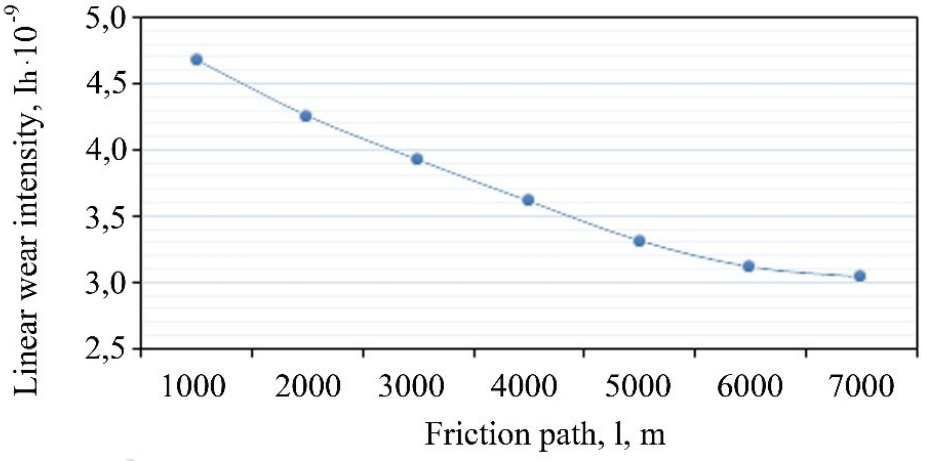

Fig.4. The influence of the length of the friction path (l, m) on the linear wear intensity of a polymer composite with a fibre content of 7.5 vol%.

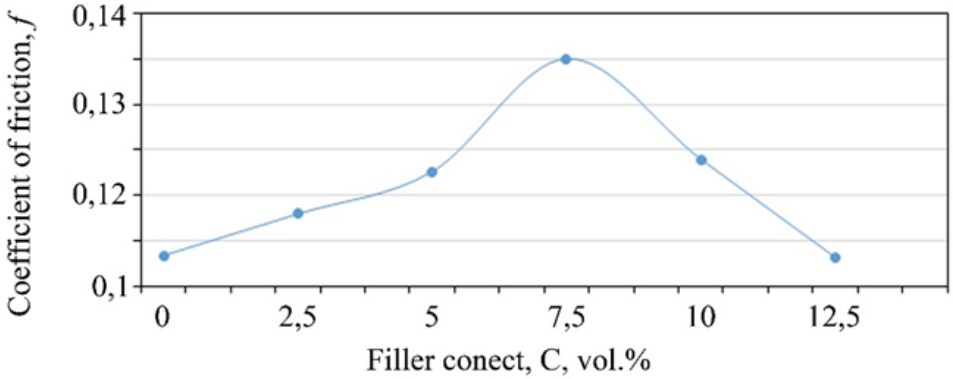

Fig.5. Dependence of the coefficient of friction (*f*) of polytetrafluoroethylene on the volume content of polyimide fiber (C, vol%)

We should note that with an increase in the PI fibre content to 12.5 vol%, a decrease in the wear resistance and hardness of the PCM is observed. This is likely due to the difficulty in uniformly distributing the filler throughout the PTFE volume, which results in a decrease in the interfacial adhesion between the polymer and the fibre. As a result, microcracks, cavities, and other defects form in the PCMs structure, negatively affecting its functional properties [14].

For PCM with an effective fibre content of 7.5 vol%, we conducted a set of tribological tests to determine the critical values of the sliding speed (υ, m/s) and load (P, MPa) that affect the linear wear intensity. From the data shown in Fig. 6, it is clear that their increase leads to a decrease in the wear resistance of the PCM.

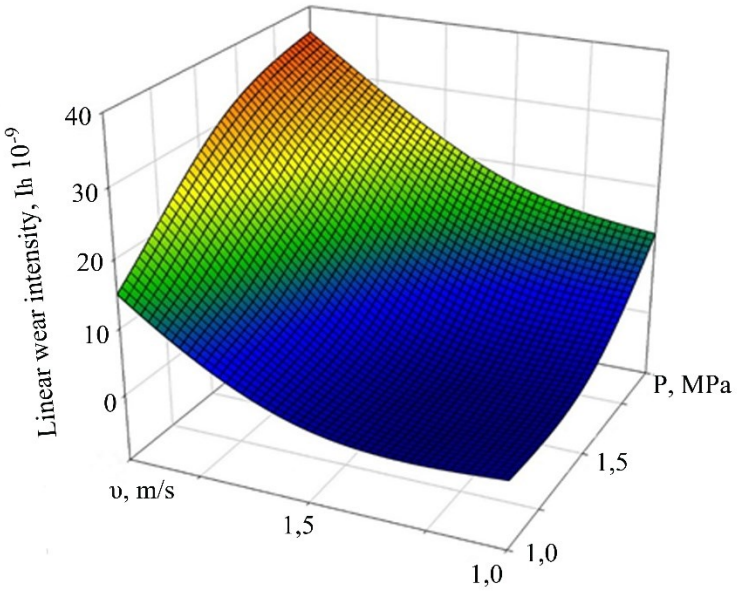

Fig.6. Dependence of the linear wear intensity index (I_h) of a composite containing 7.5 vol% PI fibre on the sliding velocity (υ, m/s) and load (P, MPa)

We can explain this dependence by the thermomechanical processes occurring in the friction zone, particularly the increase in temperature. For example, at a load of P=1.5 MPa and a sliding speed of υ=1.5 m/s, the temperature reached T=423 K, while at P=2.0 MPa and υ=2.0 m/s, it was already T=473 K, which brings it closer to the maximum operating temperature of PTFE (533 K). This increase in temperature causes a deterioration in the functional properties of the PCMs friction surface and a violation of the adhesive bond between polytetrafluoroethylene and the fibre [15].

Conclusions

Analysis of the conducted studies revealed that the introduction of polyimide fibre into the PTFE composition in amounts of 2.5-12.5 vol% results in a significant decrease in linear wear intensity by almost 370 times, with an optimal effective content of 7.5 vol%. The increase in wear resistance occurs because of a nearly twofold increase in the hardness of the PCMs, which enhances the resistance of the friction surface to deformation. This is due to the formation of strong intermolecular bonds at the "PTFE-PI fibre" interface and an increase in the structural homogeneity of the material. The formation of a stable transfer film on the counterbody surface during friction additionally increases the wear resistance of the PCMs by 1.5 times. The introduction of the fibre leads to

an increase in the friction coefficient, which is due to its high rigidity and insufficient thermal conductivity, which complicates the effective removal of heat from the friction zone. Increasing the fibre content to 10-12.5 vol% leads to a decrease in the wear resistance and hardness of the PCMs due to the difficulty in uniformly distributing the Fl, a decrease in interfacial adhesion, and the formation of structural defects (microcracks and cavities). Tribological tests under various operating conditions revealed that an increase in sliding speed and load results in a corresponding rise in temperature within the friction zone. This, in turn, deteriorates the functional properties of the surface and leads to the degradation of the adhesive bond between PTFE and PI fibre, thereby reducing the wear resistance of the PCMs.

References

1. A.S. Kobets Application of polymer composites in the agricultural industry. Monograph. Dnipro: Zhurfond, 2022. 356 p.

2. O. Kabat, V. Sytar, K. Sukhyy Antifrictional polymer composites based on aromatic polyamide and carbon black. Chem. Chem. Technol. 2018. Vol.12, No.3. P. 326–330.

3. Kabat O.S., Sytar V.I., Yermachenok D.V., Davydov S.O., Heti K.V. Polymer composite materials for friction units of space and aviation equipment. System Design and Analysis of Aerospace Engineering. 2017. Vol. XXIII. P. 40–48.

4. Myshkin N.K., Pesetskii S.S., Grigoriev A.Ya. Polymer composites in tribology. VIII International scientific conferene «BALTTRIB 2015».Kaunas, 2015. P.152–1565.

5. K.V. Berladir; T.P. Hovorun, O.A. Bilous, S.V.Baranova The modeling of the composition and properties of functional materials based on polytetrafluoroethylene. Functional Materials. 2018. Vol.25, No2. P. 342–347.

6. O. Burya, Ye. Yeriomina, O. Lysenko, A. Konchits, A. Morozov, Polymer composites based on thermoplastic binders, Dnipro: Srednyak T. K. Press. 2019. 239 p.

7. K.V. Berladir, V.A. Sviderskiy Designing and examining polytetrafluoroethylene composites for tribotechnical purposes with activated ingredients. Eastern-European Journal of Eenterprise Technologies. 2016. Vol.84. No.6. P. 14–21.

8. O. Yeromenko, A.-M. Tomina, I. Rula Effect of discrete basalt fiber on operational properties of polytetrafluoroethylene. Problems of Tribology. 2022. Vol. 27. No. 4/106. P. 39–44.

9. J. Dong, C. Yin, W. Luo, et al. Synthesis of organ-soluble copolyimides by one-step polymerization and fabrication of high performance fibers. Journal of Materials Science. 2013. No.48 (21). P. 7594–7602.

10. X. Dai, F. Bao, L. Jiao, et al. High-performance polyimide copolymer fibers derived from 5-anino-2-(2-hydroxy-4-aminobenzene)-benzoxazole: preparation, structure and properties. Polymer. 2018. Vol.150. P. 254–266.

11. K.R. Voloshina, A.-M.V. Tomina, Yu.E. Hranitskyi The influence of polyamide fiber on the wear intensity of polytetrafluoroethylene. Comprehensive quality assurance of technological processes and systems (KZYATPS -2025): materials of the abstracts of the XV International Scientific and Practical Conference (Chernihiv, May 22–23, 2025): in 2 vols. / National University "Chernihiv Polytechnic" [et al.] ; editor: Prystupa Anatoliy Leonidovych [et al.]. – Chernihiv: NU "Chernihiv Polytechnic", 2025. Vol. 2. P.136.

12. O.I. Burya, S.V. Kalinichenko, A.-M.V. Tomina, I.I. Nachovniy The impact of organic tanlon fiber on performance indicators of polychlorotrifluoroethylene. Journal Problems of Tribology. 2019. Vol.92. No.2. P. 61–66.

13. Buria O.I., Tomina A.-M.V. Organoplastics of tribotechnical purpose. Prospects and priorities of research in science and technology: collective monograph. Riga, Latvia: «Baltija Publishing». 2020. Vol.2. P. 240–257.

14. M.A. Ibrahim, H. Çamur, M. Savaş, S.I. Abba. Optimization and prediction of tribological behaviour of filled polytetrafluoroethylene composites using Taguchi Deng and hybrid support vector regression models. Scientific Reports. 2022. Vol.12. No.1. P. 10393

15. S. Kolhe, A. Deshpande, K. Wangikar. Wear behavior of polytetrafluoroethylene composites: A review. In: Smart Technologies for Energy, Environment and Sustainable Development. 2019. P. 571-584.

Томіна А-М.В., Волошина К.Р., Predrag Dašić, Граніцький Ю.Є. Вплив поліімідного волокна на трибологічні властивості політетрафторетилену

У статті досліджено вплив дискретного поліімідного волокна на трибологічні властивості політетрафторетилену в умовах тертя без змащення за схемою «диск-колодка». Встановлено, що введення наповнювача у кількості 2,5-12,5 об.% сприяє зростанню зносостійкості політетрафторетилену до 370 разів. При цьому коефіцієнт тертя дещо підвищується, досягаючи максимального значення за вмісту волокна 7,5 об.%. Зменшення інтенсивності лінійного зношування політетрафторетилену обумовлено підвищенням твердості майже в два рази. Покращення зносостійкості можна пояснити формуванням міцних міжмолекулярних зв'язків на межі поділу «матриця–волокно», підвищенням структурної однорідності та утворенням стабільної плівки переносу в процесі тертя. Морфологічний аналіз поверхонь тертя підтвердив зменшення інтенсивності пошкоджень для наповнених композитів. На поверхні тертя чистого політетрафторетилену виявлено сліди пластичної деформації, численні борозни проорювання та ознаки мікрорізання, що свідчить про переважання адгезійно-втомного механізму зношування. Натомість поверхні композитів характеризуються меншою кількістю та глибиною дефектів, що свідчить про зменшення впливу адгезійної складової сили тертя та перехід до псевдопружного механізму зношування. При збільшенні вмісту волокна понад 10 об.% спостерігається погіршення властивостей матеріалу через нерівномірний розподіл наповнювача та формування структурних дефектів. Для полімерних композиційних матеріалів із ефективним вмістом волокна 7,5 об.% проведено комплекс трибологічних випробувань з метою визначення критичних значень швидкості ковзання та навантаження, що впливають на інтенсивність лінійного зношування. Отримані результати досліджень дозволяють встановити граничні умови експлуатації, за яких полімерний композит із вмістом волокна 7,5 об.% може успішно застосовуватися у виробництві деталей трибологічних з'єднань різноманітної техніки без використання мастильних матеріалів.

Ключові слова: політетрафторетилен, поліімідне волокно, об'ємні відсотки, інтенсивність лінійного зношування, коефіцієнт тертя, твердість